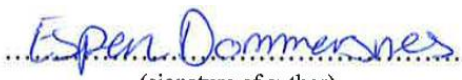




Universitetet
i Stavanger

FACULTY OF SCIENCE AND TECHNOLOGY

MASTER'S THESIS

Study programme/specialization: Petroleum Technology/Drilling	Spring semester, 2019 Open
Author: Espen Dommersnes	 (signature of author)
Supervisor: Dr. Mahmoud Khalifeh (UiS) Industrial Advisor: Lene Tørå (ConocoPhillips)	
Title of master's thesis: Potential Utilization of Neutron Logging for Casing Cement Evaluation	
Credits: 30 ECTS	
Keywords: Neutron Logging Cement Bond Log Cement Evaluation	Number of pages: 100 + supplemental material/other: 3 Stavanger, 14.06.2019

ACKNOWLEDGEMENT

This thesis concludes my Master of Science degree in Petroleum Engineering at the University of Stavanger. I would like to extend my gratitude to my supervisor Dr. Mahmoud Khalifeh at the University of Stavanger for valuable guidance throughout the semester working on this project, for good chats and for devoting so much time to your students. It is highly appreciated.

I am also grateful to Lene Tørå and Jakob Toftkaer at ConocoPhillips for accepting me to present the idea behind this work and for providing me with knowledge and answering questions throughout the semester. Thank you to Amit Govil (Schlumberger) for valuable guidance when commencing this project.

Lastly, a massive thank you goes to student colleagues for making the past five years memorable and to friends and family for continuous support.

*Espen Dommersnes
June 2019, Stavanger*

ABSTRACT

Verification of casing cement integrity is crucial to ensure that the cement fulfills its purpose of zonal isolation, for optimal production and safety. This thesis introduces cement evaluation technology on the market today and highlights advantages and current limitations of each. The scope of this work was to assess neutron logging for the same purpose, and cases such as good cement, cement with channels, foamed cement and a through-tubing configuration has been modelled in a basic preliminary analysis. Results were compared to highlight relative differences in neutron attenuation. Other aspects of the neutron logging technology are assessed for a comprehensive review.

This preliminary analysis has shown that neutrons have the potential to reach the cement-formation interface and be backscattered to the detector for all cases considered. Neutrons experience large attenuation in liquids present in or near the wellbore, while it is less attenuated for gas and foamed cement. For a single casing configuration, results indicate distinguishable results between good and channeled cement. For a through-tubing configuration it cannot be concluded the same as final energy were either too close to the good cement base case or undetectable.

Assessment of other aspects has shown that adding tracer material to the cement can be beneficial in terms of increased absorption and neutron spectroscopy. While specific neutron sources have HSE concerns, there are available alternatives on the market. Neutron logging could present an increased cost which must be weighed against potential gains of applying this technology as a replacement or complimentary to existing cement evaluation methods.

Based on the outcomes of this thesis, a paper to be published is drafted (Appendix C).

NOMENCLATURE

Symbol	Denotes	Unit
A	Area	[cm ²]
c	Speed of Light	[m/s]
C	Concentration	[%]
D	Diameter	[in, mm]
E	Energy	eV
L	Length	[cm, ft, in]
m	Mass	[g]
M	Molecular Mass	[g/mole]
n _i	Number of element i	
N _A	Avogadro's Number	[atoms/mole]
N _i	Atomic Number Density of Element i	[atoms/cm ³]
P	Pressure	[psi, atm]
R	Gas Constant	
s	Seconds	
S _w	Water Saturation	[%]
t	Thickness	[mm, in.]
T	Temperature	[°C, °F]
u	Atomic Mass	
V	Volume	[cm ³]
α	Collision Parameter	
ρ	Density	[g/cm ³ , ppg]
σ	Microscopic Cross Section	[barns, 10 ⁻²⁴ cm ²]
σ _{abs}	Absorption σ	[barns, 10 ⁻²⁴ cm ²]
σ _s	Scattering σ	[barns, 10 ⁻²⁴ cm ²]
σ _{coh}	Coherent σ	[barns, 10 ⁻²⁴ cm ²]
σ _{inc}	Incoherent σ	[barns, 10 ⁻²⁴ cm ²]
Σ	Macroscopic Cross Section	[cm ⁻¹ , capture units (c.u.)]
Σ _t	Total Σ	[cm ⁻¹ , capture units (c.u.)]
Σ _{abs}	Absorption Σ	[cm ⁻¹ , capture units (c.u.)]
θ	Scattering Angle	[degrees]

ABBREVIATIONS

Am-Be – Americium-Beryllium	NCS – Norwegian Continental Shelf
CBL – Cement Bond Log	OBM – Oil Based Mud
CNL – Compensated Neutron Log	OD – Outside Diaeter
DAS – Distributed Acoustic Sensing	P&A – Plugging and Abandonment
DCS – Distributed Chemical Sensing	PAF – Plugging and Abandonment Forum
DPS – Distributed Pressure Sensing	PNG – Pulsed Neutron Generator
D-T – Deuterium-Tritium	PNL – Pulsed Neutron Logging
DTS – Distributed Temperature Sensing	ppg – Pounds Per Gallon
EMI – Electrical Micro Imager	ppm – Parts Per Million
FQ – Foam Quality	RCBL – Radial Cement Bond Log
FWI – Free Water Index	SNP – Sidewall Neutron Porosity
HI – Hydrogen Index	SSLT - Slim Array Sonic Logging Tool
HSE – Health, Safety, Environment	TOC – Top of Cement
ID – Inside Diameter	TDT – Thermal Decay Tool
LCM – Lost Circulation Material	USIT – Ultrasonic Imaging Tool
LWD – Logging While Drilling	USD – United States Dollars
NAS – National Academies of Science	WBM – Water Based Mud
NRC – Nuclear Regulatory Commission	

Cement Notation

<i>Formula</i>	<i>Abbreviation</i>
CaO	C
SiO ₂	S
Al ₂ O ₃	A
Fe ₂ O ₃	F
H ₂ O	H

TABLE OF CONTENTS

ACKNOWLEDGEMENT	i
ABSTRACT.....	ii
NOMENCLATURE	iii
ABBREVIATIONS	iv
1 INTRODUCTION.....	1
1.1 Cement Evaluation Techniques	1
1.1.1 Cement Bond Log.....	2
1.1.2 Ultrasonic Cement Evaluation Tools.....	4
1.1.3 Temperature Log.....	5
1.1.4 Fiber Optics.....	6
1.1.5 X-Rays	8
2 OBJECTIVES	9
3 NEUTRONS AND NEUTRON LOGGING	11
3.1 Neutron Sources.....	11
3.1.1 Neutron Generator Source	11
3.1.2 Chemical Neutron Source	13
3.2 Neutron Interactions.....	13
3.3 Energy Dependence of Neutron Cross Sections	16
3.4 Hydrogen Index	17
3.5 Effects on Neutron Logging.....	18
3.5.1 The Hydrocarbon Effect	18
3.5.2 The Shale Effect.....	18
3.5.3 The Chlorine Effect.....	18
3.6 Neutron Detection and Tools	18
3.7 Neutron Attenuation.....	20
3.8 Applications of Neutron Log	21
3.8.1 Traditional Application.....	21
3.8.2 Spectroscopy	22
3.8.3 Developments in Applications of the Neutron Log.....	22
3.9 Advantages and Possible Limitations of Neutron Logging Technology for Cement Evaluation	23
4 MATERIALS	25
4.1 Casing	25
4.2 Cement	26
4.2.1 Cementing Operations	26
4.2.2 Portland Cement.....	27

4.2.3	Cement Placement	29
4.2.4	Cement Hydration and Composition	31
4.2.5	Foamed Cement	33
4.3	Oil-Based Mud.....	34
4.4	Gas	36
5	ANALYSIS AND RESULTS	37
5.1	Neutron Interaction with Different Material.....	37
5.1.1	Spacing Sensitivity Analysis.....	41
5.1.2	Case 1: Good Cement	43
5.1.3	Case 2: Foamed Cement	44
5.1.4	Case 3: Cement Defect with OBM	45
5.1.5	Case 4: Cement Defect with Gas	46
5.1.6	Summary – Case 1-4.....	48
5.1.7	Case 5: Through-Tubing Logging	48
5.2	Neutron Backscattering.....	51
5.3	Health, Safety and Environmental Concerns	54
5.4	Tool.....	55
5.5	Cost.....	56
5.6	Alternative Approach to Utilize the Technology; Tracer for Neutron Cement Evaluation 58	
5.6.1	Injection of Neutron-Absorbing Solution	58
5.6.2	Neutron Attenuation in Tagged Concrete	59
5.6.3	Gamma Ray for Cement Tracing.....	60
5.6.4	Tracer for Neutron Log Cement Evaluation	61
5.6.5	Tracer Calculations	64
5.6.5.1	Neutron Attenuation in Tracer Material	64
5.6.5.2	Neutron Absorption in Tracer Material	66
5.6.5.3	Spectroscopy for Tracer Logging	67
5.7	Alternative Approach to Utilize the Technology; Polarization Analysis	68
6	DISCUSSION	71
6.1	What Are Detectable Results?	71
6.2	Neutron Transmission Calculations	71
6.2.1	Casing	71
6.2.2	Foamed Cement	72
6.2.3	Channeled Cement	72
6.2.4	Through-Tubing Logging	73
6.2.5	Limitations of the Analysis	73
6.3	Tool, HSE and Cost	75
6.4	Cement Evaluation by Neutron Tracer Logging.....	76

6.4.1 Neutron Attenuation in Cement with Tracer Material	76
6.4.2 Spectroscopy for Cement Evaluation.....	77
7 SUGGESTIONS FOR FUTURE WORK.....	79
8 CONCLUSION	81
REFERENCES	82
APPENDIX A – DATA INTERPOLATION	89
APPENDIX B – THERMAL NEUTRON CALCULATIONS	90
APPENDIX C – PAPER TO BE SUBMITTED	91

LIST OF TABLES

Table 3-1: Atomic mass of selected elements. Adapted from Sears et al. (2012)	12
Table 3-2: Cross sections of some elements in unit barns. Based on Munter (2017).....	16
Table 3-3: Current advantages and limitations of applying neutron logging technology for cement evaluation. Based on Kahlifeh (2017).....	23
Table 4-1: Casing specifications. Based on Gabolde and Nguyen (2006)	26
Table 4-2: Composition of L-80 casing. Adapted from Continental Alloys & Services (2019)...	26
Table 4-3: Mineralogical composition of a classic Portland cement clinker. Based on Guillot and Nelson (2006).....	28
Table 4-4: Sample composition of class G cement.....	28
Table 4-5: Recipe for cured Portland class G cement.....	32
Table 4-6: Foam quality of different substances. *Depending on nitrogen amount.....	33
Table 4-7: Composition of selected class G cement.....	34
Table 4-8: Capture cross sections of different liquids. Based on SPE-International (2015c)	35
Table 4-9: Composition of selected OBM	36
Table 4-10: Selected composition of natural gas	36
Table 5-1: Dimensions for analysis	38
Table 5-2: Atomic number densities of material	39
Table 5-3: Average Deviation of Σ_t from class G cement	40
Table 5-4: Elemental atomic number densities of natural gas	47
Table 5-5: Analysis results and deviance from base case.....	48
Table 5-6: Results from Case 5 – $E_0 = 14.1$ MeV	51
Table 5-7: Capture cross sections of some selected elements. Uncertainties in parenthesis. Based on Munter (2017).....	63
Table 5-8: Results for tracer analysis at different E_0	66

LIST OF FIGURES

Figure 1-1: A fully cross sectional and vertical cement barrier. Adapted from NORSOK D-010 (2013).....	1
Figure 1-2: Sonic wave travel path. Adapted from Guillot and Nelson (2006).....	2
Figure 1-3: Attenuation of signal depends on bonding. Adapted from Guillot and Nelson (2006)	3
Figure 1-4: Cement curing is an exothermic process which may be detected as anomalies from normal temperature gradient. Adapted from Guillot and Nelson (2006).....	6
Figure 1-5: Basic principle of fiber optics. Adapted from Fidaner (2017).....	6
Figure 2-1: Attenuation of radiation through different material. Adapted from Mirion (2019).....	9
Figure 3-1: Atomic structure exemplified by the beryllium-9 atom. Not to scale. Adapted from Sharp (2017).....	11
Figure 3-2: D-T neutron generator principle. Adapted from Khalifeh (2017)	12
Figure 3-3: Energy spectra of different neutron sources. Adapted from Badruzzaman (2019)	13
Figure 3-4: Lifecycle of a neutron from generation to capture. Adapted from Ellis and Singer (2007).....	14
Figure 3-5: Slowing down of neutrons at different energy levels for different elements. Glover (2000).....	15
Figure 3-6: The target nucleus releases a gamma ray upon absorption (Das, 2017)	16
Figure 3-7: Energy dependence of (total) neutron cross section. Based on NNDC (2011).....	17
Figure 3-8: Neutron tool in cased hole. Based on Glover (2000).....	19
Figure 3-9: Neutron log response to different formations. Rider and Kennedy (2011)	21
Figure 3-10: Spectral stripping of the capture gamma rays shows individual elemental contributions (Schlumberger, 2018)	22
Figure 4-1: The neutron must reach the cement/formation interface and return	25

Figure 4-2: Wellbore construction. Adapted from Encana (2016)	25
Figure 4-3: Requirements for a hydraulically sealed cement sheet. Adapted from Guillot and Nelson (2006).....	27
Figure 4-4: Steps in a typical primary cementing job. Adapted from Guillot and Nelson (2006)	30
Figure 4-5: Cement defects. Based on Cameron (2013).....	31
Figure 4-6: Hydration of cement components. Adapted from Hewlett and Lea (2003).....	32
Figure 4-7: Foamed cement, fluid and air distinguished on neutron log (track 1). Adapted from Harness and Frank (1996).....	34
Figure 5-1. Calculated energy dependent macroscopic cross sections (Σ_t)	40
Figure 5-2: Analysis Process	41
Figure 5-3: Neutron traveling length increases with spacing.	41
Figure 5-4: Sensitivity analysis of source-detector spacing	42
Figure 5-5: Dimensions for 12 in. spacing.....	43
Figure 5-6: Dimensions for case 1 - Good Cement	43
Figure 5-7: Transmission calculations for case 1	44
Figure 5-8: Dimensions for case 2: Foamed Cement.....	44
Figure 5-9: Transmission calculations for case 2	45
Figure 5-10: Case 3: Dimensions for 10% and 20% OBM-filled channel	45
Figure 5-11: Transmission calculations for case 3	46
Figure 5-12: Case 3: Dimensions for 10% and 20% gas-filled channel	47
Figure 5-13: Transmission calculations for case 4	47
Figure 5-14: Transmission results - All cases.....	48
Figure 5-15: Case 5: Dimensions for a logging through tubing.	49
Figure 5-16: Sensitivity Analysis, Case 5 for $E_0 = 4.5$ MeV.....	50
Figure 5-17: Sensitivity Analysis, Case 5 for $E_0 = 14.1$ MeV.....	50
Figure 5-18: Results for Case 5 – $E_0 = 14.1$ MeV	51
Figure 5-19: Center of mass system. Adapted from Ragheb (2006)	52
Figure 5-20: Energy loss as function of scattering angle.....	52
Figure 5-21: The neutron beam spreads spherically. Adapted from Pynn (2009).....	53
Figure 5-22: Inelastic interactions mainly occurs at higher energy. Adapted from Ellis and Singer (2007).....	53
Figure 5-23: Radiation weighting factors plotted against neutron energy in MeV. Modified from ICRP (2007).....	55
Figure 5-24: Reduction in near and far counts due to presence of boron solution (borax). Adapted from Sommer and Jenkins (1993).....	59
Figure 5-25: Measured signal against radius of annulus behind casing. Adapted from Kline et al. (1986).....	60
Figure 5-26: Comparison between caliper radius and cement radius from gamma ray tracer log. Adapted from Kline et al. (1986).....	61
Figure 5-27: Σ_t of cements with tracers	64
Figure 5-28: Cement with tracer transmission analysis. $E_0 = 4.5$ MeV.....	65
Figure 5-29: Cement with tracer transmission analysis. $E_0 = 2.5$ MeV.....	66
Figure 5-30: Absorption probabilities of cements with and without tracers	67
Figure 5-31: Inelastic cross section of selected elements.	68
Figure 5-32: Polarization analysis. To the left: Nickel. To the right: Vanadium. Adapted from Schweika (2012)	69

LIST OF EQUATIONS

Eq. 3-1.....	12
Eq. 3-2.....	12
Eq. 3-3.....	12
Eq. 3-4.....	13

Eq. 3-5.....	15
Eq. 3-6.....	15
Eq. 3-7.....	16
Eq. 3-8.....	16
Eq. 3-9.....	17
Eq. 3-10.....	17
Eq. 3-11.....	17
Eq. 3-12.....	20
Eq. 3-13.....	20
Eq. 3-14.....	20
Eq. 3-15.....	20
Eq. 4-1.....	31
Eq. 4-2.....	31
Eq. 4-3.....	33
Eq. 4-4.....	33
Eq. 5-1.....	38
Eq. 5-2.....	38
Eq. 5-3.....	39
Eq. 5-4.....	42
Eq. 5-5.....	42
Eq. 5-6.....	46
Eq. 5-7.....	51
Eq. 5-8.....	51
Eq. 5-9.....	60
Eq. 5-10.....	63
Eq. 5-11.....	63
Eq. 5-12.....	63
Eq. 5-13.....	64
Eq. 5-14.....	66
Eq. 5-15.....	68

1 INTRODUCTION

The main purpose of any cementing operation is to provide zonal isolation. As cement is placed in the annular space between casing and formation, we must be able to verify that fluids are incapable of flowing uncontrolled up or down in channels or void space as a result of a poor cement job. About 15% of all cementing operations are unsuccessful, therefore detecting any cement defects early is useful for efficient remedial cementing operations and reduce production losses (Guillot and Nelson, 2006). The cement must provide integrity not only during the producing years of the well, but also post-abandonment. If cement integrity can be ensured outside the casing when the well is due for plugging, a cement plug can be placed inside the casing to achieve the requirement of a fully cross sectional barrier as described by NORSOK (2013) (Figure 1-1).

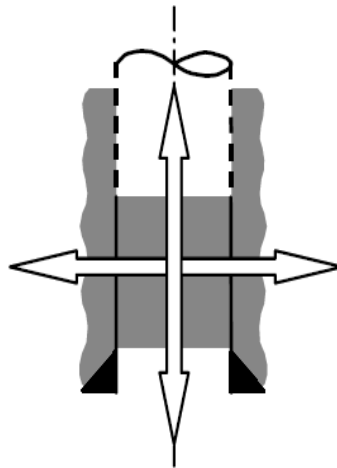


Figure 1-1: A fully cross sectional and vertical cement barrier. Adapted from NORSOK D-010 (2013)

1.1 Cement Evaluation Techniques

Since the 1950's, cement integrity has been attempted to be verified by use of different tools (Benge, 2014). As will be discussed in the following sections, these techniques to evaluate cement have both strengths and limitations. Discussed technologies include:

- Cement Bond Log
- Ultra-sonic Tools
- Temperature Log
- Fiber Optics
- X-rays

1.1.1 Cement Bond Log

The principle of the cement bond log (CBL) is the same as that of the acoustic log, namely to measure the transit time of p-waves on different interfaces. Transit time refers to the time spent by the sonic wave to travel from the transmitter through wellbore fluids to the casing, along the casing-cement interface, and from casing through wellbore fluids back to the receiver (Figure 1-2). There are several possible configurations of a CBL tool but having two receivers helps to eliminate the effect of wellbore fluids and isolate the casing travel time. The acoustic wave is generated by an acoustic transmitter. At one particular angle, the critical angle, the wave is refracted along the casing. This is the arrival of interest, which ultimately will be measured by the receiver as the primary arrival due to the high acoustic velocity in steel (Guillot and Nelson, 2006).

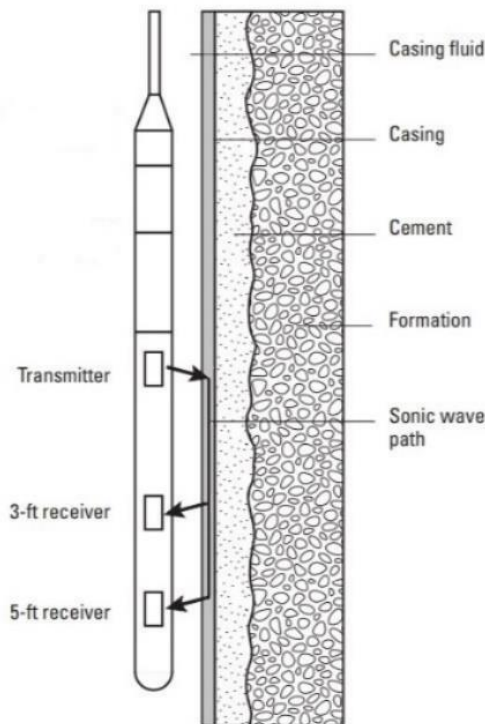


Figure 1-2: Sonic wave travel path. Adapted from Guillot and Nelson (2006)

As the name suggests, the purpose of the log is to evaluate the bonding between the casing and cement, which is derived from the attenuation of the acoustic wave. This is because the signal loses energy as a function of shear coupling between the traveled medium and nearby material (Guillot and Nelson, 2006). The principle is the same as hitting a glass with a spoon. If you wrap your hand around the glass, i.e. create bonding between your hand and the glass, there will be much more attenuation of the sound than if your hand did not touch the glass at all. Consequently, the more attenuated the received signal, the better bonding (Figure 1-3).

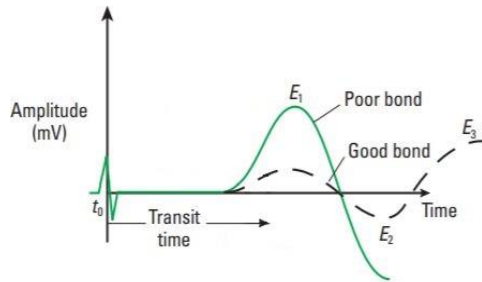


Figure 1-3: Attenuation of signal depends on bonding. Adapted from Guillot and Nelson (2006)

Advantages of the CBL include but are not limited to (Benge, 2014; Guillot and Nelson, 2006):

- Can be a very effective measure of bonding if combined with sufficient information on the cement job itself, additives and design of the cement slurry as well as knowledge of the objectives and limitations of the cementing operation (Benge, 2014).
- Safe to handle
- Non-destructive method

Several challenges and limitations exist for the CBL. While technical solutions, special interpretation methods and corrections exist for many of them, some difficulties remain. Fertl et al. (1974) mentioned that CBL “[...] is probably one of the most abused, misused, and misunderstood logs used in the oil field today. Miscalibration, inadequate information, and a severe lack of standardization are enough to push petroleum engineers into a morass of bewilderment.” By some this is still considered to be true today (Benge, 2014; Gowida et al., 2018) and the CBL is described in literature as “complicated and somewhat subjective” (Johnson and Pile, 2006). Some of the challenges include:

- Cement channels. Can be for example due to casing eccentricity or fluid flow in the cement prior to curing. Cement channels will yield a high reading on the CBL (Johnson and Pile, 2006).
- Thin cement sheaths. Cement with thickness of less than $\frac{3}{4}$ in. will not have significant dampening effect on the CBL and hence will read too high values. This is for example the case for a $8\frac{1}{2}$ in. hole with 7-in. casing (Pilkington, 1992).
- Microannulus, or small gaps in bonding. These small voids may be so small that fluids are unable to pass through, so to some extent one can say that integrity and bonding is still intact, however it will still affect the CBL log to show values close to free pipe (Johnson and Pile, 2006)
- The tool averages response around the wellbore, making the tool unreliable for determining isolation of small intervals (Benge, 2014).

- Fast formations. These are formations of so low porosity and high density that it can transmit acoustic waves as fast or faster than steel. The formation arrival will arrive before the casing arrival. (Johnson and Pile, 2006).
- Properties of wellbore fluids. Nayfeh et al. (1986) showed significant free-pipe amplitude differences for various types of brine.
- Wellbore conditions. Deep wells have higher temperatures and pressures, which will affect the traveling velocity of sound (Guillot and Nelson, 2006).
- Detection of lightweight cement. These cements, such as foamed cement, have low attenuation effect on the acoustic signal and may be mistaken as free pipe (Thomas et al., 2016). The same is the case for gas-cut (contaminated) cement (Johnson and Pile, 2006).
- Requires well re-entry which can be costly (Wu et al., 2017).
- Not a continuous log, provides a snapshot in time (Wu et al., 2017).

1.1.2 Ultrasonic Cement Evaluation Tools

One of the earliest ultrasonic cement evaluation tools was the pulse-echo tool. Usually arranged with eight transducers phased at 45 degrees, the tool emits high frequency pulses of 250-650 kHz to make the casing vibrate perpendicularly. Vibrations, and the following attenuation of these, are a function of the acoustic impedance of wellbore fluids, casing and cement. The tool takes the difference of measurements in uncemented and cemented intervals, and it is assumed that the only changing factor is whatever is behind casing. Hence, the acoustic impedance of the cement is isolated. For an uncemented interval the pulse will fade away slowly, while if there is good cement the pulse will be dampened rapidly (Guillot and Nelson, 2006).

Sharing the same principles as that of the pulse-echo tool, more recent ultrasonic imaging tools (USIT) include rotating transducers to achieve coverage of the whole circumference of the casing (Benge, 2014). The advantages of USIT can be simply summed up in that it deals with some of the limitations of the CBL:

- Evaluates cement around the whole casing (Benge, 2014).
- Less sensitive to the effects of micro-annulus (Pilkington, 1992).
- Where CBL is limited to the casing/cement interface, pulse-echo technology has deeper depth of investigation and has potential for cement evaluation behind two casing strings (Morris et al., 2007).

Despite this, there exist some limitations to this technology (Gowida et al., 2018; Guillot and Nelson, 2006):

- The tool is sensitive to corrosion on the inside of the casing.

- The tool is sensitive to casing weight.
- The casing cannot be thicker than 0.59 in.
- There is an upper limit for how heavy mud weight the tool can handle.

1.1.3 *Temperature Log*

Curing of cement is an exothermic process, and the temperature log essentially looks for deviations in the temperature gradient behind casing to verify presence of cement. By detecting sudden increases in temperature (Figure 1-4) this log can detect the top of cement (Benge, 2014). It is a time-restricted process as the peak temperature occurs after 4-12 hours and it has been shown that the temperature gradient returns to normal after about 24 hours (Pilkington, 1992). Advantages of temperature logging include (Guillot and Nelson, 2006):

- When knowing the top of cement, this can be compared to what was expected by considering pumped volume and the volume of the annulus. From this, the displacement efficiency can be determined and say something about whether the cement job has been successful.
- The temperature log can give indication of channeling in the cement. If run after some time, fluctuations from a normal temperature gradient may indicate that fluids are flowing behind casing. It can also be monitored by active injection of fluids.

Possible limitations include but are not limited to:

- Low density cements. Due to less heat produced in the curing process, temperature anomalies can be difficult to detect (Guillot and Nelson, 2006).
- Because heat rises there are uncertainties related to detection of top of cement (TOC) (Benge, 2014). It could be solved by running the log several times and study the differential temperature, which is time consuming.
- Limited time window (Pilkington, 1992).
- Dependent in many factors such as annulus size, cement height, circulation time, additives and density of the cement (Guillot and Nelson, 2006).
- As the log itself only measures temperature, evaluation of cement as hydraulic seal using this technology is difficult.

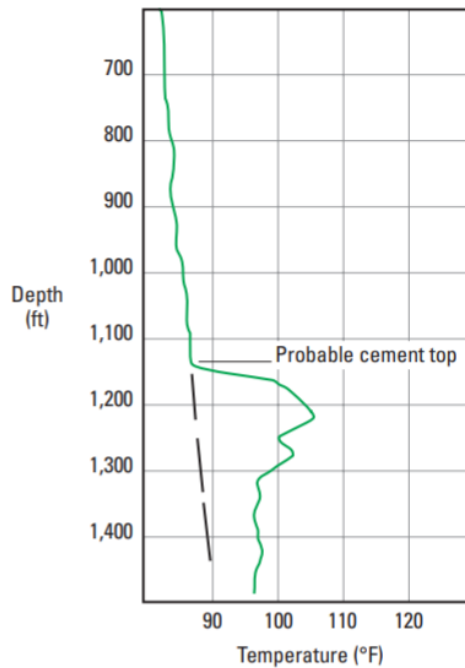


Figure 1-4: Cement curing is an exothermic process which may be detected as anomalies from normal temperature gradient. Adapted from Guillot and Nelson (2006)

1.1.4 Fiber Optics

While most people relate fiber optics to communication technology, it has also seen applications in the oil-field industry since the 1990s (Rambow et al., 2010). Generally speaking, the principle of fiber optics revolves around the response of light generated from a pulsed laser. The laser is connected to an optical fiber (Figure 1-5) and studying the different components of the backscattered light gives information about passed media.

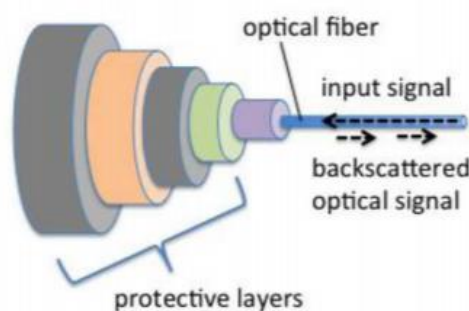


Figure 1-5: Basic principle of fiber optics. Adapted from Fidaner (2017)

Components of the backscatter include Raman band, Brillouin band and Rayleigh band. Depending on how the Raman band is scattered, it can be dependent on temperature. This technology is called distributed temperature sensing (DTS). Similarly, the Rayleigh band is studied in distributed acoustic sensing (DAS), and it is used for leak detection, fracture modelling etc. Distributed pressure sensing (DPS) and distributed chemical sensing (DCS) are technologies still in the research stage (Hveding and Bukhamsin, 2018).

The fiber optic cable can be installed both permanently, semi-permanently or intervention-based (Hveding and Bukhamsin, 2018):

- Permanent installation is achieved by cementing the cable in place. By applying DTS, properties such as TOC can be measured in a similar fashion as for temperature logs.
- Semi-permanent installation involves strapping the fiber to the tubing, and thereby expose the fiber to the tubing-casing annulus primarily with leak detection in mind. If the tubing is removed, so is the fiber.
- In cases where fiber optics were not part of the initial installation, it can be run either embedded in a coiled tubing, wireline or a composite carbon rod. This installation method is useful for monitoring production, injection or flow behind casing.

A study by Wu et al. (2017) demonstrated the potential of using fiber optic distributed sensing for monitoring the curing process of cement and for detection of hydrocarbons behind casing. A hybrid of Rayleigh and Brillouin technology was used, which are sensitive to shifts in temperature and strain. Through laboratory experiments, the exothermic curing process of cement was successfully monitored in real-time. Furthermore, different degrees of contaminated cement were detected, which can be used to estimate displacement efficiency. Hydrocarbons in cement defects behind casing were detected by a specially developed cable consisting of an optical fiber covered in a polymer which swells upon contact with hydrocarbons.

Applying fiber optics for temperature logging can also be used in an opposite fashion as demonstrated by Sun et al. (2018). In this study water jets, normally used for cleaning the inside of the wellbore, were used to inject water and thereby cool down the casing at arbitrary depths. This was done in two trial wellbores, where three different fibers were placed outside of the casing. The jets were dragged upwards at different speeds. By the response of the distributed fiber optic sensing system it was possible to evaluate cement integrity as measured temperature anomalies had good correlation with Radial Cement Bond Log (RCBL) and Electrical Micro Imager (EMI) run over the same interval.

Advantages of fiber optics include but are not limited to:

- Continuous real-time measurement, rather than a snapshot in time provided by standard logs (Walker and Carr, 2003).
- Not sensitive to internal corrosion of pipe (Walker and Carr, 2003).
- Economically favorable. Reduces need for intervention if installed permanently/semi-permanently. Low operational cost (Hveding and Bukhamsin, 2018).
- Wide variety of possible applications such as TOC estimation, leak detection in casings,

fracture monitoring, multiphase flow monitoring, seismic, subsidence monitoring and casing imager (Hveding and Bukhamsin, 2018; Rambow et al., 2010).

- Shows promising results in evaluation of cement with different contaminations (Wu et al., 2017).

Possible limitations include but are not limited to:

- Heat release from curing cement is affected by contamination (Wu et al., 2017)
- The Rayleigh-Brillouin hybrid cement evaluation presented above was carried out with fiber permanently cemented to the casing (Wu et al., 2017). This is not possible on already cemented intervals.
- Technology still fairly young and many techniques are still in the research phase (Hveding and Bukhamsin, 2018).
- Hydrogen-induced effects (Walker and Carr, 2003).

1.1.5 X-Rays

X-rays are mostly known for their applications in the medical field. However, studies have been done to investigate their applicability for the petroleum industry. X-rays are photons with wavelengths of 10^{-8} to 10^{-12} meters. This is considerably shorter than visible light, but longer than gamma rays and have energy of 10^2 to 10^5 electron volts (eV) (Stark, 2018).

A previous MSc thesis investigated the potential of utilizing X-rays for cement evaluation (Haddad, 2017), with associated advantages and limitations (Khalifeh et al., 2017). The thesis concluded that X-rays experience high attenuation through steel and did therefore not have enough energy to reach the cement and travel back to the receiver. Limitations identified where:

- The X-rays must be of very high energy to penetrate steel
- Providing the power to generate X-rays of sufficiently high energy to penetrate steel without generating too much heat.
- Radioisotopes could provide the needed energy but the disposal of these were a concern.

2 OBJECTIVES

In Haddad (2017) and Khalifeh et al. (2017) it was suggested to consider the application of neutron logging for cement evaluation for future research. The main argument for applying neutrons is that it is most slowed down by substances of low atomic mass. Because steel is a mixture of mainly iron and carbon, neutrons would therefore be less attenuated than X-rays when passing through it.

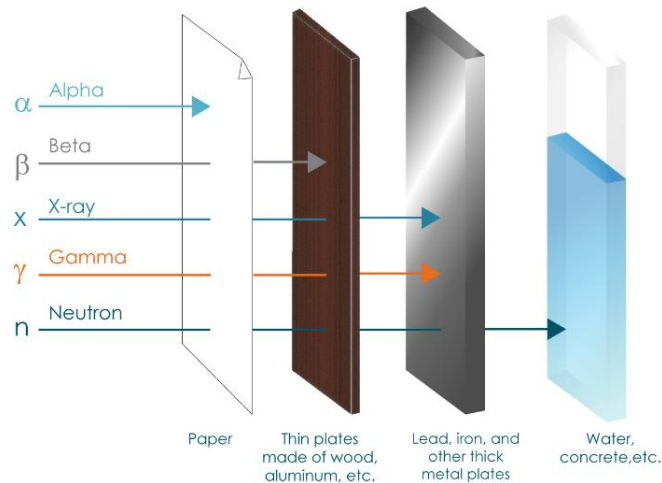


Figure 2-1: Attenuation of radiation through different material.
Adapted from Mirion (2019)

Based on the stated challenges and limitations with current logging techniques discussed above, the potential of utilizing neutron logging for cement evaluation will be investigated. Points to be assessed are the following:

- How do neutrons interact with a single casing and a through-tubing well design?
- How do neutrons interact with cement and presence of fluids in channeled cement?
- How do neutrons interact with foamed cement?
- Can neutrons be emitted from the neutron source and be backscattered to the detector?
- Define a list of other requirements the technology must fulfill to be adequate for the desired application, and assess defined list for neutron logging technology.

In the following chapter, different aspects of neutron logging will be presented from neutron generation to detection. Next, the material to be investigated is introduced to lay the foundation for the following analysis. The neutron response through the different material is simulated in a preliminary analysis including simple modelling in MATLAB and Excel. Promising results in this work will be encouraged for further analysis in more advanced software or laboratory experiments. Furthermore, other relevant aspects of the technology will be assessed by review of relevant literature to give a comprehensive review of the technology for cement evaluation.

3 NEUTRONS AND NEUTRON LOGGING

To understand where neutrons originate from, we must study atoms. The core of an atom, the nucleus, consists of protons and neutrons. Protons, having about one atomic mass, are positively charged particles while neutrons are of similar mass but has no charge. Orbiting around the nucleus are electrons, which are relatively much smaller in size and negatively charged (Trefil et al., 2018) (Figure 3-1).

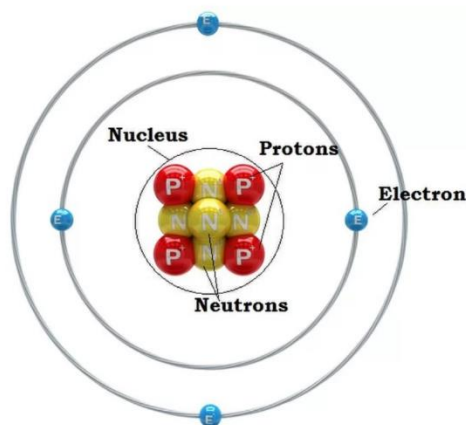


Figure 3-1: Atomic structure exemplified by the beryllium-9 atom. Not to scale. Adapted from Sharp (2017)

When logging using neutrons, we essentially bombard the formation with neutrons and record the response as they collide with encountered atoms and slow down (Glover, 2000). Three important processes determine what we detect; neutron generation, formation interaction and absorption. The following sections will go into detail on these processes in order to explain how neutron logging works.

3.1 Neutron Sources

There are two main types of sources for generating neutrons; a chemical source and neutron generators. This section will elaborate on the main differences between these.

3.1.1 Neutron Generator Source

The neutron generator source generates neutrons by fusing the heavy hydrogen isotopes deuterium and tritium. It is therefore known as a D-T source (Rider and Kennedy, 2011). In the generator, deuterium is contained in the filament (Figure 3-2a) and is released upon heat increase from an induced current. A second current causes a cathode to release electrons (Figure 3-2b) which upon interaction leaves the deuterium positively charged (Figure 3-2c). Tritium is also released by heating a tritium-source known as the target (Figure 3-2d) which in turn interacts with the

deuterium to produce alpha particle (${}^4_2\text{He}$) and a neutron (Figure 3-2e). The process is described by Eq. 3-1 and Figure 3-2 (Sears et al., 2012).

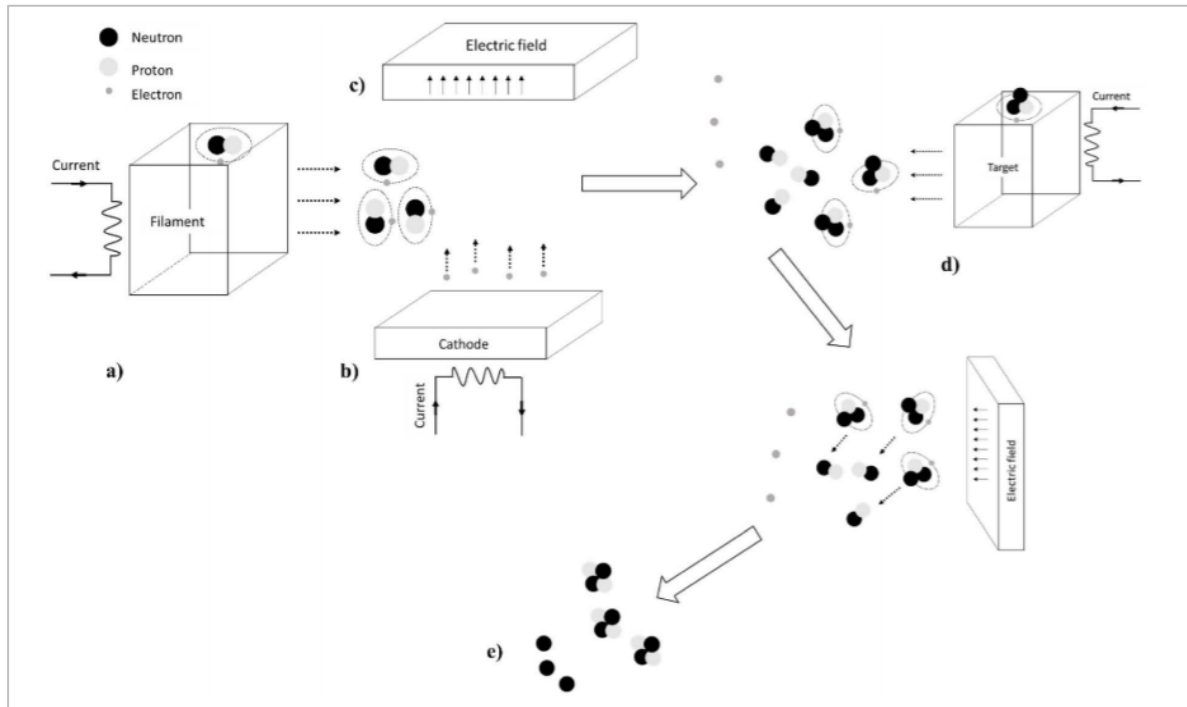


Figure 3-2: D-T neutron generator principle. Adapted from Khalifeh (2017)

The energy released in the reaction can be calculated from the mass-energy equivalence (Sears et al., 2012):

$$E = mc^2 \quad \text{Eq. 3-2}$$

Table 3-1: Atomic mass of selected elements. Adapted from Sears et al. (2012)

Element/Isotope	Atomic mass [u]
Hydrogen	1.007825
Deuterium	2.014102
Tritium	3.016049
Helium	3.016029
Helium ⁴	4.002603
Neutron	1.008665

Inserting values for atomic mass (m) from Table 3-1 into Eq. 3-2 we get:

$$E = (2.014102 + 3.016049 - 4.002603 - 1.008665)u * 931.5 \frac{\text{MeV}}{u} \quad \text{Eq. 3-3}$$

$$= 17.6 \text{ MeV}$$

Due to the helium atom being about 4 times heavier than the neutron, momentum and energy conservation dictates that the neutron will carry about 80% of the energy (Sears et al., 2012). Thus, the neutron generator emits neutrons of about 14.1 MeV (mega electron volts). This generation occurs in pulses, or short bursts, thereby the name pulsed neutron generator (PNG) is used. One of

the advantages of this tool is that it can be switched on and off when desired. Furthermore, due to the high energy and initial velocity, the PNG has higher depth of investigation (Zhou et al., 2018).

3.1.2 Chemical Neutron Source

The chemical neutrons source consists of a beryllium-9 source and an unstable nuclide such as americium, plutonium, radium or californium. As the unstable nuclide decay, it emits α -particles (${}^4_2\text{He}$) which react with the beryllium to produce a broad spectrum of neutrons with average at around 4.5 MeV (Glover, 2000) (Figure 3-3).



The chemical americium-beryllium (Am-Be) source is the most widely used today as it is technology that has been available for a long time, and thus a much larger database has been gathered for well log analysis using this source. Typically, this neutron source yield in the vicinity of 10^8 neutrons per second (Rider and Kennedy, 2011). There exist concerns in applying radioactive sources for logging purposes, and alternative sources are sought. This is discussed in the later chapters.

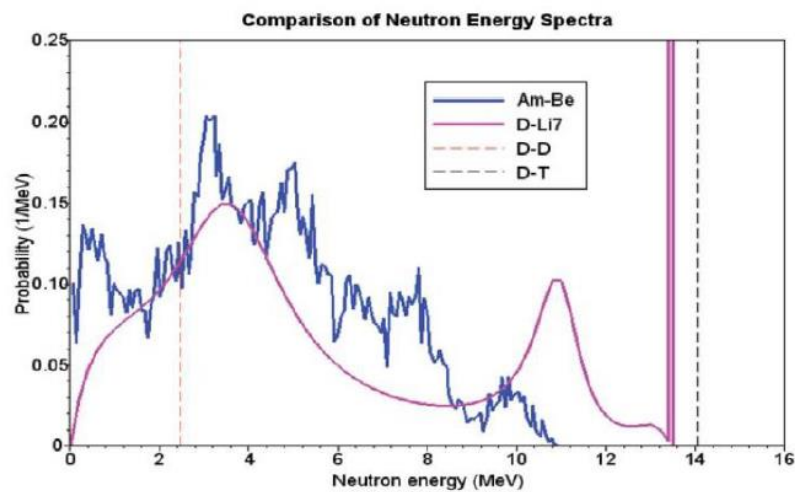


Figure 3-3: Energy spectra of different neutron sources. Adapted from Badruzzaman (2019)

3.2 Neutron Interactions

As the neutrons are generated and bombarded into the formation, they collide with encountered nuclei. This is referred to as scattering. We differentiate between elastic and inelastic scattering. For elastic scattering, there is no loss of kinetic energy in the system. For inelastic collisions there is a loss of kinetic energy used to excite the nucleus with which the neutron collides. For the nucleus to return to the ground state, it emits a gamma ray of a characteristic energy spectrum.

A 4 MeV neutron has an initial velocity of about 2800 cm/ μ s, and at these energy the interactions with the surroundings is a complex conglomeration of highly energy dependent attenuation, scattering and absorption. However, within few microseconds of interactions in the

formation, high energy neutrons have slowed down considerably. As it reaches about 10 eV, usually after a lifetime of 5-50 μs , the neutron is called epithermal. When slowed down even further to about 0.025 eV after about 70-500 μs , it is called a thermal neutron (Hilchie et al., 1969; Rider and Kennedy, 2011). The neutrons are now thought of as diffusing and can both lose and gain small amounts of energy. The diffusion stage lasts until the neutron is terminated by the third and final stage mentioned previously, namely absorption (Ellis and Singer, 2007). Figure 3-4 illustrates the lifecycle of the neutron from generation to capture.

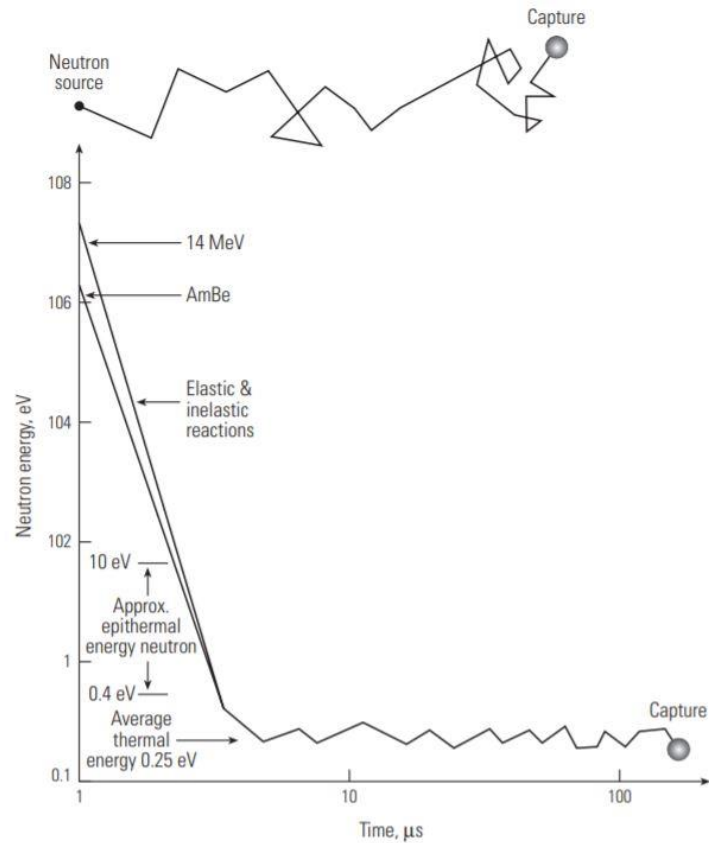


Figure 3-4: Lifecycle of a neutron from generation to capture. Adapted from Ellis and Singer (2007)

Even though interactions occur with all encountered elements, the neutron loses energy depending on the atomic mass of the nucleus it collides with. The more similar the atomic mass is to that of the neutron, the more energy it loses in each collision. As shown in Figure 3-5, hydrogen, which is the lightest substance in the periodic table, will generally slow down the neutron more than heavier atoms such as oxygen and silicon. Hydrogen therefore dominates neutron energy loss (Glover, 2000).

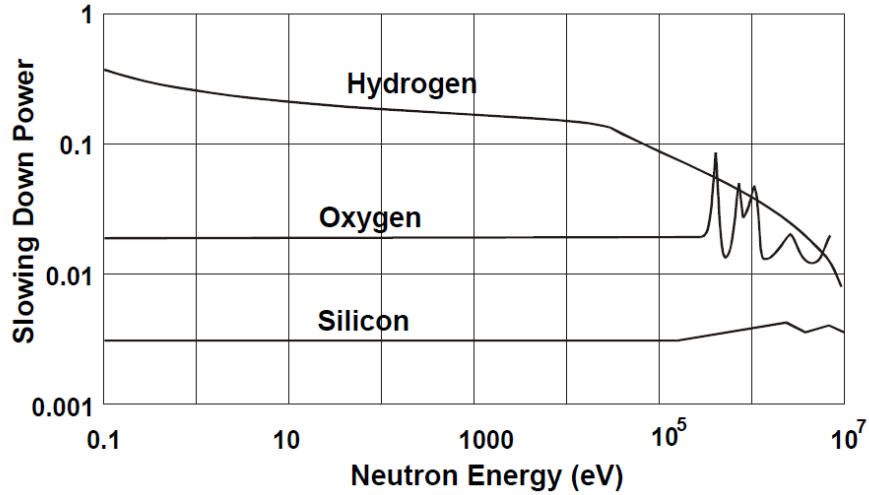


Figure 3-5: Slowing down of neutrons at different energy levels for different elements. Glover (2000)

The ability of a material to interact with the neutrons can be quantified by cross sections, which in fact is the probability of an interaction to occur between a neutron and a target nucleus. This is known as the *microscopic* cross section and is denoted σ . The same element can have a different probability to scatter and to absorb the neutron. It can therefore be differentiated between scattering cross section and absorption cross section (Elmahroug et al., 2013). Scattering cross section can in turn be divided into elastic and inelastic scattering cross section, and the sum of all are referred to as the total cross section (Pynn, 2017).

$$\sigma_t = \sigma_{abs} + \sigma_s = \sigma_{abs} + \sigma_{el} + \sigma_{inel} \quad Eq. 3-5$$

The unit of σ is given in barns, which equals 10^{-24} cm^2 . The unit makes sense if visualizing the area of a target; a larger target area gives a higher probability to hit the target. If we also consider the number of nuclei existing in this area (the atomic density, N), we get the *macroscopic* cross section, called sigma (denoted Σ) (Zhou et al., 2016). While the microscopic cross section can be referred to as the area of a target nucleus, the macroscopic cross section accounts for the area of all nuclei accommodated in the target material and can be referred to as the attenuation coefficient:

$$\Sigma = \sigma * N = \sigma * \frac{\rho * N_A}{M} \quad Eq. 3-6$$

N	Atomic number density [atoms/cm ³]
ρ	Density [g/cm ³]
N_A	Avogadro's number, $6.022 * 10^{23}$ atoms/mole
M	Molecular mass [g/mole]
Σ	Macroscopic cross section [cm ⁻¹]
σ	Microscopic cross section [barns, 10^{-24} cm^2]

It can be observed from Table 3-2 that hydrogen has significant scattering cross section but will not dominate neutron absorption. Hence oftentimes one can say that attenuation of neutrons is proportional to hydrogen content. This is further discussed in section 5.2. Chlorine and especially boron, on the other hand, have large absorption cross section. It is important to note that values for the cross sections vary since neutron interaction is an energy dependent process. The values below are for thermal neutrons, i.e. neutrons of 0.025 eV or 2200 m/s velocity.

Table 3-2: Cross sections of some elements in unit barns. Based on Munter (2017)

Element	σ_s	σ_{abs}
H	81.9	0.334
B ¹⁰	3.14	3835
O	4.23	0.0001
Cl ³⁵	16.8	33.5
Fe ⁵⁶	12.4	2.59

When a neutron is absorbed by a nucleus, the nucleus emits a gamma ray (Figure 3-6) (Eq. 3-6, Eq. 3-7) in a similar fashion as for inelastic scattering.



Following the large absorption cross section of chlorine, capture gamma rays suggests the presence of saline formation water and can be used to calculate water saturation of the formation.

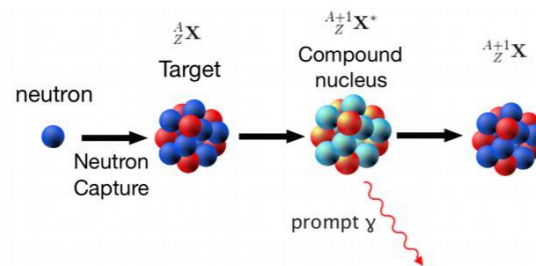


Figure 3-6: The target nucleus releases a gamma ray upon absorption (Das, 2017)

3.3 Energy Dependence of Neutron Cross Sections

Neutron interaction with atoms is a short-range process, thus slow neutrons generally have larger probability to interact with target nucleus as they stay close for a longer time. Consequently, neutron cross section generally increases with lower energy. Energy dependent cross sections are available in National Nuclear Data Center databases, and Figure 3-7 shows this energy dependence exemplified by plutonium-239 (NNDC, 2011).

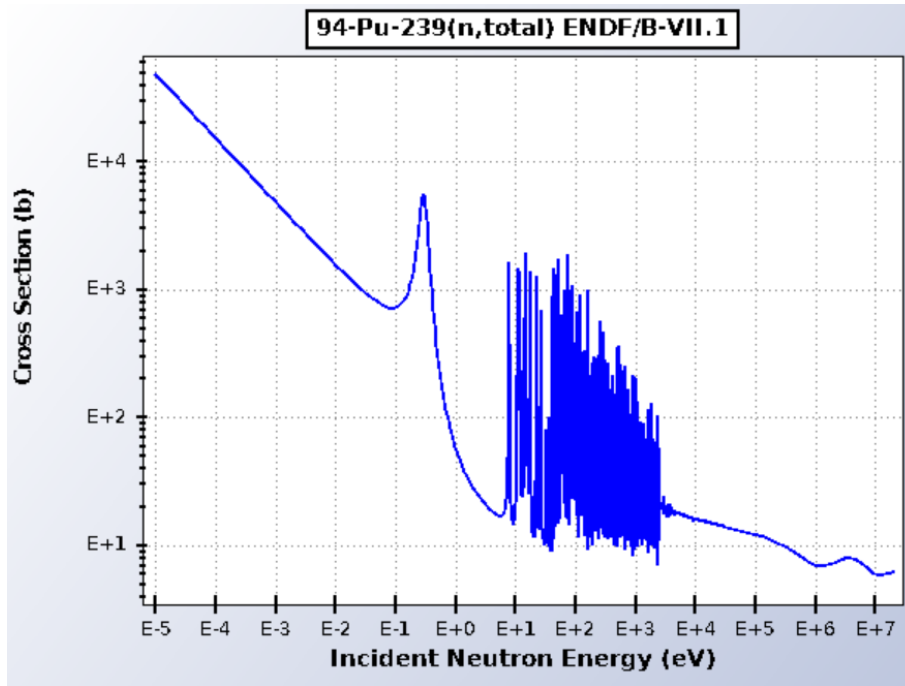


Figure 3-7: Energy dependence of (total) neutron cross section. Based on NNDC (2011)

At very high energy, called the fast region, the cross section generally increases. At higher energy there can be observed some distinct oscillations in cross section values by order of magnitudes. Their origin is beyond the scope of this thesis, but are called resonance peaks and are related to sharp peaks in absorption probability when the energy of the neutron is the same as a resonance level in the encountered nucleus. Not all elements, particularly light elements such as hydrogen, have a noticeable resonance region as they are more abundant the heavier the element (Sowerby and Forrest, 2017). In the low energy range, the total cross section increases inversely proportional to the velocity of the neutron and it is often referred to as the “1/v” region.

3.4 Hydrogen Index

The hydrogen index is a well-known property and it is a measure of the hydrogen content of the formation, or “the density of hydrogen relative to that of water” (Schlumberger, 2019a). It can be computed by the following equations:

$$HI = \frac{(C_H)_{vol}}{(C_H)_{vol,H_2O}} \quad Eq. 3-9$$

$$(C_H)_{vol} = (C_H)_{mass} * \rho \quad Eq. 3-10$$

$$(C_H)_{mass} = \frac{\text{mass of hydrogen in compound}}{\text{molecuar mass of compound}} \quad Eq. 3-11$$

where C_H is the concentration of hydrogen, ρ is the bulk density of encountered compound. For example, for water (H_2O), $(C_H)_{mass}$ would be $\frac{2*1}{2*1+16} = \frac{1}{9}$.

The tool itself is calibrated in limestone, hence the HI is equivalent to the porosity in a water saturated limestone. For other rocks it must be corrected using available charts. This means that HI=1 is equivalent to a pure limestone with 100% porosity filled with water (Glover, 2000).

3.5 Effects on Neutron Logging

The assumption that all observed hydrogen and chlorine represents formation water is not always true; however, by making this assumption and correct for possible other scenarios, we are able to obtain good measurements. This section discusses three effects which must be accounted for.

3.5.1 The Hydrocarbon Effect

Assuming that all pore space in the formation contains water, we could say that all hydrogen detected on the neutron log represents this water. However, the obvious goal in the oil and gas industry is to find hydrocarbons which also contains hydrogen and occupies pore space. Oil has similar HI as water, as the difference in hydrogen content is balanced by the difference in density. Gases, however, have very low density. Thus, natural gas contains much less hydrogen atoms per unit volume and the measured porosity will be underestimated. This must be corrected for and it is known as the hydrocarbon effect (Glover, 2000).

3.5.2 The Shale Effect

Shales have high hydrogen content due to bound water in the clay. However, the porosity of shales is very low, and this must be corrected for on the neutron porosity logs. As a rule of thumb, this effect must be corrected for when the volume of shale is above 5% (Johnson and Pile, 2006). This is called the shale effect and was demonstrated by Burt et al. (2018), who identified gas where a traditional neutron log would suggest oil.

3.5.3 The Chlorine Effect

As chlorine has significant capture cross section, all of its occurrence in a well must be accounted for. Not only does chlorine occur naturally in formation brine, but it is also often found dissolved in drilling mud and mud filtrate (Glover, 2000). This effect, the chlorine effect, must be corrected for as it will yield overestimated neutron porosity.

3.6 Neutron Detection and Tools

Neutron detectors are potentially quite different in terms of what they measure and their arrangements. The tools can be arranged both for logging while drilling (LWD) and run on wireline,

and measure either the gamma rays emitted from scattering or the epithermal and thermal neutrons themselves.

Neutron detectors detect thermal or epithermal neutrons. The common denominator is that they can only measure neutrons of low energy, hence some attenuation must have occurred before detection. It is only the small fraction of low-energy neutrons that ultimately end up near the detector which are counted. The tool itself traditionally contains an amount of Helium-3, which has large capture cross section and therefore absorbs the low energy neutrons. The chemical reaction releases a small electrical pulse which is counted (Rider and Kennedy, 2011).

To isolate the epithermal neutrons, the principle of shielding is used. The detectors are covered with a strong neutron absorber to capture thermal neutrons and thereby only allow the epithermal neutrons to reach the sensor. Like discussed, neutron attenuation is proportional to hydrogen content, while absorption is dominated by mainly chlorine among the naturally occurring elements in and around the wellbore. As epithermal neutrons are not absorbed, detecting these is useful because it will isolate the hydrogen response and make corrections for the chlorine effect less necessary. On the contrary, epithermal detectors have lower count rates than thermal detectors and hence receive less data (Rider and Kennedy, 2011).

The neutron logging tools can be sensitive to borehole effects such as fluids in the wellbore (mud, brine etc.), hole size, casing steel and materials behind casing such as cement (Hilchie et al., 1969). To account for this, there can be applied two detectors positioned near and far from the source, typically about 30 and 60 cm. The ratio of the near and far detector is used to correct the response for borehole effects, and these types of logging tools are usually referred to as

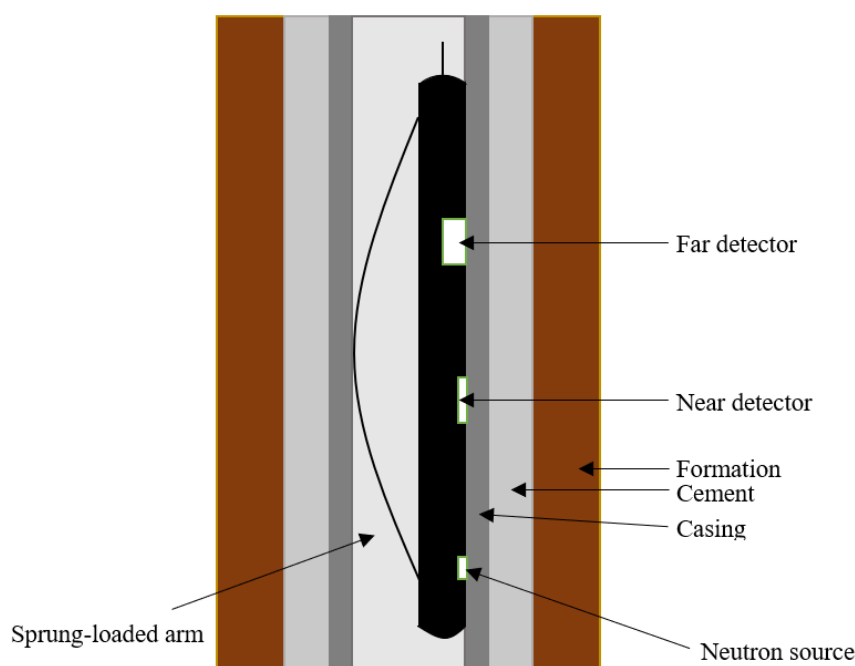


Figure 3-8: Neutron tool in cased hole. Based on Glover (2000)

compensated neutron logging (CNL) tools (Rider and Kennedy, 2011). The source and detector can also be pressed against the sidewall, eliminating the wellbore fluids from the neutron path (Figure 3-8). This is limited to wireline applications (SPE-International, 2015b).

A tool equipped with a PNG and one or more gamma ray detectors/counters is called Pulsed Neutron Logging (PNL) tools. The principle is to detect either inelastic or capture gamma rays. An example of this is the Thermal Decay Tool (TDT). It counts the captured gamma rays with a scintillator, but rather than relating this to hydrogen index and porosity, it is designed to detect the capture cross section of logged material. By in turn relating this to chlorine content and thereby formation brine, it can be used to estimate the water saturation of the formation, S_w . More recent TDT tools utilize two detectors, one near and one far, to give more accurate information about the formation (Darling, 2005).

The tools themselves vary in size according to the application, but can be down to 1 11/16 in. (Dewan et al., 1973; Glover, 2000). Exemplified by Schlumberger's Pulsar tool, it can be run in minimum and maximum casing size of 2 3/8 in. and 9 5/8 in. It is 18.3 ft. long and is rated to temperatures of 175°C and pressure of 15 000 psi (Schlumberger, 2018).

3.7 Neutron Attenuation

The energy of a neutron traveling through a medium can be estimated as (Ellis and Singer, 2007):

$$E(x) = E_0 * e^{-\Sigma_t * x} \quad \text{Eq. 3-12}$$

where Σ_t is the total capture cross section of penetrated material, E_0 is the initial energy of beam, and E describes remaining neutrons as function of distance x in cm.

The calculation for macroscopic cross section, Σ_t , is given in Eq. 3-6 as the probability of an interaction with an atom to happen (σ_t) multiplied by the number of atoms per unit volume. For compounds, we must take into account the number of atoms from the k number of individual elements and sum up thereafter (Holbert, 2014; McAllister, 2016).

$$N_i = \frac{\rho * N_A}{M} * n_i \quad \text{Eq. 3-13}$$

$$\Sigma_i = N_i * \sigma_{t,i} \quad \text{Eq. 3-14}$$

$$\Sigma_t = \sum_{i=1}^k \Sigma_i \quad \text{Eq. 3-15}$$

N_i	Atomic number density of element i [atoms/cm ³]
ρ	Density of compound [g/cm ³]
n_i	Number of atoms of element i in compound
N_A	Avogadro's number, $6.022 * 10^{23}$ [atoms/mole]
M	Molecular mass [g/mole]
Σ	Macroscopic cross section [cm ⁻¹]
σ	Microscopic cross section [barns, 10^{-24} cm ²]

3.8 Applications of Neutron Log

3.8.1 Traditional Application

The traditional use of neutron log is to estimate formation porosity and water saturation. This is because hydrogen and chlorine are the main neutron affecting elements naturally present in the near-wellbore area. Like previously mentioned, it is assumed that most hydrogen in the subsurface comes from water, which exists in pores or as bound water. Likewise, chlorine is dominating the thermal neutron capture. Consequently, the response of the neutron tool can be treated as a measurement of water in the formation (S_w) and be directly correlated to porosity with some corrections (Rider and Kennedy, 2011).

It can also be used in combination with other logs, particularly density log, and they are often presented in the same track when evaluating well logs. From the separation between the logs, one can identify fluid-bearing formation and distinguish between some lithologies. If there is a high

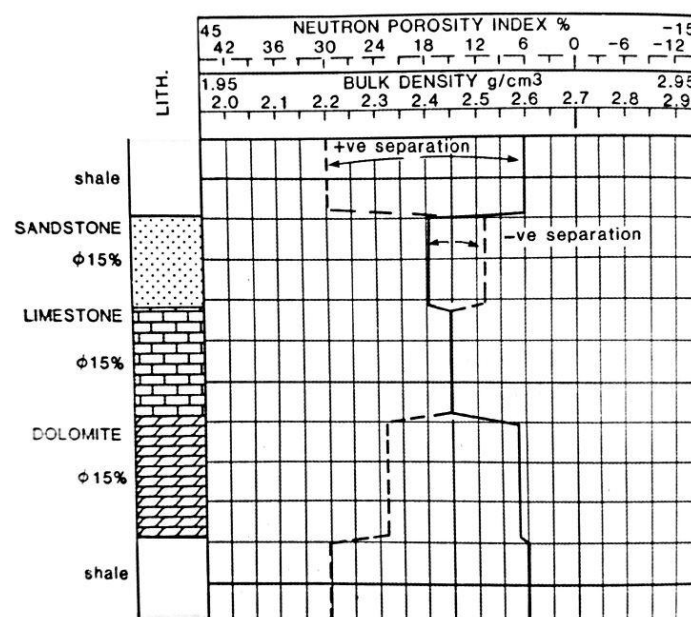


Figure 3-9: Neutron log response to different formations. Rider and Kennedy (2011)

neutron porosity and high density measurement, the spacing is called positive (Figure 3-9). The opposite is called negative separation and the magnitude of negative separation is an excellent way of distinguishing oil from gas-zones (Rider and Kennedy, 2011).

3.8.2 Spectroscopy

As previously mentioned, the neutrons may collide and excite encountered atoms which in turn releases a gamma ray of a certain energy spectra. This is the case for both inelastic collisions and thermal neutron capture. By measuring these energy spectra, we can retrieve information on the elemental composition of the encountered media.

Elements such as C, O, Si, Ca, Fe and S have significant *inelastic* cross section. The ratio between the content of C and O is a useful quantity, simply known as the C/O ratio. It is applicable in fields with low or unknown salinity (chlorine), where a PNL log would be less useful in estimating the water saturation. As water does not contain carbon and oil does not contain oxygen, the C/O ratio can effectively determine water and oil saturations regardless of salinity.

Similarly, Figure 3-10 illustrates how the concentrations of different elements such as H, Cl, S, Fe, Ca and Si can be determined from the energy of released *capture* gamma-rays. By knowing which elements are present in different rock, this measurement can aid in lithology assessment (Johnson and Pile, 2006).

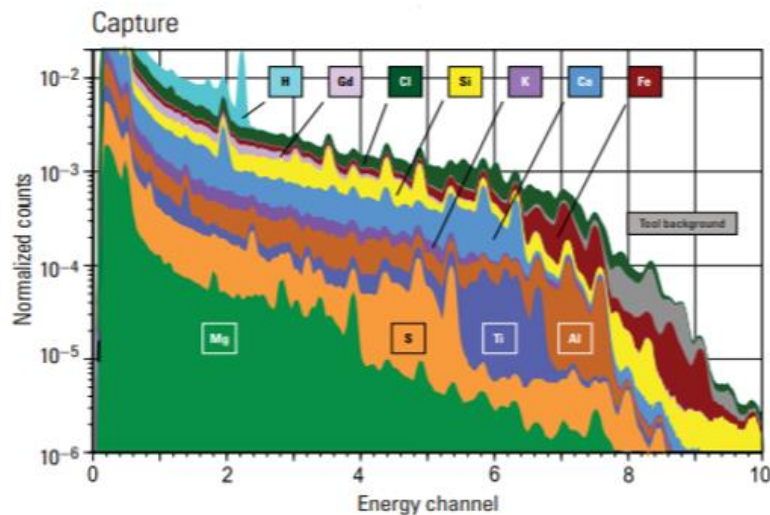


Figure 3-10: Spectral stripping of the capture gamma rays shows individual elemental contributions (Schlumberger, 2018)

3.8.3 Developments in Applications of the Neutron Log

Due to the insufficient supply of helium-3 for neutron detectors and restrictions to using chemical sources, alternatives are sought. Materials used in recent tools include cerium-doped lanthanum bromide (LaBr₃:Ce) scintillators (Grover, 2017) and lithium-6 (Li-6) glass detectors (Nikitin et al., 2011).

New tools also have the ability to, in addition to the traditional uses, perform subtler lithological analysis such as distinguishing tight formations from gas-filled formation, and mineral-based formation evaluation with the mentioned spectroscopy. Furthermore, detection of water flow/entry and evaluation of gravel pack are applications possible in the late neutron tools, in addition to general improvements such as larger detectors for higher count rates and higher temperature resistance (Schlumberger, 2019c; Simpson et al., 1998). Another feature is that modern tools can run in different modes including sigma-, inelastic capture-, C/O- and TOC-mode depending on what is the objective to measure (Schlumberger, 2018).

Zhou et al. (2018) presented a tool able to self-compensate for borehole effects by considering ratios between measured near and far detector responses. They used the principle that near detectors are sensitive to inelastic scattering gamma rays of high-energy neutrons, which will be different from far detectors sensitive to capture gamma rays. By considering two different time gates (time since pulse), ratios were calculated for the burst period (burst ratio) and some time after burst (capture ratio). The formation response corrected for borehole conditions was then estimated based on the balance of the near/far ratios at different times.

3.9 Advantages and Possible Limitations of Neutron Logging Technology for Cement

Evaluation

Based on this chapter, the main challenges and possible advantages neutron logging could have over conventional techniques are listed below with cement evaluation in mind. Some of the limitations have solutions presented earlier in this chapter.

Table 3-3: Current advantages and limitations of applying neutron logging technology for cement evaluation. Based on Kahlifeh (2017)

<i>Advantages</i>	<i>Current Limitations</i>
<ul style="list-style-type: none"> • Commercial technology already exists. • PNL is already being used in cased hole environments, indicating its potential to evaluate what is behind casing. • Small diameter tools. • Can verify presence of certain individual elements by spectroscopy. • PNL can be switched on and off. 	<ul style="list-style-type: none"> • Borehole conditions can affect accuracy, including wellbore fluids, hole size, casing steel and annulus fluid behind casing. • Current neutron logging data may have gone through processing and be corrected for borehole effects, thus potentially eliminating the response we are interested in being the cement. • The use of americium as neutron source has HSE concerns.

4 MATERIALS

For the neutrons to be able to evaluate cement, it must pass through several media (Figure 4-1). Assuming the tool is pressed against the casing, neutrons must first travel through the casing, which was shown to give problems for X-ray logging technique. Secondly is the cement itself. For full cement evaluation, it is assumed that the neutrons must travel from the source to the cement-formation interface and back. This chapter will study these different media and how they potentially could affect the neutrons. If the cement job has been unsuccessful, it could have channels which is assessed later in this chapter and in the analysis.

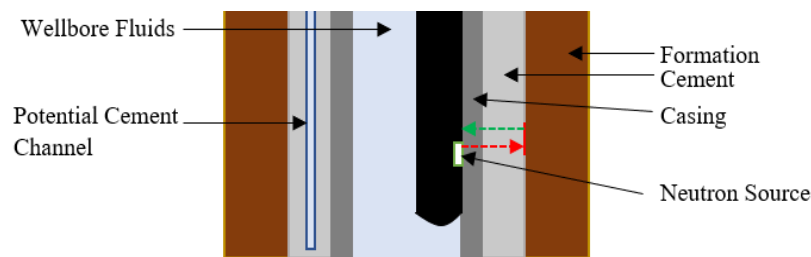


Figure 4-1: The neutron must reach the cement/formation interface and return

4.1 Casing

When drilling a well, it is important to prevent hole collapse. Therefore, steel pipes called casings are installed inside the wellbore. This goes on in an alternating and telescoping fashion; drill a section, install casing inside, drill a smaller diameter hole inside previous casing, place a smaller casing inside (Figure 4-2). Casings differ in thickness, weight and composition and are designed depending on what pressures, temperatures and other environmental conditions the casings must

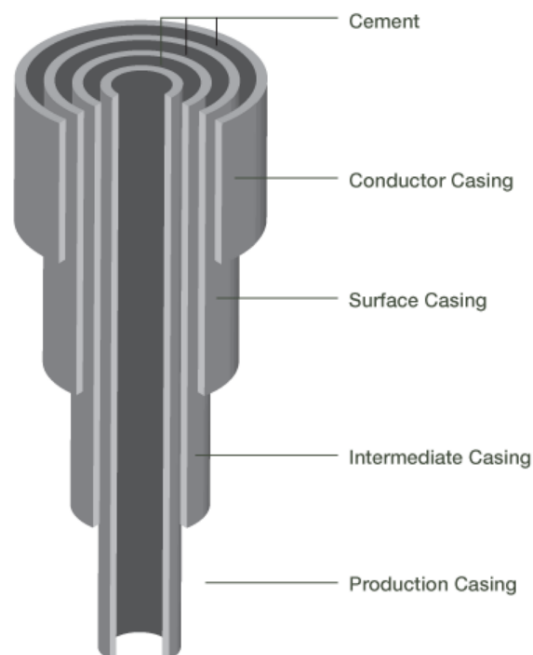


Figure 4-2: Wellbore construction. Adapted from Encana (2016)

withstand. The purpose of the casing also differs depending on where in the well it is installed, and from this it gets its name. From shallow to deep setting depth is the conductor, surface casing, intermediate casing, production casing and liner (Azar and Samuel, 2007).

Greene and Thomas (1969) studied the attenuation of 14 MeV neutrons through steel. They found that a 17 cm thick steel transmitted about 25% of the neutrons. Typical casing wall thicknesses do not exceed 2.2 cm (Gabolde and Nguyen, 1999), hence transmission can be expected to be much higher for casings.

A 9 5/8 in., L-80 grade casing is selected for further analysis in this work (Table 4-1). The composition of L-80 casing for further analysis is given in Table 4-2. As can be seen, iron is the major constituent of the casing.

Table 4-1: Casing specifications. Based on Gabolde and Nguyen (2006)

<i>Grade</i>	<i>Nominal Weight [lb/ft]</i>	<i>Outside Diameter [in. (mm)]</i>	<i>Thickness [in. (mm)]</i>
L-80	43.50	9 5/8 (244.48)	0.435 (11.05)

Table 4-2: Composition of L-80 casing. Adapted from Continental Alloys & Services (2019)

<i>Element</i>	<i>C</i>	<i>Mn</i>	<i>Ni</i>	<i>Cu</i>	<i>P</i>	<i>S</i>	<i>Si</i>	<i>Fe</i>
%	0.430	1.90	0.250	0.350	0.030	0.030	0.450	96.56

4.2 Cement

The scope of this section is to give background theory on cement, cementing operations and chemistry of the cement curing process for further understanding of how neutrons interact with this material.

4.2.1 Cementing Operations

Primary cementing is the process of placing a volume of cement in the annulus between the casing and formation after drilling the wellbore and running the casing itself. Reasons for cementing are many depending on the casing type, but the first and foremost goal of any cementing operation is to achieve zonal isolation in the well (Guillot and Nelson, 2006). The purpose of primary cement in this case is therefore to create a hydraulic seal to prevent cross-flow of formation fluids between formations or to surface (Figure 4-3).

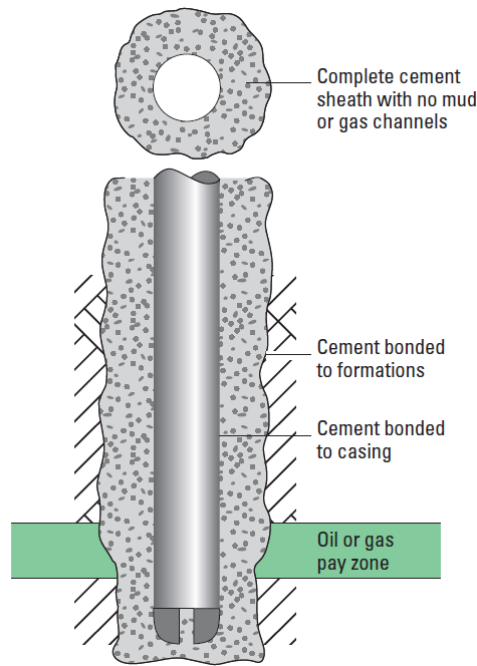


Figure 4-3: Requirements for a hydraulically sealed cement sheath. Adapted from Guillot and Nelson (2006)

In addition to primary cementing, cementing operations can also be necessary some time after the primary cementing stage is completed. These are referred to as remedial or secondary cementing and gathers the following main concepts (Guillot and Nelson, 2006):

- Squeeze cementing; local placement of cement under high hydraulic pressure to ensure intact cement sheet. Can be to fill voids, micro-annuli, repair leaking casing or to close perforations.
- Plug cementing; place a volume of cement inside the well. Can be for example to prepare well for abandonment, to plug old wellbore in preparation for a sidetrack or directional drilling, or to stop losses to a circulation zone.

4.2.2 Portland Cement

Cement used in the petroleum industry differs somewhat from traditional construction industry cement. In construction, cement is a constituent of concrete when mixed with water and sand/gravel. In the petroleum industry properties such as density, viscosity, compressional strength and curing time are of fundamental interest and are controlled by different additives in the cement slurry along with water (Hossain, 2016).

First manufactured by Joseph Aspdin in 1824, the Portland cement was a mixture of clay and limestone. He thought the blend reminded him of a rock he had seen in England, at the Isle of Portland, and thereby gave it its name. With the purpose of shutting off water, Portland cement was first used in the petroleum industry in 1903. Today it remains the most widely used type of

cement and is the one used when investigating the interactions between cement and neutrons in this thesis (Hossain, 2016).

The recipe of Portland cement remains more or less the same as from 1824, with the main components being limestone and clay or shale. The components are grounded and mixed to the desired composition, before the mixture undergoes a high temperature treatment of up to 3000°F. This burning process creates a material called clinker. Many steps along the way affects the final properties of the cement, including the cooling process. For high compressive strength it is desirable that the clinker is cooled slowly to allow crystallization. Finally, the cement is ground resulting in a fine cement powder before storing (Azar and Samuel, 2007; Schlumberger, 1984).

The American Petroleum Institute (API) has divided Portland cement into classes depending on what depth they are placed in a well and thereby what pressures and temperatures they will be exposed to during their lifetime. Currently there are eight classes, named from A through H. Based on the raw material, the composition of Portland clinker is mostly made up of the oxides CaO, SiO₂, Al₂O₃ and Fe₂O₃ shown in Table 4-3 (Guillot and Nelson, 2006). Note the conventional cement notation.

Table 4-3: Mineralogical composition of a classic Portland cement clinker. Based on Guillot and Nelson (2006)

Oxide	Cement Notation	Name	Concentration (%)
Ca_3SiO_5	C ₃ S	Alite	55-65
Ca_2SiO_4	C ₂ S	Belite	15-25
$Ca_3Al_2O_6$	C ₃ A	Aluminate	8-14
$Ca_4Al_2Fe_2O_{10}$	C ₄ AF	Calcium Aluminoferrite	8-12

An example of a Portland class G cement clinker recipe is given in Table 4-4 based on Guillot and Nelson (2006); Guner et al. (2016).

Table 4-4: Sample composition of class G cement

Oxide	Concentration (%)
CaO	65
SiO ₂	22
Al ₂ O ₃	4
Fe ₂ O ₃	4
Other (MgO, K ₂ O, SO ₃ ...)	< 5%

4.2.3 Cement Placement

After drilling of the well, the casing is going to be placed and cemented. There are many ways of doing this depending on the casing type, casing diameters and formation characteristics. The common way to primary cement, is a single-stage process where cement is pumped down the casing (alternatively through drillpipe) and up the annulus.

For a successful cementing operation, cuttings and residual mud filtrate on the borehole wall called mudcake must be removed from the well. To do so, mud is circulated throughout the well known as conditioning. Conditioning also allows displacement of drilling fluid to a lighter fluid in the well which in turn will be easier to displace during the cementing operation (Lavrov and Torsæter, 2016). If mud has been static for some period it will start gelling, which makes restarting circulation more difficult. With the casing in place, the annular flow area is much smaller than with the drillpipe in place, resulting in a higher flow velocity. The increased velocity decreases the gel-strength of the mud, helps transport cuttings and remove mudcake. Additional pre-flush fluids or mechanical devices can be used if removal of mudcake is difficult or the mud has developed high gel-strength (Azar and Samuel, 2007; Guillot and Nelson, 2006).

A sequence of fluids is prepared and pumped down the casing in sequence, as illustrated in Figure 4-4. Usually such a sequence consists of the following:

- Wash; helps removing mud and mudcake and ensures good bonding of cement to the casing and formation. Can be fresh water, however chemicals are normally added for adequate dispersal and compatibility for bonding (Azar and Samuel, 2007; Chilingarian and Vorabutr, 1983).
- Spacer; as the name suggests, separates drilling fluids from the following cement to prevent contamination. Can be pumped both before and after the cement, depending on the cementing procedure (Guillot and Nelson, 2006). It has very specific density (should be between that of the mud and lead cement) and viscosity, and additives are used to carefully control these properties (Schlumberger, 2019d).
- Lead cement; the first volume of cement entering the annulus and will be located closest to the fluids that are present in annulus prior to cementing. It is a relatively cheap and weak cement because even though spacer is pumped in front there could still be some intermixing with displaced fluid, which will affect the cement properties (Guillot and Nelson, 2006).
- Tail cement; the bottom part of the cement column. Is placed deeper in the wellbore and must be of higher strength to handle stress, temperature and pressure to ensure the integrity of the casing shoe (SPE-International, 2013)
- Displacement fluid; could be water or mud. Pumped with the purpose of displacing the cement out of the casing into the annulus (Guillot and Nelson, 2006).

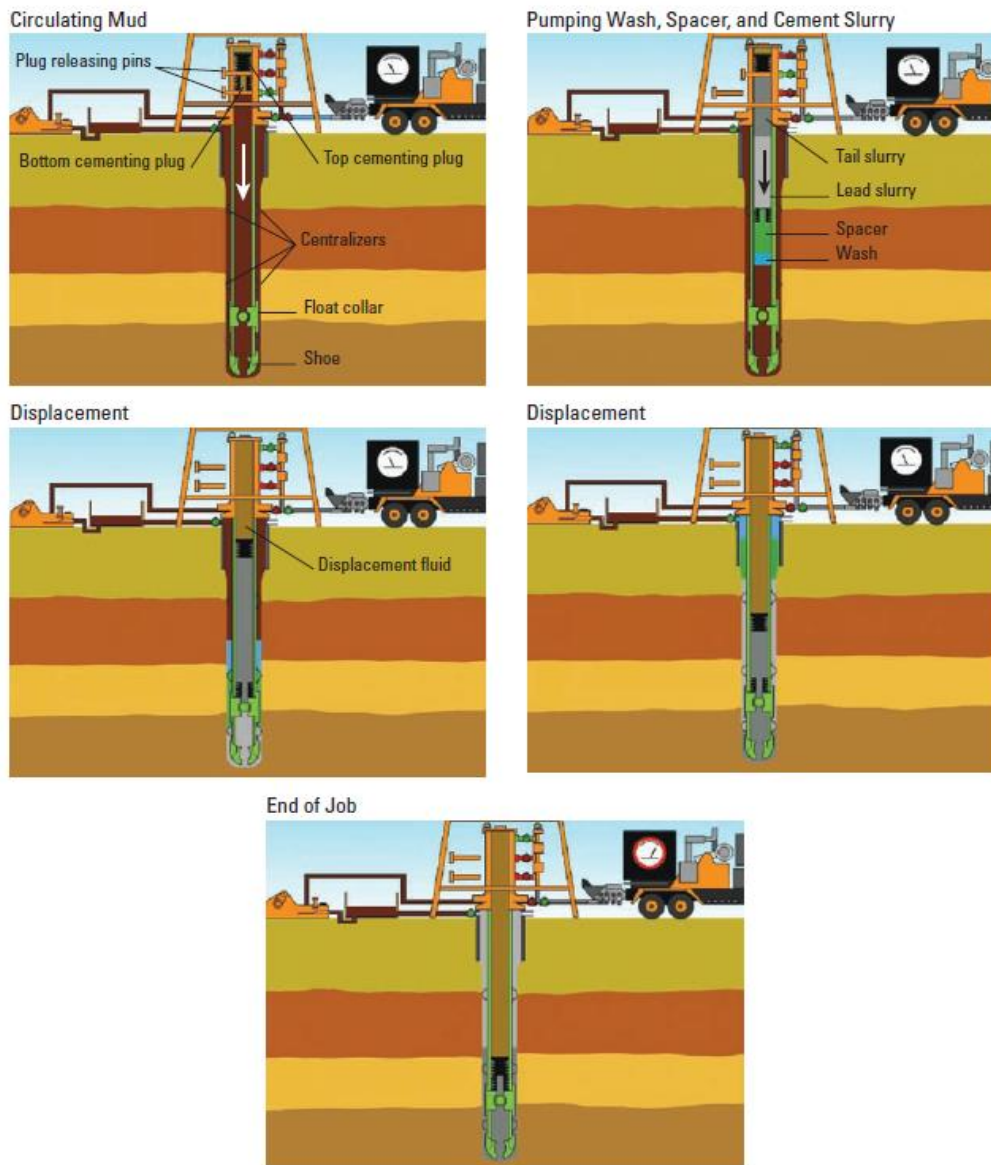


Figure 4-4: Steps in a typical primary cementing job. Adapted from Guillot and Nelson (2006)

In front of the sequence of fluids a hollow plug (bottom plug) containing a disk is pumped. It is pushed in front of the cement as the cement train is displaced down the pipe, serving as both a wiper of the casing inside as well as displacing the mud in front of the cement. The plug lands at the bottom of the well, and pressure increases on the disk which eventually ruptures. At the back of the train is another plug which displaces the cement up the annulus. When the cement is successfully displaced, the top plug will land on the bottom plug causing a pressure increase which can be measured at surface. This is known as “bumping the plug” and is an indication to the operator of a successful displacement (Azar and Samuel, 2007).

Cement displacement is a crucial part of any cementing operation. Some factors to ensure good displacement jobs are (McLean et al., 1967):

- Centered casing; if casing is not centered in the well, annular velocities and thus flow regimes will vary around the circumference of the casing. Turbulent flow gives best

displacement. Difference in displacement velocities will affect mud displacement resulting in potential mud channels. This is particularly challenging in horizontal/highly deviated wells. Eccentric casing should be mitigated using centralizers.

- Separation of mud and cement; isolate mud and cement by mechanical plugs or spacer. Also maintain a 2 ppg density contrast to avoid intermixing of fluids.
- Pipe movement; by rotating or reciprocating the casing while displacing cement, occurrence of mud channels can be mitigated.

The potential consequences of a failed displacement job are illustrated in Figure 4-5, and make the background for the analysis in this thesis. Failure modes that can cause occurrence of micro-annuli include cement shrinkage during hydration, cyclic temperature and pressure effects and changes in formation stress (Bois et al., 2011).

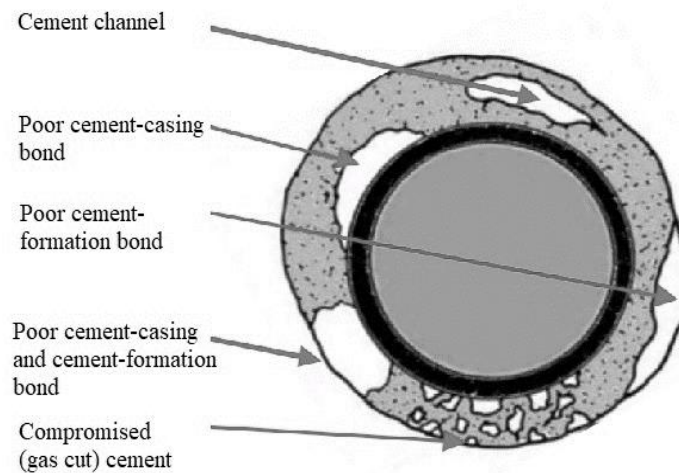
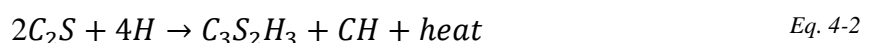
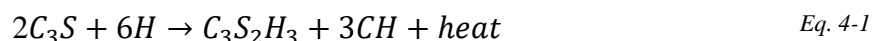


Figure 4-5: Cement defects. Based on Cameron (2013)

4.2.4 Cement Hydration and Composition

When logging the cement, it has gone through mixing with water, been placed and cured. It is the properties of the cured cement we are logging, and hence it is appropriate to understand the chemistry of the complex curing process of cement.

Cement hydration is a process which is not fully understood, but in general it is a reaction between oxides and water which forms hydrates. The C_2S reaction (Eq. 4-2) generates much of the heat which is detectable on temperature logs. The C_3S reaction (Eq. 4-1) is component responsible for early strength development of hydrate cement. When mixed with water, the exothermic reactions can be summed up as follows (Mason and Lea, 2018):



To summarize it is observed that the addition of water to the cement causes formation of calcium silicate hydrate (or C-S-H in cementing notation, equivalent to $\text{CaO} - \text{SiO}_2 - \text{H}_2\text{O}$), and calcium hydroxide. The C-S-H phase will form as a coating around the cement grains, while the latter will develop in void space or pores (Lavrov and Torsæter, 2016). The hydration process is highly complex and is dependent on several factors such as abundance of the different components, how the clinker was prepared, temperature and mixing water ratio and content. Therefore the notation $\text{C}_3\text{S}_2\text{H}_3$ is not exact. Gabrovšek et al. (2006) reported an approximate formula of $\text{C}_{1.7}\text{S}_1\text{H}_{1.5}$. Furthermore, the time of hydration is very different for the oxides both in terms of when and how fast it occurs (Figure 4-6). According to Guillot and Nelson (2006) the C-S-H phase and calcium hydroxide, known as portlandite, accounts for about 65% and 15-20% of hydrated cement respectively.

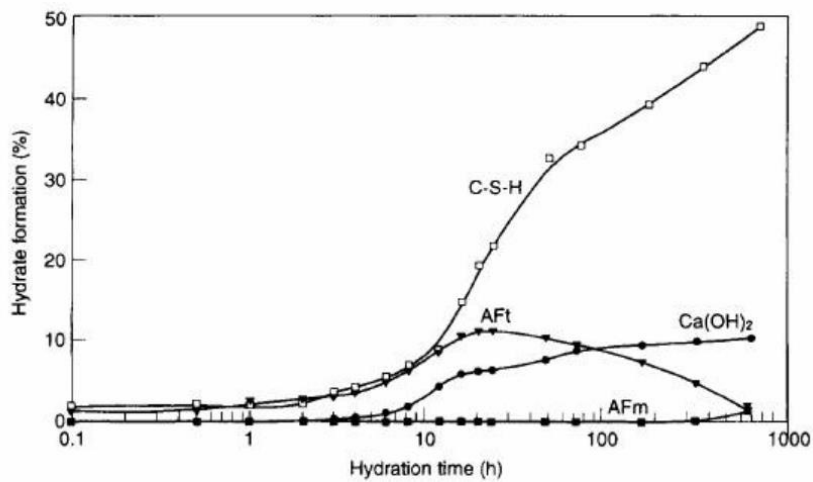


Figure 4-6: Hydration of cement components. Adapted from Hewlett and Lea (2003)

The hydration of C_3A can be controlled by addition of gypsum, however assuming no gypsum is added the C_3A will eventually form an aluminoferrite monosulphate (AFm) phase called hydrogarnet (Guillot and Nelson, 2006). A similar reaction will happen to C_4AF to produce aluminoferrite trisulfate (AFt). However, as the hydration progresses the AFt content decreases and may become totally removed as the AFt phase converts to an AFm phase (Hewlett and Lea, 2003). For simplicity, based on Table 4-4 it is therefore assumed that hydrogarnet makes up the remaining 15% of fully hydrated cement, and that there are equal amounts of aluminum and iron. This gives the final recipe in Table 4-5.

Table 4-5: Recipe for cured Portland class G cement

Component	$1.7\text{CaO} \cdot \text{SiO}_2 \cdot 1.5\text{H}_2\text{O}$	$\text{Ca}(\text{OH})_2$	$\text{Ca}_3[\text{Al}(\text{OH})_6]_2$	$\text{Ca}_3[\text{Fe}(\text{OH})_6]_2$	Sum
%	65	20	7.5	7.5	100
Name	C-S-H gel	Calcium Hydroxide	Hydrogarnet (AFm phase)		

The hydration process of alite has been studied by FitzGerald et al. (1998). By exploiting that 99% of the hydrogen in a cement slurry originates from the mixing water, they were able to monitor how much water was still liquid in the cement. This is known as the Free Water Index (FWI). The water content in hydrated cement is described as bound water, similar to that of clays which is known to affect neutrons (section 3.5.2). From this it can be argued that the water mixed with cement must be accounted for when considering neutron detection effects because the hydrogen atoms remain in the cement as hydrates and hydroxides.

4.2.5 Foamed Cement

Foamed cement is a type of cement characterized by ultra-low density, i.e. less than 10 ppg or 1.2 g/cm³. These types of cements are becoming more frequently used, primarily in formations susceptible to fracturing which would not handle conventional density cements. By use of foamed cement, potential losses of wellbore fluids to the formation are mitigated. The low density is achieved by injecting a standard cement slurry with a gas, commonly nitrogen (Harness and Frank, 1996). Foamed cement can be characterized by its foam quality (FQ), which is given by (Guillot and Nelson, 2006; Harness and Frank, 1996):

$$FQ = \frac{V_{gas}}{V_{foam}} = 1 - \frac{\rho_{cement,final}}{\rho_{cement,base}} \quad Eq. 4-3$$

Where V_{gas} is the volume of gas and V_{foam} is the total volume of the foamed cement. Logically, $FQ = 0$ indicates neat cement while $FQ = 1$ is indicative of pure gas. The foam quality can be related to the hydrogen index of neutron logs linearly by (Harness and Frank, 1996):

$$HI_{final} = HI_{initial} - HI_{initial} * FQ \quad Eq. 4-4$$

Based on Eq. 3-4 it can be understood that hydrogen index decreases with foam quality. Thus, a neat cement of $HI = 1$ which is nitrified until reaching $FQ = 0.4$ will get a final $HI = 0.6$.

Due to the similar response of foamed cement and fluids on the CBL log, Harness and Frank (1996) studied the application of neutron log for foamed cement evaluation. By running a base log before casing and cementing, and a following log afterwards with corrections for borehole effects they were able to distinguish air, foamed cement and fluid behind casing by relating measured hydrogen index to the foamed quality as illustrated in Figure 4-7 and Table 4-6.

Table 4-6: Foam quality of different substances. *Depending on nitrogen amount

Material	FQ
Foamed Cement	30-40%*
Fluid	0%
Air (void)	100%

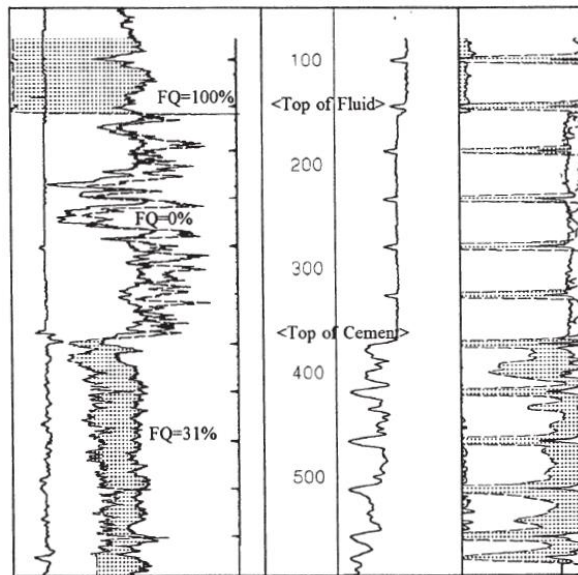


Figure 4-7: Foamed cement, fluid and air distinguished on neutron log (track 1). Adapted from Harness and Frank (1996)

The composition of the foamed cement is assumed the same as for class G cement, but with a foam quality of 40%. This gives the following composition:

Table 4-7: Composition of selected class G cement

Component	$1.7CaO \cdot SiO_2$	$Ca(OH)_2$	$Ca_3[Al(OH)_6]_2$	$Ca_3[Fe(OH)_6]_2$	N_2	Sum
%	39	12	4.5	4.5	40	100
Name	C-S-H gel	Calcium Hydroxide	Hydrogarnet (AFm phase)			

4.3 Oil-Based Mud

This subchapter will discuss properties of oil-based mud found in a well and how it can affect neutrons. It is difficult to give a comprehensive overview of all drilling fluids due to the wide range of possible combinations of additives and chemicals, thus one simple recipe is assumed for analysis.

The two main types of muds are oil-based and water-based. Additionally, freshwater or seawater (brine) can be used which are a subcategory of the water-based muds (Azar and Samuel, 2007). During drilling, fluids are usually circulated down inside the drill string and back up outside. Reasons for circulating fluids in the well are many, some of the most important include (Azar and Samuel, 2007):

- Removal and transport of drilling cuttings to surface.
- Maintain pressure against the formation fluid pressure to avoid inflow.
- Balance pressure against formation rock to stabilize wellbore and avoid collapse or instabilities due to chemical reactions.

Fluid selection and additives must be based on criteria such as what type of well is being drilled, the casing program, environmental considerations, formation type and fluid content. When the fluids are mixed with a clay substance, they are referred to as muds. The typical clay used is bentonite and controls the viscosity of the mud. Typical additives in addition to viscosity modifiers are weighting material, lost circulation material (LCM), emulsifiers etc. Barite is a typical weighting material found in many muds (Guillot and Nelson, 2006).

Often used as a non-inhibitive option to water-based mud (WBM), oil-based mud (OBM) is essentially a mud where oil is the continuous phase. It is normally used in higher temperature wells to reduce friction effects such as torque and drag/stuck pipe, or in wells with anticipated shales which swells upon contact with water-based fluids. Despite oil being the continuous phase, it still contains some water. Normal ratios of oil to water is in the range of 70/30 to 90/10 (SPE-International, 2015a). Of oil types, diesel is most commonly used (Chilingarian and Vorabutr, 1983). Since oil is composed of long chain of hydrocarbons (thereby consisting of hydrogen and carbon) it is fair to assume that OBM will affect the neutron log. Zhou et al. (2016) reported a theoretical sigma for diesel of 23 capture units (c.u.) , which according to Table 4-8 is similar to that of oil and fresh water. The higher salinity solutions are denoted parts per million (ppm). A salinity of 35 000 ppm essentially means 35 000 grams of salt per million grams of solution. Neutron response is expected to take effect by mixing water depending on the water-to-oil ratio and salinity, i.e. the chlorine content.

Table 4-8: Capture cross sections of different liquids. Based on SPE-International (2015c)

<i>Material</i>	Σ (c.u)
<i>Oil</i>	18-22
<i>Fresh Water</i>	22
<i>Diesel</i> (Zhou et al. (2016))	23
<i>Water: 35 000 ppm (sea water)</i>	33-35
<i>Water: 50 000 ppm</i>	35-40
<i>Water: 200 000 ppm</i>	95-100

In the following analysis, it will be defined cases to investigate what effects the presence of channels in cement will have on neutron logs. If there exist channels, it is likely that drilling fluids will be present in these corresponding to an insufficient displacement job. OBM is chosen as the drilling fluid because it is expected to yield less response on the neutron log compared to WBM. Thus, if OBM yields a detectable response it can be expected that WBM also will considering Table 4-8. The following recipe is chosen for OBM based on practical laboratory exercises from PET210

(UiS, 2016), where the mineral oil EDC 95/11 is used as base oil. Additives of small concentration are neglected:

Table 4-9: Composition of selected OBM

<i>OBM</i>		<i>Density [g/cm³]</i>	<i>Wt%</i>
<i>Mineral oil [ml]</i>	206	0.814	0.48
<i>CaCl₂ solution (8 wt%) [ml]</i>	60	1.07	0.185
<i>Barite (BaSO₄) [g]</i>	115	4.48	0.335
<i>Sum</i>			1

Based on the safety data sheet of EDC 95/11, the mineral oil consists of “paraffinic and cyclic hydrocarbons having a carbon number range predominantly of C15-C20” (Total, 2014). As paraffinic hydrocarbons are on the form C_nH_{2n+2} (Carey, 2018), the composition of the mineral oil is assumed to be C₁₅H₃₂. The density of the OBM is 1.19 g/cm³.

4.4 Gas

Gas, as discussed in 3.5.1, is known to influence the neutron log. This is primarily related to when the formation contains gas, thus it is of interest to investigate how much a gas pocket in the cement will affect neutron log response.

The occurrence of gas in cement can have several causes depending the time since cementing operation. Gas influx only a few hours after the cementing operation indicates lost hydrostatic pressure while cementing, while if the influx occurs a day or more later it indicates the presence of a micro-annulus. Influx occurring even later indicates factors such as damaged or permeable cement, or that there existed a mud channel which has lost hydrostatic pressure (Guillot and Nelson, 2006).

Similar to oil, natural gas consists of primarily hydrogen and carbon. The most abundant component of natural gas is methane, CH₄ (80-95%). Moreover, heavier hydrocarbons such as ethane, propane and butane make up a total of 3-10%. Small fractions of nitrogen and carbon dioxide could also be present (Boye, 2009). Based on this, the basic recipe in Table 4-10 is chosen for gas.

Table 4-10: Selected composition of natural gas

<i>Component</i>	CH ₄	C ₂ H ₆	N	CO ₂	Sum
<i>%</i>	90	5	2.5	2.5	100
<i>Name</i>	Methane	Ethane	Nitrogen	Carbon dioxide	

5 ANALYSIS AND RESULTS

To give a comprehensive evaluation of the potential for utilizing neutron log for casing cement evaluation the following list of requirements is defined:

- Tool must produce neutrons of sufficient energy to not be completely attenuated through material defined in previous cases.
- Neutrons must be affected by material it penetrates to leave a recognizable, detectable result.
- As sender and receiver are placed inside the wellbore, signal must have the ability to be backscattered.
- Health, Safety and Environment (HSE); must not present an increased risk to environment or people.
- Tool must be small enough to fit inside smallest expected casing (or potentially tubing).
- Cost; should not be overly expensive compared to alternative approaches. Potential gains of applying this technology must be compared relative to potential losses by not doing so.

The following sections are dedicated to investigating the listed requirements in terms of modeling, analyzing obtained data and relevant literature. Furthermore, the potential of some alternative approaches using neutron log for cement evaluation is presented.

5.1 Neutron Interaction with Different Material

The analysis simulates the response of a neutron traveling through good cement, foamed cement and a cement with a channel. The purpose is to see if the neutron is theoretically able to penetrate the material encountered, and to see if the presence of a channel would give measurable response at the detector. Two cases are simulated where the channel is assumed to compose 10 and 20% of the cement thickness. The channel itself is placed in the center of the cement for simplicity. The channels will be assumed filled with OBM, representing a failed cement displacement job, and natural gas indicating gas migration during or after curing.

Five cases are defined for comparison. The first four are presented here, and the fifth is presented separately:

1. Base case: Neutron travels through a block of 11.05 mm casing and 33.34 mm cement and returns to the detector.
2. Same as case 1, but with foamed cement for direct comparison.
3. Channeled cement filled with oil-based mud. Channel composes 10 and 20% of cement thickness and is placed in the center of the cement.
4. Same as for case 3 but with natural gas filling the channel.

The following assumptions are made:

- Compositions of penetrated material as described in chapter 3 with associated assumptions.
- Standard temperature and pressure (STP), i.e. $T = 0\text{ }^{\circ}\text{C}$, $P = 1\text{ atm}$, and compositions remains the same in downhole conditions. Exception for gas, see section 5.1.5.
- 4.5 MeV neutron initial energy, similar to average energy emitted by Am-Be chemical neutron source. If attenuation is too large, 14.1 MeV is an option representing D-T neutron generator.
- Fully hydrated cement, i.e. FWI = 0.
- Tool is pressed against casing wall, i.e. no stand-off.
- No mudcake.
- Neutrons transmission is given by:

$$\frac{E}{E_0} = 100 * e^{-\Sigma_t * x} \quad [\%] \quad \text{Eq. 5-1}$$

This implies a constant Σ_t between each step in the simulation and no absorption occurs.

- Neutrons travel shortest path from source to cement/formation interface to detector, i.e. no attention given to scattering or scattering angles. This is further assessed in section 5.2.

The following dimensions are assumed:

- 12 ¼ in. wellbore.
- 9 5/8 in. outside diameter (OD) casing.
- Casing thickness of 11.05 mm (Gabolde and Nguyen, 1999).

$$t_{cement} = \frac{(12.25\text{ in} - 9.625\text{ in})}{2} * 25.4 \frac{mm}{in} = 33.34\text{ mm} \quad \text{Eq. 5-2}$$

Table 5-1: Dimensions for analysis

Material	Casing	Cement	Cement	Casing
Length [mm]	11.05	33.34	33.34	11.05
Cumulative [mm]	11.05	44.38	77.72	88.77

To perform neutron attenuation calculations (Eq. 3-12), we must first determine Σ_t of the composite materials under consideration from Eq. 3-13 and Eq. 3-14. The elemental atom number densities of the different material are calculated based on the recipes presented in chapter 4. To calculate the molecular mass, M, the individual atoms must be counted. Here exemplified by

$\text{Ca}(\text{OH})_2$ where n is number of atoms of the element in compound and u is the atomic mass of the element:

$$M_{\text{Ca}(\text{OH})_2} = n_{\text{CA}} * u_{\text{CA}} + n_{\text{O}} * u_{\text{O}} + n_{\text{H}} * u_{\text{H}} = 1 * 40 + 2 * 16 + 2 * 1.008 \approx 74 \quad \text{Eq. 5-3}$$

Running the same calculation for all molecules in the compound, taking into account their different fractions, gives the following atomic densities (Ni) based on Eq. 3-13 (gas and packer fluid (case 5) are presented separately).

Table 5-2: Atomic number densities of material

	<i>Cement</i>	<i>Foamed Cement</i>	<i>OBM</i>	<i>Casing</i>
<i>Density [g/cm³]</i>	1.89	1.20	1.19	7.89
<i>M [g/mole]</i>	194.47	116.68	185.82	55.53
<i>H</i>	2.429 E+22	1.542 E+22	6.020 E+22	-
<i>O</i>	3.226 E+22	2.073 E+22	5.790 E+21	-
<i>Ca</i>	1.027 E+22	6.521 E+21	5.752 E+19	-
<i>Fe</i>	8.779 E+20	5.574 E+20	-	8.261 E+22
<i>Si</i>	3.804 E+21	2.415 E+21	-	3.850 E+20
<i>C</i>	-	-	2.761 E+22	3.679 E+20
<i>Cl</i>	-	-	1.15 E+20	-
<i>S</i>	-	-	1.285 E+21	2.567 E+19
<i>Ba</i>	-	-	1.285 E+21	-
<i>Al</i>	8.779 E+20	5.574 E+20	-	-
<i>N</i>	-	4.954 E+21	-	-
<i>Mn</i>	-	-	-	1.626 E+21
<i>Ni</i>	-	-	-	2.139 E+20
<i>Cu</i>	-	-	-	2.995 E+20
<i>P</i>	-	-	-	2.567 E+10

The energy dependent total microscopic cross section, σ_t , for the different elements were retrieved from the 2011 evaluated neutron library of the National Nuclear Data Center of Brookhaven National Laboratory (USA) (NNDC, 2011). The datasets consisted of two columns, one with energy and one with corresponding σ . Obtained datasets were of different sizes for different elements, ranging between 80 to 8500 datapoints. The energy range was always consistent from 0.1 meV to 20 MeV. Thus, the data was imported to MATLAB for sorting and interpolation. An array of 10 000 evenly distributed points between 4.5 MeV and 0.1 meV was created, and corresponding values for σ was interpolated (see Appendix A). Next the data was exported from MATLAB to Microsoft Excel, where Σ_t for each of the elements and material under consideration was calculated according to Eq. 3-14 and Eq. 3-15. As a result, a database for Σ_t was obtained for all elements as well as for cement, casing, foamed cement and gas at 10 000 datapoints between 0.001 eV and 4.5 MeV (Figure 5-1).

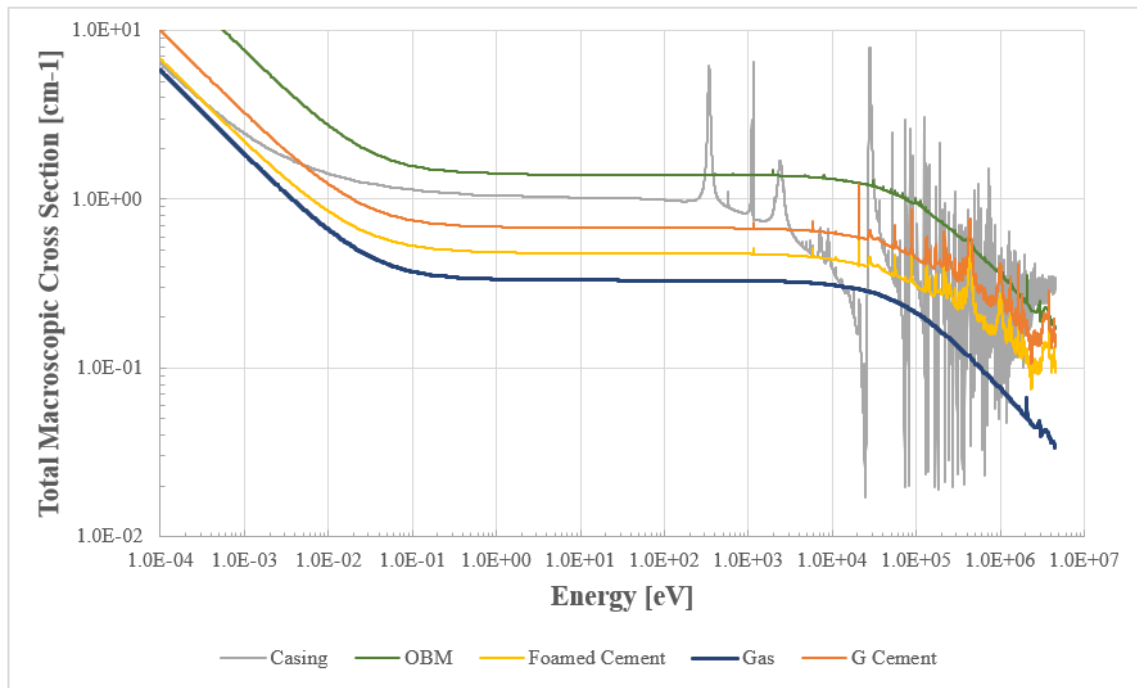


Figure 5-1. Calculated energy dependent macroscopic cross sections (Σ_t)

This figure reveals relevant information on the total attenuation power of the different material. A general observation is that class G cement seems to attenuate more than foamed cement, and OBM attenuates more than gas. The average deviations between the class G cement and the other material is given in Table 5-3. For casing there are heavy oscillations in the high energy range, corresponding to the resonance peaks of iron. In all cases, the neutron first travels through casing at 4.5 MeV, thus experiences the same attenuation coefficient so any resonance effects will be the same for all cases. When returning, the neutrons are of much lower energy where resonance peaks are less abundant.

Table 5-3: Average Deviation of Σ_t from class G cement

Average Deviation	
<i>Foamed Cement</i>	-30.5 %
<i>OBM</i>	+104.4 %
<i>Gas</i>	-72.6 %
<i>Casing</i>	+23.8 %

Transmission calculations were done in steps to account for the energy dependency of the cross sections as illustrated in Figure 5-2. Starting with initial energy $E_0 = 4.5$ MeV, the corresponding Σ_t for steel was picked from the calculated database and modelled across the thickness of the casing. For the energy outcome after this simulation, E , a new Σ_t was picked for the following material

being cement. This was repeated until the neutron had traveled through all materials, and also done for the cases of foamed cement and channeled cement.

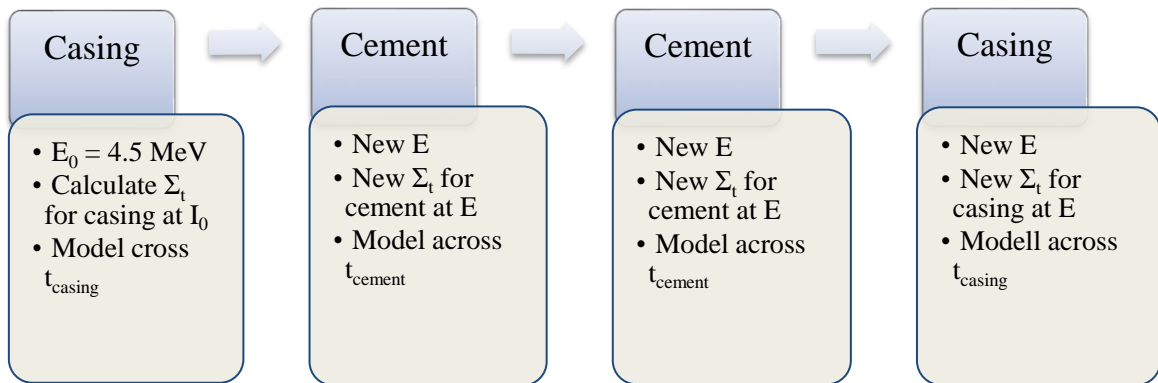


Figure 5-2: Analysis Process

Due to the many assumptions made and the relative simplicity of this model compared to more sophisticated software the results achieved in this work cannot be expected to be exact. Despite this the relative response of the different material is expected to be of relevance and can encourage to more sophisticated modelling with available software or lab testing if current analysis shows promising results.

5.1.1 Spacing Sensitivity Analysis

The first step in the analysis is to perform a sensitivity analysis on spacing between neutron source and detector. According to Guillot and Nelson (2006), the spacing in neutron tools is optimized by factoring in the material traveled through and how fast a neutron will be stopped in such material.

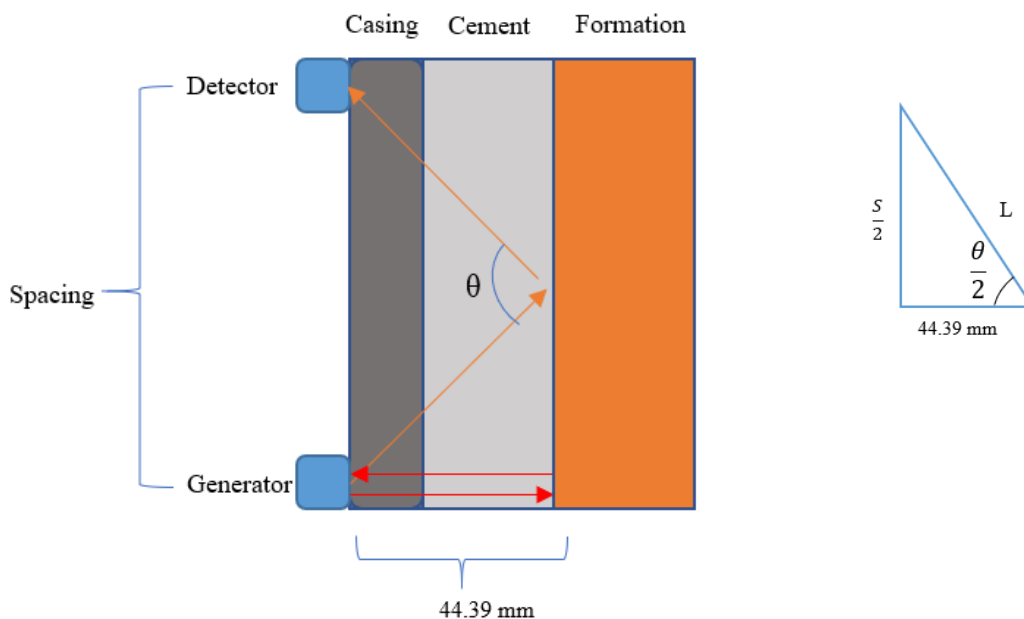


Figure 5-3: Neutron traveling length increases with spacing.

The same is done here to ensure neutrons are within detectable range. A larger spacing gives longer neutron traveling length (Figure 5-3) and hence more attenuation will occur.

The actual distance traveled as a function of spacing (S) can be determined by geometry (Figure 5-3) as follows:

$$\tan\left(\frac{\theta}{2}\right) = \frac{S/2}{44.39} \rightarrow \frac{\theta}{2} = \tan^{-1}\left(\frac{S/2}{44.39}\right) \quad \text{Eq. 5-4}$$

$$\cos\left(\frac{\theta}{2}\right) = \frac{44.39}{L} \rightarrow L = \frac{44.39}{\cos\left(\frac{\theta}{2}\right)} \quad \text{Eq. 5-5}$$

By inserting Eq. 5-4 into Eq. 5-5 we obtain an expression for the (one-way) distance traveled (L) as function of spacing, S. The procedure explained in Figure 5-2 was repeated for various spacings, with the purpose of calibrating the spacing so that neutrons reaches detectable energy at the detector with basis in the good cement base case. Detectable energy range is here assumed to be below 10 eV, corresponding to the approximate epithermal energy range (section 3.2) and a transmission of $\frac{10}{4.5 \cdot 10^6} * 100\% = 2.22 * 10^{-4} \%$. The results are presented in Figure 5-4. It should be noted that the x-axis on the plot is traveled length projected to horizontal for direct comparison between the cases, and that the y-axis is logarithmic scale. Solid vertical lines illustrate the different interfaces between material, here being casing-cement-cement-casing.

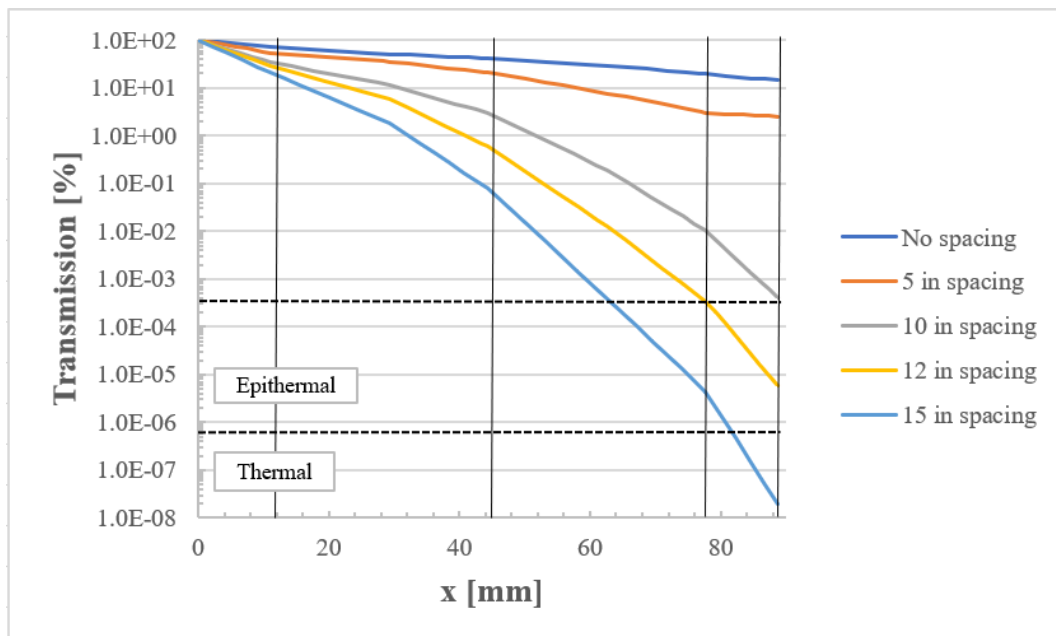


Figure 5-4: Sensitivity analysis of source-detector spacing

Based on this sensitivity analysis, it is evident that spacing is important for getting detectable results. 12 in. spacing is selected for further analysis, as it falls into the detectable range using epithermal detectors and is not far from thermal energy range. 12 in. spacing gives the dimensions illustrated in Figure 5-5.

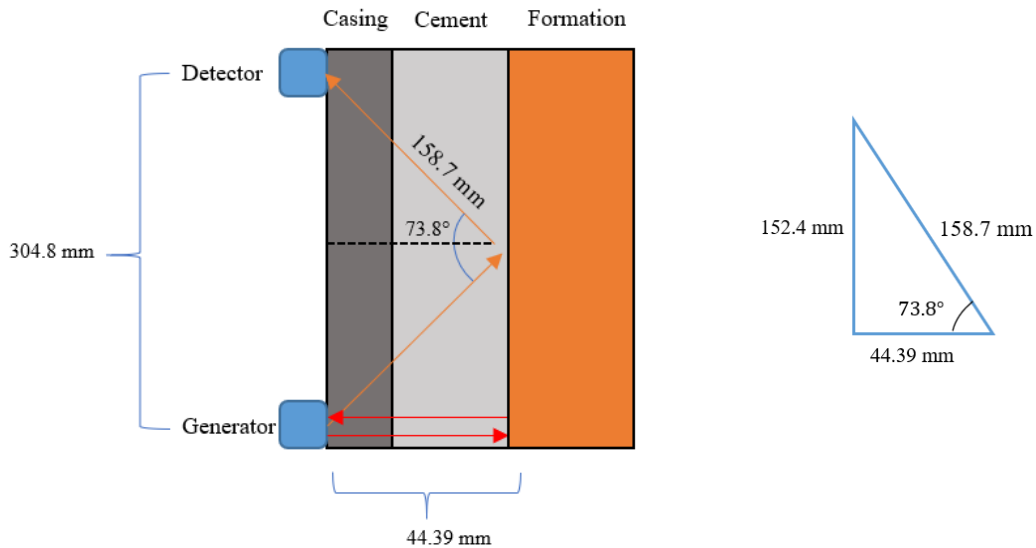


Figure 5-5: Dimensions for 12 in. spacing

In the following sections the results for each case under consideration is presented in semi-log plots. The lengths on the x-axis are in millimeters and represent the projected horizontal distance (red arrows in Figure 5-5) for easier visualization across the different interfaces.

5.1.2 Case 1: Good Cement

The first case to be considered for modelling is the case of intact cement. This is referred to as a base case and represents a successful cement job. The effect of other defined cases can be compared to this case for evaluation. Involved dimensions are illustrated in Figure 5-6. Transmission results are presented in Figure 5-7 where we can see that the spacing sensitivity analysis has ensured final neutron energy to be below 10 eV. Now we can model the remaining cases for direct comparison.

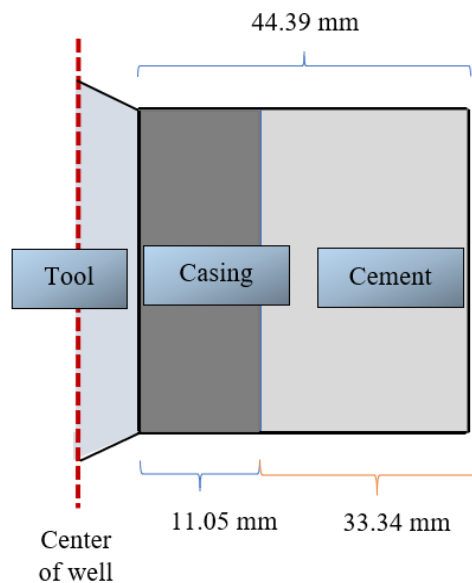


Figure 5-6: Dimensions for case 1 - Good Cement

The different shadings represent the different material to better visualize the horizontally projected lengths.

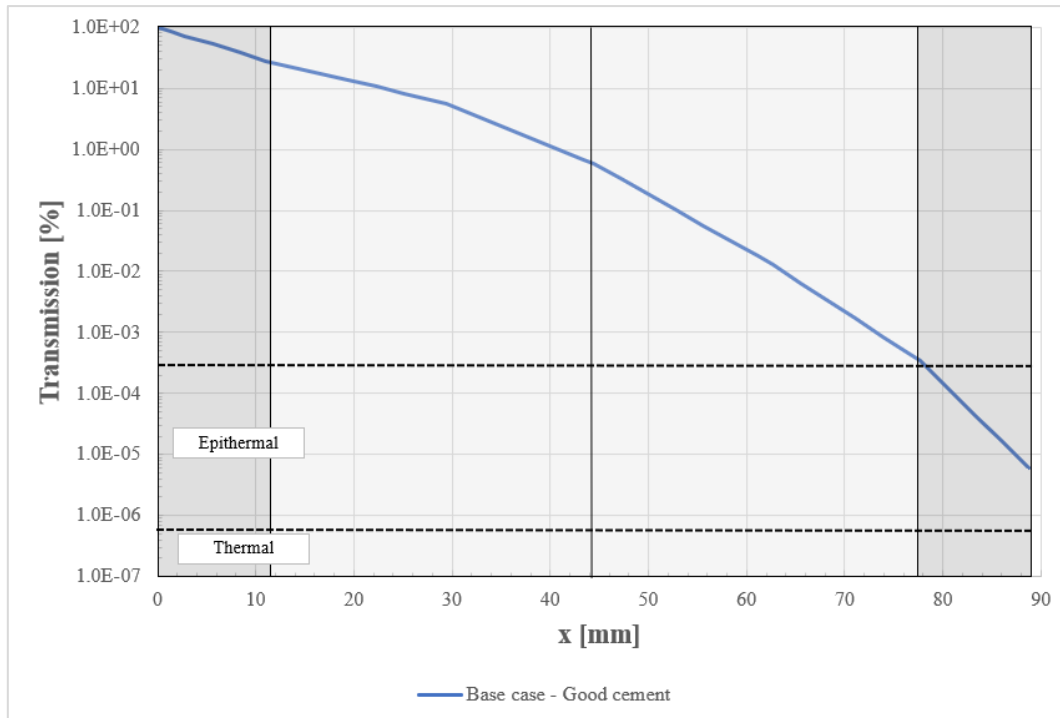


Figure 5-7: Transmission calculations for case 1

5.1.3 Case 2: Foamed Cement

The second case is the same as case 1, but with foamed cement rather than regular class G cement (Figure 5-8). The transmission results are plotted in the same plot as class G cement for direct comparison (Figure 5-9). We can observe a clear separation, and the difference seems to grow within the cement interface.

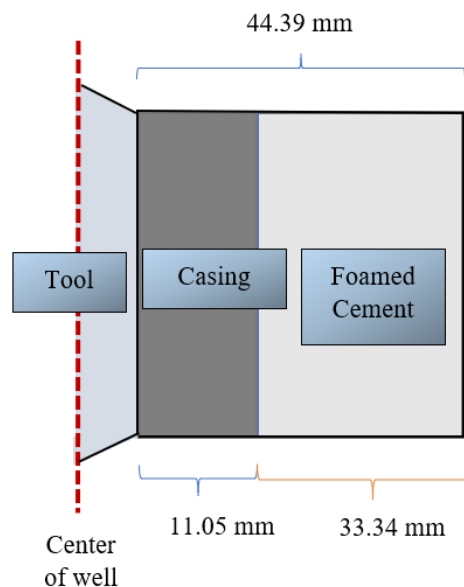


Figure 5-8: Dimensions for case 2: Foamed Cement

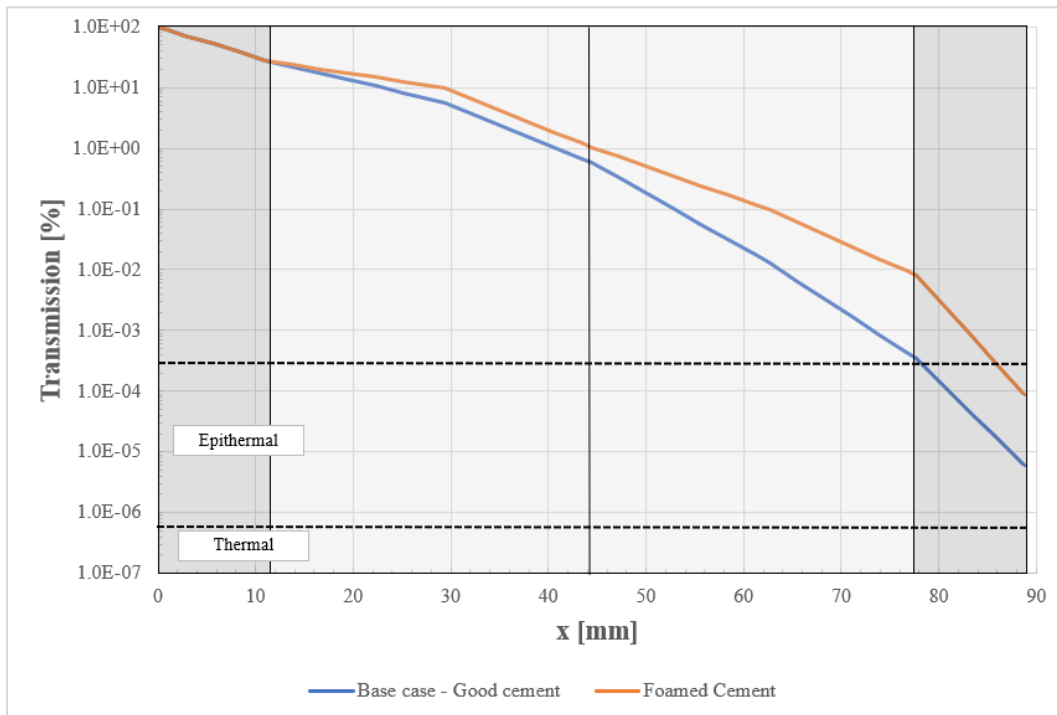


Figure 5-9: Transmission calculations for case 2

5.1.4 Case 3: Cement Defect with OBM

The third case is the same as case 1 except a channel is added in the center of the cement. The channel is assumed to comprise 10% and 20% of the cement thickness (Figure 5-10). The results in Figure 5-11 show that the transmission is clearly affected by the channels, and that the attenuation increases with channel thickness.

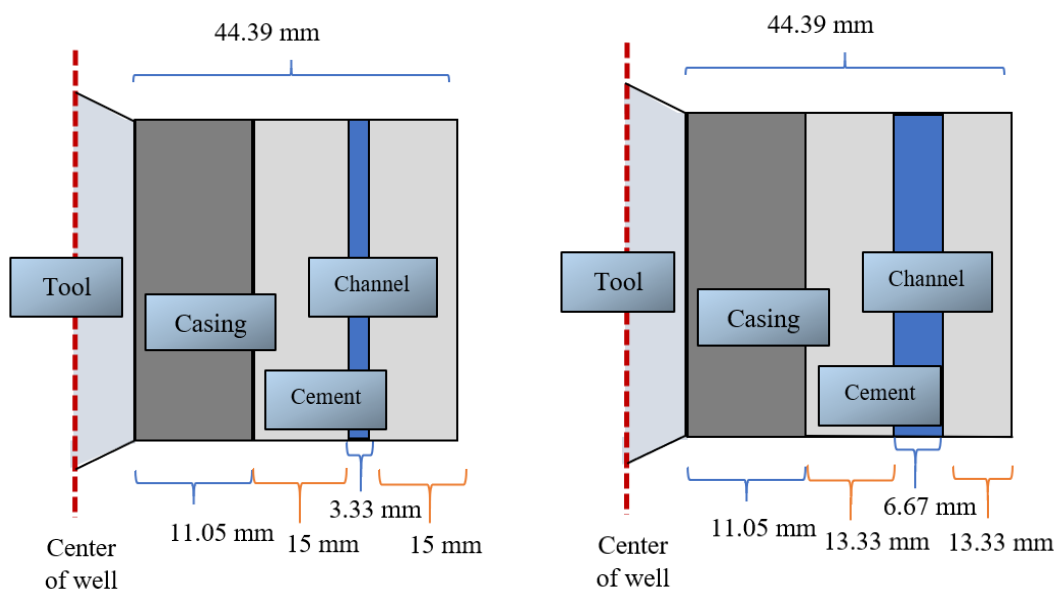


Figure 5-10: Case 3: Dimensions for 10% and 20% OBM-filled channel

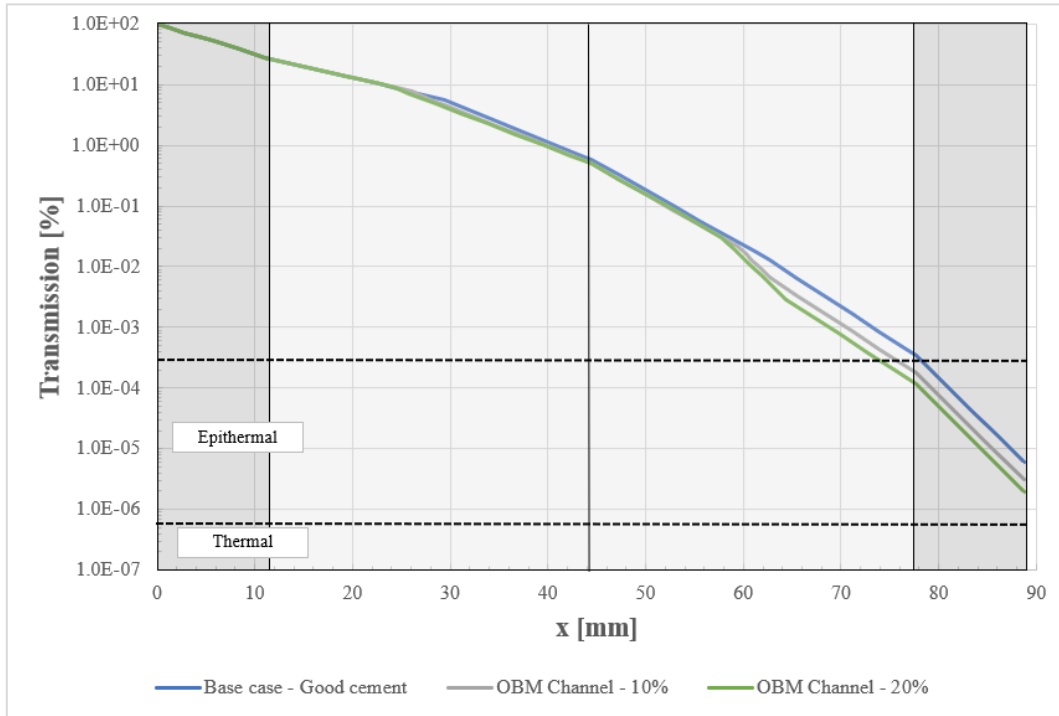


Figure 5-11: Transmission calculations for case 3

5.1.5 Case 4: Cement Defect with Gas

Gas density varies considerably with pressure and temperature, and the assumption of density at standard conditions will not hold. Therefore, the density of gas must be corrected. Assuming:

- Standard conditions (STP) is $P = 1 \text{ atm}$, $T = 0^\circ\text{C}$ or 273.15 K
- True vertical depth of 1000m
- Normal pressure gradient of $0.1 \text{ bar per meter depth}$, i.e. $P = 10.1 \text{ MPa}$
- Normal temperature gradient of $30^\circ\text{C per km depth}$, i.e. $T = 303.15 \text{ K}$
- Gas composition as given in section 4.4.
- Gas considered to be ideal.

The density of the gas is calculated following the ideal gas law (Eq. 5-6) and is found to be 0.071 g/cm^3 .

$$\rho = \frac{M * P}{R * T} \quad \text{Eq. 5-6}$$

Where $R = 8.3145 \frac{\text{cm}^3 * \text{MPa}}{\text{mol} * \text{K}}$, M is calculated according to Eq. 5-3, T is temperature and P is pressure.

The atomic number density, N , of the different constituents is calculated and presented in Table 5-4. The dimensions involved and analysis results are presented in Figure 5-12 and Figure 5-13. It seems clear that the channels with gas cause a similar but opposite effect to those with OBM.

Table 5-4: Elemental atomic number densities of natural gas

Gas	
Density [g/cm ³]	0.071
M [g/mole]	17.74
O	1.205 E+20
H	9.400 E+21
C	2.471 E+21
N	1.205 E+20

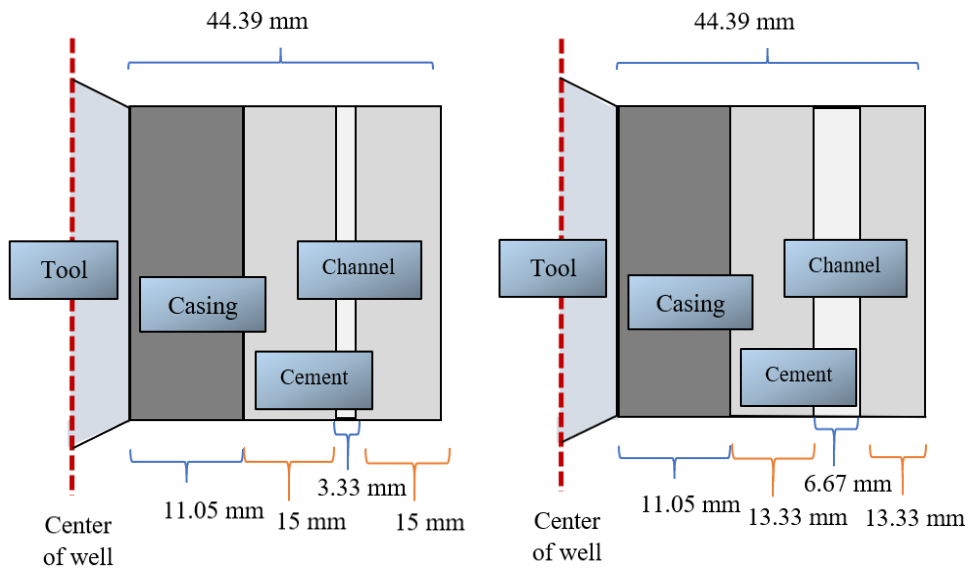


Figure 5-12: Case 3: Dimensions for 10% and 20% gas-filled channel

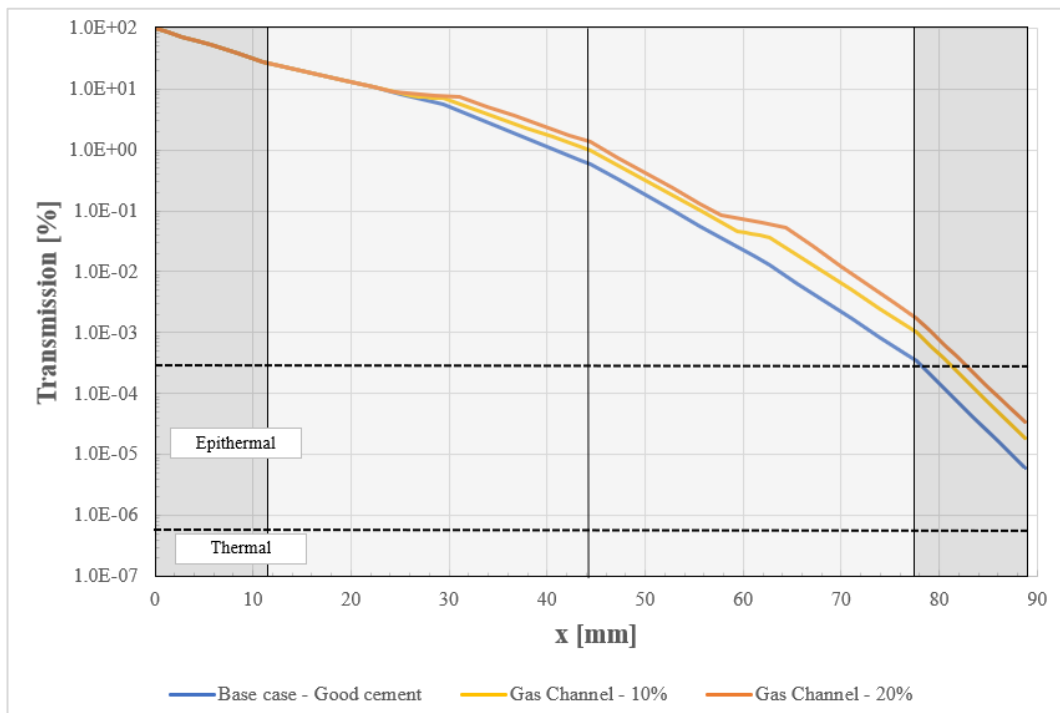


Figure 5-13: Transmission calculations for case 4

5.1.6 Summary – Case 1-4

The final results and final neutron energy that is predicted to reach the detector of case 1-4 is presented in Figure 5-14 and Table 5-5. The effect of channels are observed at around 25 mm and 60 mm which causes separation of these cases relative to the base case. Foamed cement also clearly deviates from the base case after the first intersection. The final neutron energy of all cases falls below 10 eV which is assumed to be detectable.

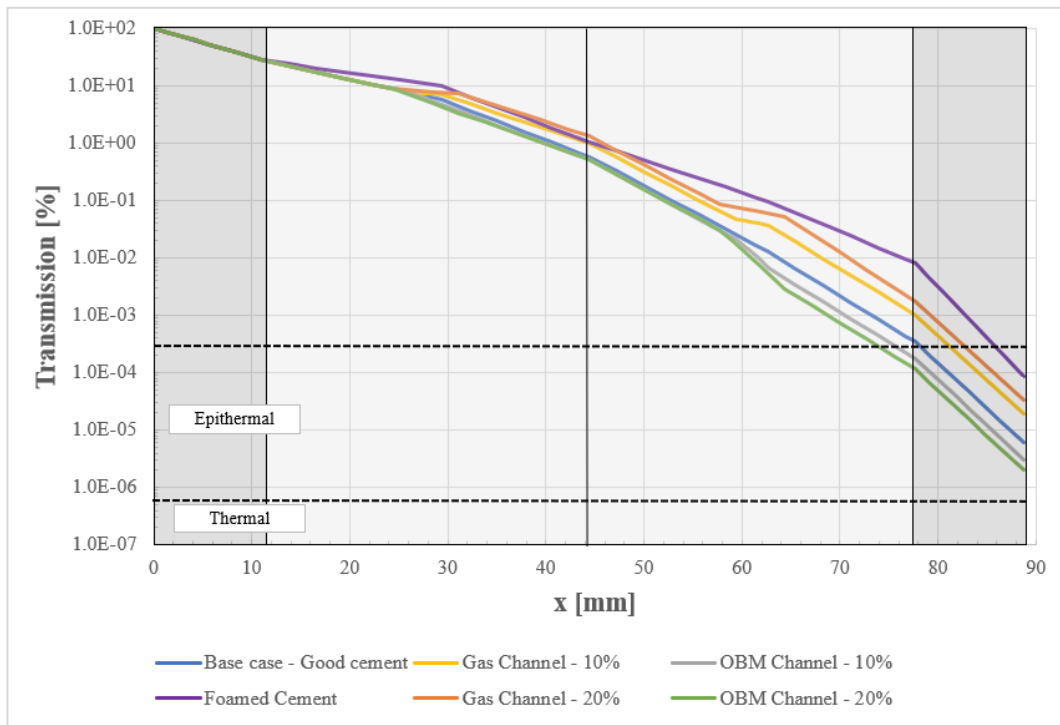


Figure 5-14: Transmission results - All cases

Table 5-5: Analysis results and deviance from base case

Case	Final Neutron Energy [eV]	Percent Deviation From Base Case
Base case – Good cement	0.273	-
Foamed Cement	4.003	+1366 %
OBM-filled channel (10%)	0.051	-81.3 %
OBM-filled channel (20%)	0.014	-94.9 %
Gas-filled channel (10%)	0.852	+212 %
Gas-filled channel (20%)	1.530	+460 %

5.1.7 Case 5: Through-Tubing Logging

When a well is due for permanent plugging and abandonment (P&A), cement plugs are placed in the well to restore the function of the cap rock with an eternal perspective (NORSOK, 2013). If hole is cased, we can verify the cement behind casing by logging and thereby place a cement plug of adequate length to produce a fully cross sectional and vertical barrier (Figure 1-1).

Logging through two strings was mentioned among the key technical challenges and needs in field decommissioning at the annual Norwegian Oil and Gas P&A Forum (PAF) (Thorstensen, 2019), as cement plugs can only be set where cement outside casing is verified. If the production

tubing can be left in the wellbore in a manner that satisfies plugging and abandonment guidelines, it would imply great savings in cost and time (Wilson, 2017). It has been shown in literature that neutrons have the potential to penetrate multiple casing strings (Blount et al., 1991; Desport and Crowe, 2008).

The final case is to simulate neutron attenuation in a well with production tubing in place. With the production tubing in place, there is usually also a production packer in place, and packer fluid filling the annulus between tubing and casing string. The purpose of the packer fluid is primarily to provide hydrostatic pressure. This is to avoid failure of sealing elements and casing by extensive differential pressure. Furthermore, it can shield elastomers and steel in the annulus from corrosion (Schlumberger, 2019b). It is here assumed a non-corrosive oil-based packer fluid, where the main component is diesel (Simpson, 1969).

The following assumptions are made for case 5:

- Same configuration for wellbore and casing.
- 5 ½ in. L-80 production tubing, nominal weight 20 lb/ft, thickness 0.361 in (9.17 mm) (Figure 5-15) (Gabolde and Nguyen, 1999).
- For simplicity it is assumed the same composition and density as for the 9 5/8 in. casing.
- Diesel as the main component filling annulus between tubing and casing, with average chemical formula of $C_{12}H_{23}$ (Date, 2011) used to calculate Σ_t .

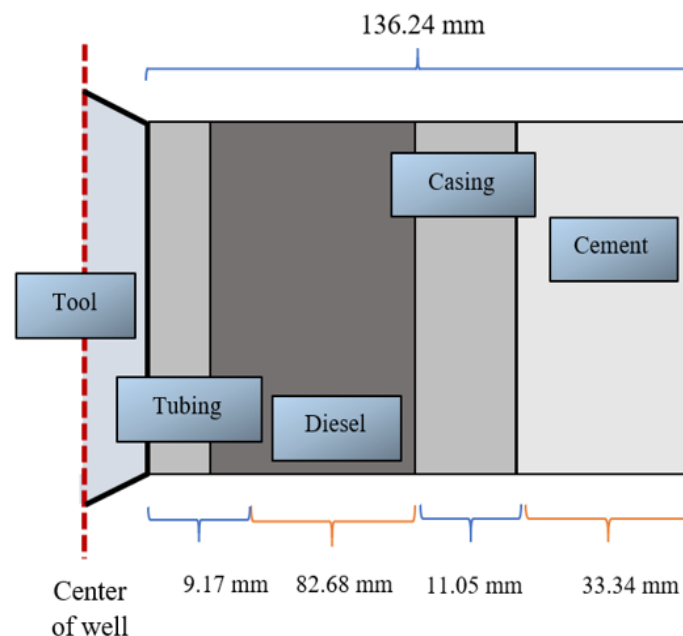


Figure 5-15: Case 5: Dimensions for a logging through tubing.

Due to the added interfaces, a new spacing sensitivity analysis is performed in the same manner as for previous cases to ensure the neutrons are within detectable energy range. The result in Figure 5-16 shows that due to significantly higher attenuation in the packer fluid it must be assumed 5 in. or no spacing between the source and detector. This is unrealistic in practice, and therefore it was

decided to perform this analysis with 14.1 MeV initial energy resembling a D-T neutron generator. Using a higher initial energy not only gives more room for attenuation, but the attenuation coefficients themselves are lower at higher energy. Therefore Σ_t was calculated for the new energy range in the same procedure as before. The result of the sensitivity analysis with new initial energy is shown in Figure 5-17. Again the solid vertical lines represent the different interfaces, as reflected in Figure 5-15.

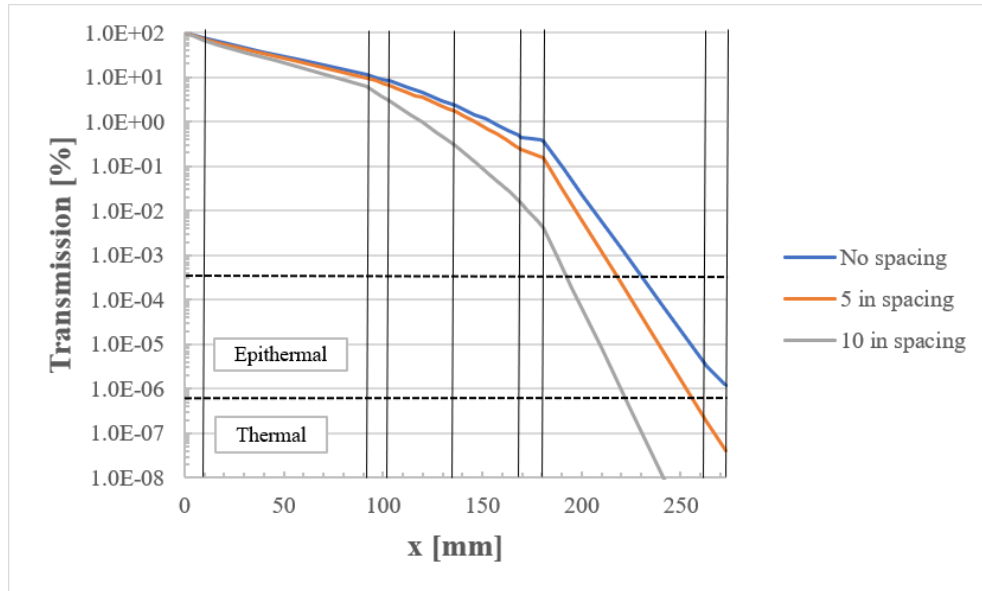


Figure 5-16: Sensitivity Analysis, Case 5 for $E_0 = 4.5 \text{ MeV}$

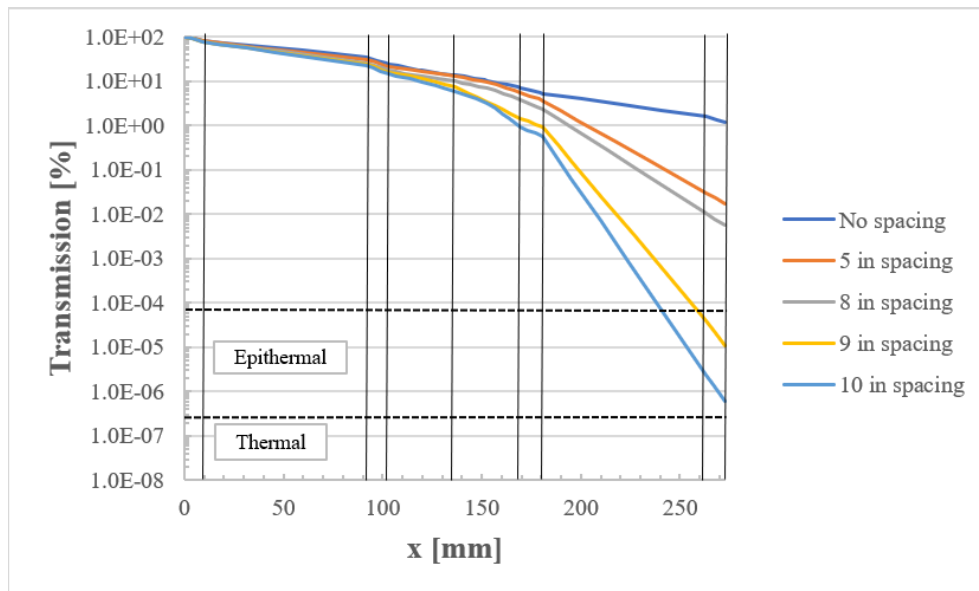


Figure 5-17: Sensitivity Analysis, Case 5 for $E_0 = 14.1 \text{ MeV}$

From this sensitivity analysis it was chosen 9 in. spacing. Performing the analysis in the same manner as for cases 1-4 yielded the results presented in Figure 5-18 and Table 5-6. The results show that only case 3 with OBM falls inside the detectable energy range. However, these have very similar final neutron energy to the base case and can hardly be distinguished in the graph.

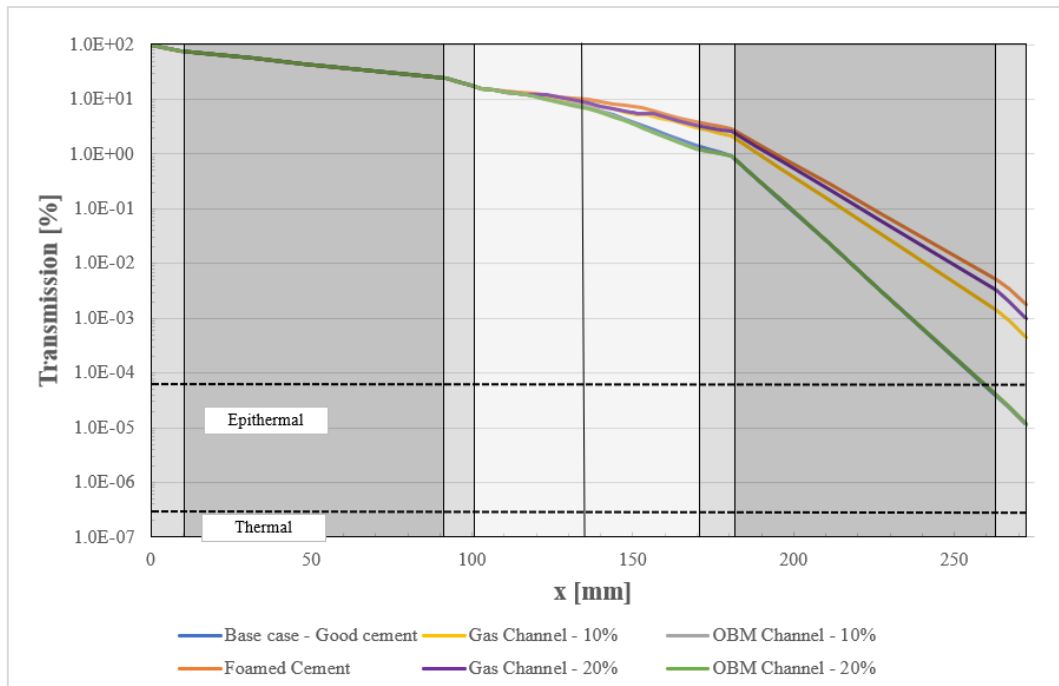


Figure 5-18: Results for Case 5 – $E_0 = 14.1$ MeV

Table 5-6: Results from Case 5 – $E_0 = 14.1$ MeV

Case (Through-tubing configuration)	Final Neutron Energy [eV]	Percent deviance from base case
Base case – Good cement	1.579	-
Foamed Cement	259.330	+16324 %
OBM-filled channel (10%)	1.609	+1.9 %
OBM-filled channel (20%)	1.652	+4.6 %
Gas-filled channel (10%)	62.574	+3862 %
Gas-filled channel (20%)	139.2	+8715 %

5.2 Neutron Backscattering

It is not only neutron attenuation behavior which is of significance when evaluating if neutron logging is suitable for casing cement evaluation. The signal must also have potential to be backscattered to the detector located inside the wellbore. Ragheb (2006) derived a relationship for neutron energy loss as function of scattering angle. The derivation is based on elastic collisions in a center of mass system (Figure 5-19) which is isotropic, total momentum is zero and magnitude of the particle velocities remain unchanged following a collision. The resulting equations are:

$$E' = \left[\frac{(1 + \alpha) + (1 - \alpha)\cos\theta}{2} \right] E \quad \text{Eq. 5-7}$$

$$\alpha = \left(\frac{M - 1}{M + 1} \right)^2 \quad \text{Eq. 5-8}$$

Where E' is energy of neutron after collision and M is the mass of target nucleus. α is here known as the collision parameter and θ denotes the scattering angle.

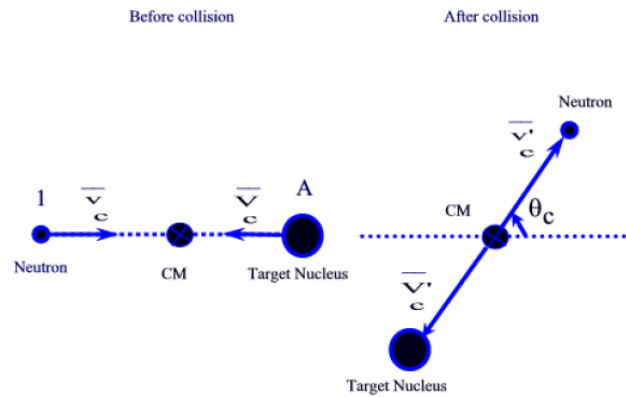


Figure 5-19: Center of mass system. Adapted from Ragheb (2006)

The following observations are made from the equations:

- If there is no collision, i.e. $\theta = 0$ then the energy remains unchanged. $E' = E$.
- Lower atomic mass substances cause larger energy loss for each collision.
- Maximum energy loss occurs at $\theta = 180^\circ$, i.e. for direct backscattering collisions. At this angle we get $E' = \alpha E$. The collided neutron thus falls in the range $[E, \alpha E]$ with equal probability of any final energy within this range. This is illustrated in Figure 5-20 where the final energy E' can fall anywhere between the solid line for a representative mass and initial energy E_0 (here exemplified with $E_0 = 4.5$ MeV).
- For hydrogen ($M \approx 1$), neutron can be completely attenuated in one collision at $\theta=180^\circ$ (Figure 5-20).

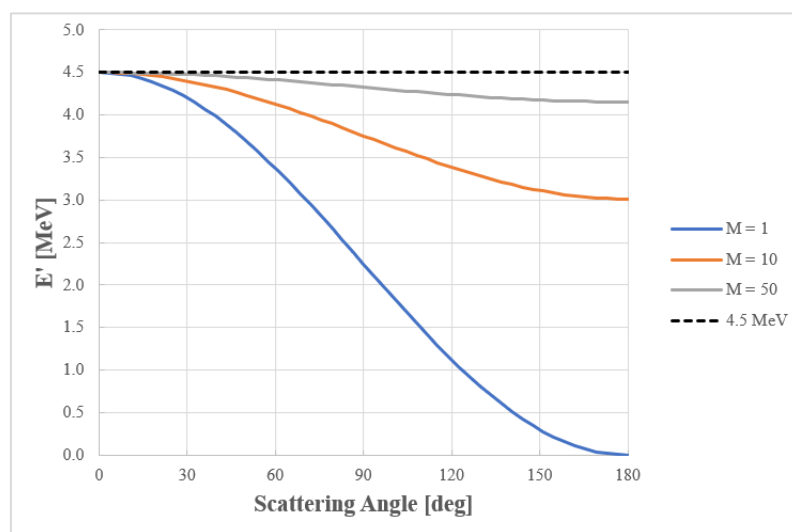


Figure 5-20: Energy loss as function of scattering angle

The equations above have illustrated that neutron backscattering is possible for elastic collisions. The probability of scattering at a certain angle is equal in all directions assuming the

center of mass system since there is equal probability of falling within $[E, \alpha E]$. Considering the neutron beam as a wave, the wave front will spread out spherically (Figure 5-21) (Pynn, 2009). This works to the advantage of the petroleum industry, where the transmitter and detector must be placed inside the wellbore thus detecting the neutrons ending up in the wellbore vicinity after interacting with surrounding environment.

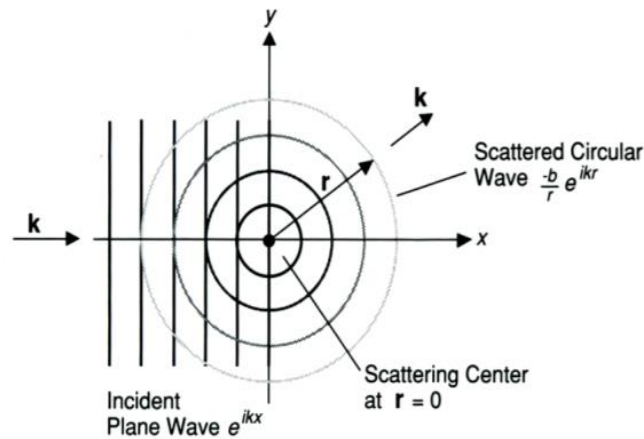


Figure 5-21: The neutron beam spreads spherically. Adapted from Pynn (2009)

It has been shown that neutrons can indeed be backscattered through elastic collisions. Inelastic scattering on the other hand can be more difficult to describe since parts of the energy is spent exciting the target nucleus which in turn emits a gamma ray. Because inelastic collisions are more abundant at higher energy (Figure 5-22), starting around the keV (10^3) energy range, and inelastic cross sections in general are smaller than elastic cross sections, elastic scattering is considered the most likely event (Rinard, 1991) and the main manner of slowing down neutrons (Yip, 2014). Consequently, neutrons which have undergone elastic collisions is mainly what will be measured by thermal/epithermal neutron detectors. Inelastic collisions are of more relevance for inelastic gamma ray detectors. Furthermore, the molecular masses of the considered material in section 5.1

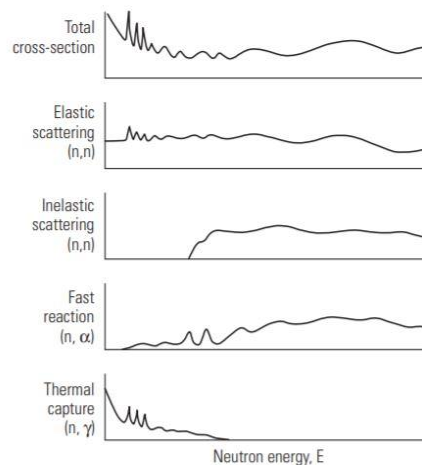


Figure 5-22: Inelastic interactions mainly occurs at higher energy. Adapted from Ellis and Singer (2007)

gives α in the range of 0.93 to 0.98. An exception is for gas where α is 0.80, but the small distance traveled in gas combined with the low probability of final neutron energy being αE backs up the assumption of neglecting energy loss due to scattering.

5.3 Health, Safety and Environmental Concerns

The chemical neutron source, as explained in section 3.1.2, uses radioactive isotopes to generate alpha-particles which in turn interacts with beryllium to produce neutrons. The use of the chemical Am-Be neutron source does present environmental and personnel health concerns in terms of radioactivity. Regulations exist for tool transportation, handling of radioactive material, how tools are stored when not in use and finally obligations when it comes to disposal of such tools (Aitken et al., 2002).

Alpha particles have poor penetration capabilities and are unable to penetrate human skin and even a thin sheath of paper. Consequently, americium is only a health treat if inhaled or ingested (NRC, 2017). However, the United States Nuclear Regulatory Commission (NRC) defines five categories for classification of radioactive source, where category 5 are sources not presenting risk of permanent damage to humans while category 1 is a radiation source which could be fatal if a human is exposed for more than a few minutes (NRC, 2019). Am-Be logging tools are placed in category 2 (NAS, 2008).

On the Norwegian Continental Shelf (NCS) there has previously been concerns related to logging tools being stuck or lost in a wellbore. This has led to plugging back wellbores with the logging tool remaining inside. Particularly directional drilling is of concern due to increased risk of equipment becoming stuck. This has led to several cases where radioactive logging equipment is being left in the subsurface. This is in itself not harmful, but is indeed unwanted and makes an environmental hazard as americium-241 has a half-life of 432.7 years (Aanestad, 2000).

High activity radiation sources such as americium has the potential to be misused as so called Radiological Dispersal Devices (RDD), further known as “dirty bombs” which spreads radiation but without detonation by a nuclear reaction (REMM, 2019). Following threats from extremist groups, the US National Research Council (NAS, 2008) ordered studies to investigate ways to replace current use of radiation sources. Am-Be neutron sources are suggested replaced with D-T neutron generator or californium-252 sources. A concern using this source in addition to the lack of a long-term database for interpretation, is that californium-252 has half-life of only 2.64 years, thus would have to be replaced more frequently (about every 4-5 years) compared to Am-Be source which is recommended to replace every 15 years (NAS, 2008).

Recent studies have investigated potential Am-Be replacements such as neutron generators (deuterium-tritium (D-T), deuterium-deuterium (D-D), deuterium-lithium (D-Li⁷)) and alpha-

particle accelerators with background in mentioned HSE concerns. It is concluded that it is a challenge replacing Am-Be neutron sources, mainly because of the experience and vast library of well log data which has been accumulated over the years which is important in interpretation of the well logs (NAS, 2008). Moreover, it is reported that each technology has its benefits and shortcomings. For example, neutron generators have shown some inconsistency and has the potential to fail due to being electronically controlled. On the other hand, D-T generators operate at higher energy than Am-Be sources (section 3.1.1), can be switched on and off and can evaluate inelastic (limited to higher energy interactions) and capture gamma rays for a more exhaustive mineralogical evaluation (Badruzzaman et al., 2019).

It is also of interest to consider the harmfulness of neutrons themselves to human. This is of relevance for laboratory experiments, and the attention which must be paid to safety when handling sources of radiation. According to Ottolenghi et al. (2013), neutrons are well known to present health concerns for humans. The measure of harmfulness is often presented as a radiation weighting factor, which is a measure of the biological effectiveness of radiation type relative to X-rays and gamma rays. For neutrons, the radiation weighting factor is illustrated in Figure 5-23. It is shown to be highly energy dependent but consistently superior to X-rays and gamma rays (which have weighing factor equal to one as they represent the reference index, see dotted line in Figure 5-23). Based on this it seems evident that neutron experiments should be conducted with care and with application of shielding material to avoid human exposure.

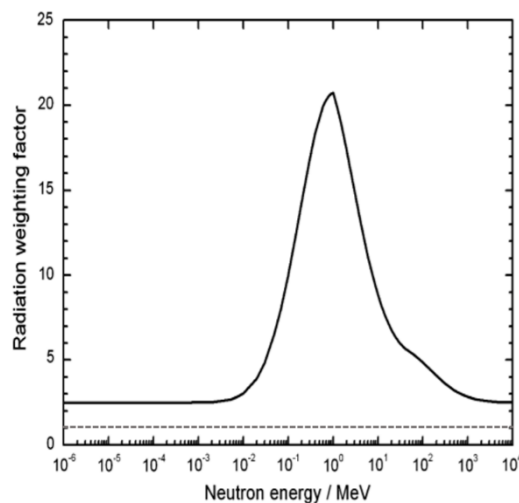


Figure 5-23: Radiation weighting factors plotted against neutron energy in MeV. Modified from ICRP (2007)

5.4 Tool

Neutron logging tools are quite small in size and hence could fit into narrow wellbores without compromising logging quality. From Schlumberger Wireline Services Catalog (Schlumberger,

2015) it is found that CNL tools are available down to 3 3/8 in. outside diameter without the bow-spring. Reservoir Saturation Tools (RST) measuring inelastic and capture gamma rays, C/O ratio and formation capture Σ , are available in as small outside diameter as 1 11/16 in. Consequently, it can be used in tubing of down to 2 3/8 in. The CNL tool requires 4.5 in borehole/inside diameter casing. Typical LWD tool sizes include 4 3/4 in., 6 3/4 in. and 8 in (Xu et al., 2010).

The depth of investigation of the mentioned tools are 9 and 10 in. respectively for the CNL and RST tool. A reduction in emitted neutron energy yields lower depth of investigation and vice versa simply because a higher energy neutron travels further into the formation before being captured (Xu et al., 2010).

When logging in a wellbore, it is important to know the direction of where one is logging. Tools emitting signal in only one direction may miss out on important information on sudden changes in properties in other directions around the wellbore. Neutron tools with a chemical source emits neutrons in all directions. Neutron generators emit neutrons around the circumference of the well, i.e. on a plane perpendicular to the tool. The tools can be either centered or pressed against the wall with a bow-spring. In the latter case, the investigated volume will not be symmetric (Kennedy, 2015).

5.5 Cost

When evaluating the cost of the neutron log, the direct cost of the measurement itself is not the only factor which should be considered. One must also consider the alternative cost of not properly evaluating the cement, given the limitations of current cement evaluation technology. According to Chen et al. (2014), many wells fail to achieve the objective of zonal isolation which in turn can affect production and thus lost revenue. Detecting this sooner rather than later is important for quick remedial actions, and thereby limiting production losses. This section will compare actual cost of available logging tools and identify potential benefits or additional expenses of the neutron log in a cost perspective.

Cost data for wireline basic neutron and cement bond logs has been provided for this thesis. There are many factors that could potentially affect the cost of running a log, such as challenging weather and other unforeseen event. Logging horizontal wells also adds an extra cost. Based on this, the following assumptions are made:

- Good weather
- No unforeseen events
- Deviated well

The total cost of a basic spectroscopy neutron logging job under these ideal conditions is estimated to be about 20% more expensive than a comparable CBL log. It is not known if neutron

log can fully replace CBL log, and another case could be that it would be beneficial to run both logs for a more comprehensive evaluation. The additional cost is not simply to add the cost of the two operations as the time spent on the total logging operation only increases slightly. It is found that running both CBL and basic neutron log in one operation increases the cost by roughly 50% compared to only running the CBL log. This is based on a “per run” calculation.

Another factor to consider is the logging speed. A faster logging speed will save both rig- and personnel time and thereby also save cost. The personnel expenditure is reported to account for 40-50% of a logging operation. However, pushing the logging speed could come at the cost of lower resolution. Logging speed varies for the different neutron logging types, configurations and purposes. There are many different neutron logging tools on the market, and each provider has their own name for their tools. For example, logging speed for inelastic measurements is reported by Schlumberger (2015) to be very slow (100 ft/hr depending on the formation) compared to the standard 1800 ft/hr of CNL tool. Typical CBL tools such as Schlumberger’s Slim Array Sonic Logging tool (SSLT) runs at 3600 ft/hr while cement mapping tools and ultrasonic tools (USIT) logs at 1800 ft/hr (Schlumberger, 2015). Thus, there is a potential doubling of running time for the log itself, and CBL could be 36 times faster than inelastic measurements.

It has been shown that a neutron logging operation is likely to be more expensive than a CBL log given the same conditions. The benefits and additional cost of running a neutron log must therefore be compared with the alternative cost of not doing so and the confidence in already existing techniques. A competent cementing operation is a prerequisite to ensure cement integrity. And any loss in revenue or increased safety risk related to a poor cementing job must be tied back to the cementing job itself. However, detection of cement defects can help mitigate such consequences. Thus, focus on both a proper cementing operation and cement logging could both reduce eventual consequences. If loss of cement integrity occurs undetected, it can potentially have consequences such as (Guillot and Nelson, 2006; Jennings et al., 2003):

- Gas migration; not only potential of lost revenue, but greatly affects operational and platform safety. Has been a problem for years in the deep gas wells of Gulf of Mexico and the Ghawar field.
- Water migration; could cause erosion of downhole steel pipes, contaminate aquifers and increase water cut of produced fluids.
- Failed zonal isolation; could lead to production of unwanted fluids i.e. lost production income. Could in turn affect artificial lift operations.

For P&A operations there exists potential cost savings. Normally in such operations completion equipment must be removed, including the tubing which can make up thousands of meters. Reliable

logging through both tubing and casing strings would make it possible to leave the tubing downhole, thereby coming one step closer to achieving rig-less P&A. Even though the cost of P&A operations vary, a study has shown that rig-time accounts for approximately 50% of the total cost (Osundare et al., 2018). Additionally, leaving the tubing downhole also presents reduction in HSE-related cost and concerns in terms of offshore heavy lifting, material transport, handling and disposal (Sørheim, 2018). There are approximately 300 planned P&A operations on the Norwegian Continental Shelf in the period 2019-2025 (Thorstensen, 2019).

5.6 Alternative Approach to Utilize the Technology; Tracer for Neutron Cement Evaluation

This chapter assesses the potential of evaluating cement with neutron logging by actively adding a substance of known properties to the cement. Aspects to be assessed are the following:

- If cement with added neutron absorbing elements causes significant neutron attenuation, this will lead to a reduced count rate and reveal the presence of cement. Consequently, top of cement can be evaluated. Furthermore, such application could also be of use for secondary cementing as the tagged cement would be highlighted on a log to ensure the cement is in place where intended.
- If tracers can produce capture or inelastic gamma rays, detection of such gamma rays could give information on cement integrity.

Literature on this topic is sparse, therefore multiple studies will be presented enlightening different aspects on such application.

5.6.1 Injection of Neutron-Absorbing Solution

Studies by Blount et al. (1991) and Sommer and Jenkins (1993) show that it is possible to detect channels in the cement in a well using neutron log. To do so, a solution containing boron is prepared. A base pass was run before injecting the solution through perforations. Due to its significant capture cross section the boron solution had noticeable effect on the following PNL pass (Figure 5-24). This was possible through two casing strings and in highly deviated wells (Blount et al., 1991). The obvious drawback is that the solution must be actively injected into the annulus, thus requiring perforations or punched holes in the casing which limits the area of investigation.

Similarly, Chen et al. (2017) applied neutron logging to image and characterize fractures induced by hydraulic fracturing operations. This was achieved by advanced simulations applying Monte Carlo N-Particle (MCNP) Transport Code. Adding small amounts (0.17%) of gadolinium oxide (Gd_2O_3) to the fracturing proppant, a massive thermal neutron absorber, the resulting anomalies in the log could be used not only to identify but evaluate a fracture in terms of geometry

and orientation. This study is not for evaluation of cement, but still is of relevance as it illustrates the possibility of using neutron absorbers as tracing material which in turn could be applicable for this work.

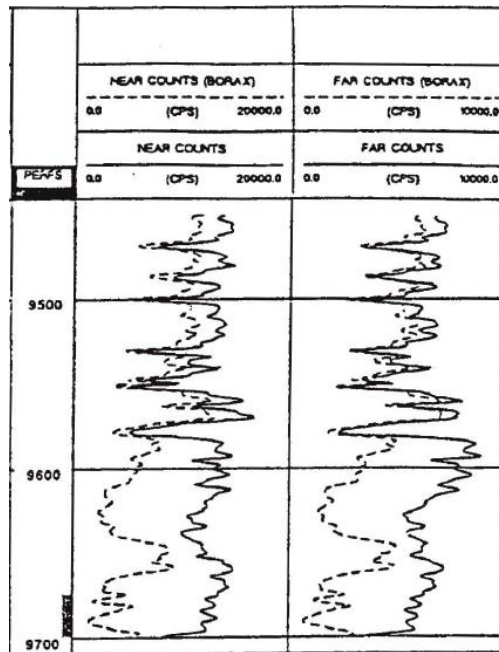


Figure 5-24: Reduction in near and far counts due to presence of boron solution (borax). Adapted from Sommer and Jenkins (1993)

5.6.2 Neutron Attenuation in Tagged Concrete

Seshadri (1989) measured transmission of 14 MeV neutrons through a 50 cm thick concrete of different densities and composition. As concrete essentially consist of cement, water and aggregates (most usually sand and gravel), it is believed that such studies on concrete could have relevant results for cement. It was found that a heavy concrete with 1% gadolinium reduced neutron transmission by 30% compared to normal concrete. It should be noted however, that a concrete thickness of 50 cm exceeds the dimensions considered in this work.

Contradictory, Piotrowski et al. (2015) concluded in their investigation of adding gadolinium to concrete shields that despite gadolinium being very effective at low energy levels there was no significant effect at higher energy. The International Atomic Energy Agency (IAEA) carried out a comprehensive study in the period 1978-1982 on the use of rare earth oxides (which includes gadolinium) in concrete shields for reactors. It was found that concrete added gadolinium is a more efficient neutron attenuator than boron for concrete thickness up to 30 cm, but the difference vanishes as the thickness increases. Furthermore there was little relative effect of increasing the concentration of the additives (Gopinath, 1983).

5.6.3 Gamma Ray for Cement Tracing

Kline et al. (1986) used the principle of tracing to monitor the placement of cement in 10 petroleum wells. The cement was tagged with the radioactive isotopes I-131, Au-198 or Br-82, and a spectral gamma ray tool was used to detect these. When the cement is tagged with isotopes emitting gamma rays different than the naturally occurring ones, contrasts in signal is assumed to be produced by contrasts in cement thickness. The tool was omnidirectional i.e. it measured the average response around the circumference of the wellbore. Hence it had to be assumed that the tracers were uniformly distributed around the wellbore.

By using the principle of spectroscopy (section 3.8.2), it was possible to discriminate the gamma ray signal of the tracer from other elements in the wellbore. The half-lives of the isotopes ranged from 1.5 - 8.1 days, and it was expected that the tracer would fade after 3 - 4 half lives. The radius of cement behind casing at a horizontal plane can be related to the detected signal by:

$$I = k \int_{r_1}^{r_2} \frac{e^{-\mu r}}{r} dr \quad \text{Eq. 5-9}$$

Where I is the intensity of detected signal, r_1 is the outer radius of casing, r_2 is the outer radius of cement, μ is the cement attenuation coefficient (similar to macroscopic cross section of neutrons) and r is the radial distance of the wellbore. All other wellbore effects on gamma rays such as that of casing and wellbore fluids were assumed constant and gathered in the constant k.

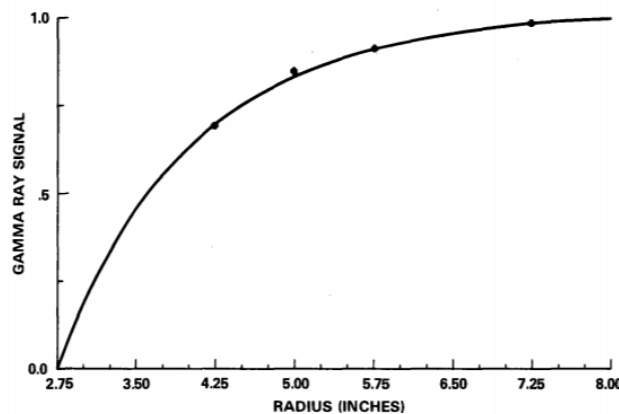


Figure 5-25: Measured signal against radius of annulus behind casing. Adapted from Kline et al. (1986)

By comparing the measured cement radius to the caliper log run before the cementing operation, the top of cement was easily detected (Figure 5-25 and Figure 5-26). Voids in the cement is indicated by the radius of cement being smaller than the caliper radius. This is not easily visible on the figure but is indicated by arrows. When the cement radius is larger than caliper it corresponds to washouts after the caliper was run.

Even though this study considers gamma ray log, it is of relevance for this work because it illustrates the possibility of using tracers in cement. Furthermore, it shows that gamma ray spectroscopy is related to cement radius. This can have applications for this work through neutron inelastic/capture gamma rays from neutron interactions.

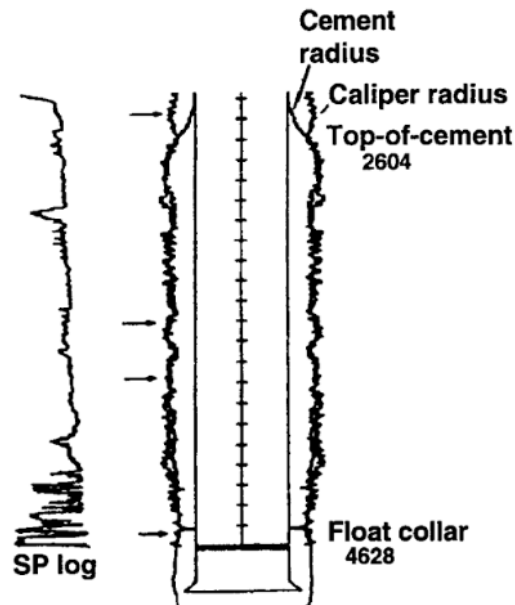


Figure 5-26: Comparison between caliper radius and cement radius from gamma ray tracer log. Adapted from Kline et al. (1986)

Gadeken and Smith Jr (1996) proposed evaluation of cement radius by spectral gamma ray logging of potassium. Potassium chloride (KCl), is a common additive in cement and bypasses concerns related to use of non-naturally occurring radioactive isotopes. This method included running a base log before casing and cementing to compare the natural radiation to the post-cementing log. Measured response was also related to cement radius by Eq. 5-9.

5.6.4 Tracer for Neutron Log Cement Evaluation

So far, this chapter has shed light on different aspects around the potential alternative methods to apply neutron log for cement evaluation. We have seen:

- Neutrons can evaluate channels in cement and fractures in the formation by actively injecting a neutron absorbing solution behind casing.
- There are arguments both for and against that concretes containing neutron absorbing elements could reduce transmission of neutrons.
- Cement can be evaluated by radioactive tracer logging using gamma ray logs which is related to cement radius.

The following sections will evaluate the potential of the elements considered in presented literature to be useful for cement evaluation using neutron log. Potential advantages based on the papers discussed include:

- Increased absorption can give anomalies to verify presence of cement.
- Inelastic scattering gamma rays could be related to cement radius.
- Non-radioactive tracers.
- Does not require punched holes or perforations to inject neutron absorbing material as it would be already mixed in the cement.
- No time limit compared to the gamma ray application studies, where decay of radioactive isotopes limited the logging.
- Can be batch cemented to ensure uniform distribution of tracers.

When determining if a tracer material is fitting for neutron tracer applications, a list of aspects to be evaluated is proposed indicating possible benefits and limitations of using this method:

- Large neutron cross section to be effectively traced.
- Compatibility with the cement and the setting process, such as not affecting bonding or compressive strength.
- For spectroscopy, element should not be already present in significant amounts in well or wellbore area.
- Availability and cost.
- Health, safety and environmental (HSE) impact.

Boron is already described by Sommer and Jenkins (1993) to be of large capture cross section, easy to handle, relatively cheap, compatible with formation and available on the market for purchase. Taking a closer look at gadolinium, the element of highest thermal capture cross section, it is found that it is categorized as one of the rare earth metals. The category name is somewhat inaccurate as the elements themselves are relatively abundant elements found in the earth in oxidized form (United States Department of Agriculture, 2005). Gadolinium has found applications as an additive to improve temperature and oxidation resistance of steel alloys (Stewart, 2012), as shielding material in nuclear reactors (Kofstad and Pedersen, 2014), as tracer in tracking movement and erosion of soil (United States Department of Agriculture, 2005) and is used within the medical field as contrast agent for magnetic resonance imaging (MRI) (Fornell, 2018; Stewart, 2012) and for neutron capture therapy of tumors (Cerullo et al., 2009).

Table 5-7: Capture cross sections of some selected elements. Uncertainties in parenthesis. Based on Munter (2017)

Isotope		Capture Cross Section [barns]	Natural Abundance [%]
Gadolinium-157	^{157}Gd	259000 (700)	15.7
Samarium-149	^{149}Sm	42080 (400)	13.9
Cadmium-113	^{113}Cd	20600 (400)	12.22
Helium-3	^3He	5333 (7)	0.00014
Boron-10	^{10}B	3835 (9)	20
Lithium-6	^6Li	940 (4)	7.5
Chlorine-35	^{35}Cl	44.1	75.77

Evaluating gadolinium using the previously presented list:

- Neutron cross section; The largest thermal capture cross section of all known elements (Piotrowski et al., 2015) (Table 5-7). Its behavior at higher energy should be investigated.
- Compatibility with the cement and the curing process, such as affecting bonding or compressive strength; Wang et al. (2000) reports that both gadolinium and boron are easily dissolved in water. No literature is found on how gadolinium interacts with cement and should be further investigated. It should be kept in mind that very small amounts is required (0.17% concentration for tracing of hydraulic proppant (Chen et al., 2017), 1% for concrete transmission (Seshadri, 1989)).
- Availability and cost; the exact availability and cost is not known, however from online sources gadolinium has about the same abundance in earth's crust as boron and lead (Helmenstine, 2018; Wikipedia, 2019) and is already being used in several applications as discussed above. According to Thompson Reuters Eikon financial software the price of gadolinium oxide per 25.02.2019 was 19 868.2 USD per metric ton. From the wellbore dimensions chosen in section 3, the annular area is:

$$A_{\text{cement}} = \frac{\pi}{4} * \left(\left(\frac{D_{\text{well}}}{2} \right)^2 - \left(\frac{D_{\text{casing}}}{2} \right)^2 \right) \quad \text{Eq. 5-10}$$

$$\begin{aligned} A_{\text{cement}} &= \frac{\pi}{4} * \left(\left(\frac{12.25 \text{ in}}{2} \right)^2 - \left(\frac{9.625 \text{ in}}{2} \right)^2 \right) * 0.0254^2 \frac{\text{m}^2}{\text{in}^2} \\ &= 0.007274 \text{ m}^2 \end{aligned} \quad \text{Eq. 5-11}$$

Assuming the cost above, concentration (C) of 1% and a density of 7.41 g/cm^3 or ton/m^3 a rough estimation for cost of gadolinium oxide in cement gives:

$$\frac{\text{Cost}}{m} = \rho * A * \frac{\text{Cost}}{V} * C \quad \text{Eq. 5-12}$$

$$7.41 \frac{\text{ton}}{\text{m}^3} * 0.007274 \text{ m}^2 * 19868.2 \frac{\text{USD}}{\text{ton}} * \frac{1}{100} = 107.1 \frac{\text{USD}}{\text{m}} \quad \text{Eq. 5-13}$$

- Health, safety and environmental (HSE) impact; Gadolinium is non-radioactive, allowing batch cement mixing to ensure uniformly distributed tracers. Gadolinium is used in contrast agents for MRI in the medical field, where it is actively injected into the human body (Ferris and Goergen, 2017). However, such applications have been topic in recent discussions on whether it can be harmful for humans and studies are initiated (Fornell, 2018). Nevertheless, such applications are not of relevance for the petroleum industry applications and it is therefore not found any reason to believe gadolinium is harmful for humans.

5.6.5 Tracer Calculations

5.6.5.1 Neutron Attenuation in Tracer Material

The literature in section 5.6 presented some contradictory results. Small amounts of gadolinium were added to hydraulic fracturing proppant to successfully evaluate fractures in terms of geometry and direction. On the other hand, some studies argue that gadolinium is not very effective at high energy levels. To investigate this, Σ_t is calculated for cements added 1% gadolinium and boron. Their σ_t is retrieved from the evaluated neutron library of the National Nuclear Data Center of Brookhaven National Laboratory (USA) (NNDC, 2011).

Taking into consideration the atomic density of each element by Eq. 3-6, Σ_t is calculated for the corresponding σ_t .

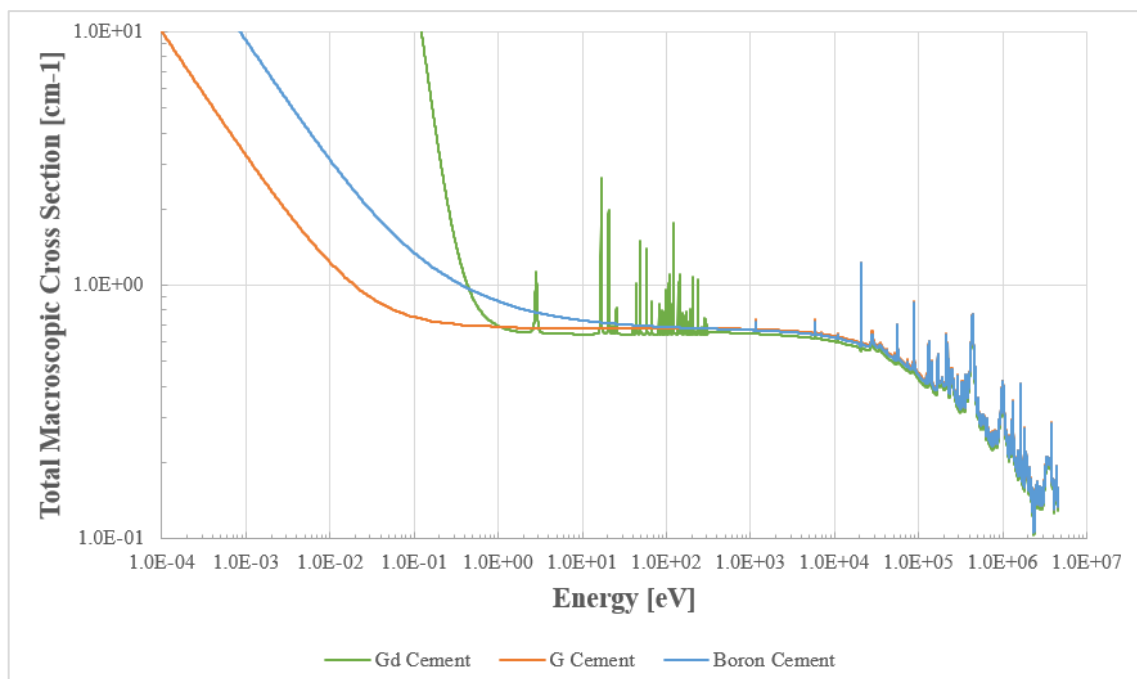


Figure 5-27: Σ_t of cements with tracers

From Figure 5-27 it is seen that the arguments made about gadolinium being only superior at low energy holds, as it only becomes dominant below 1 eV. A transmission analysis is performed similar to previous cases. Assumptions are the same as those in section 5.1, including a 1% concentration of tracer material. Additionally, the density of the cement for each case is considered the same as class G cement because of the low concentration of additives.

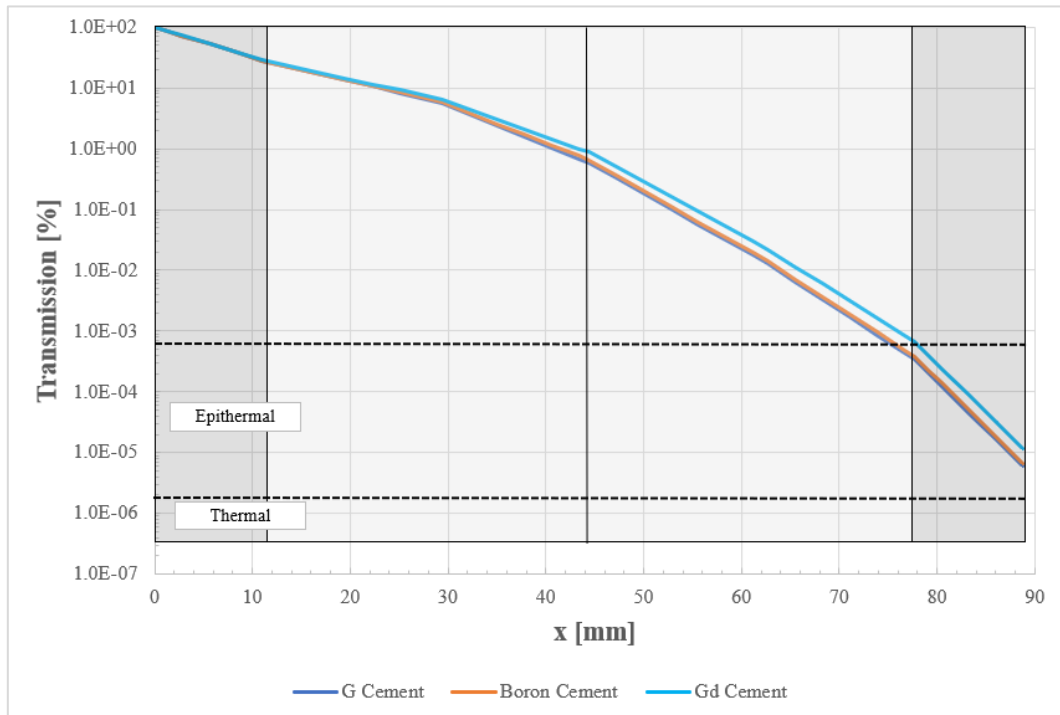


Figure 5-28: Cement with tracer transmission analysis. $E_0 = 4.5 \text{ MeV}$

The transmission analysis reveals quite small differences (Figure 5-28), and it is shown that the two cements added tracer material attenuate slightly less than class G cement. In an attempt to study this phenomenon further, a simulation is conducted where a lower initial neutron energy is assumed to study the potential effect of tracer materials given that they seem more efficient at low energy (Figure 5-27). A 2.5 MeV neutron is assumed, corresponding to the lower range of an Am-Be source, deuterium-deuterium (D-D) source and potentially the lower and of deuterium-lithium (D-Li⁷) generator (Figure 3-3). The result of this study is presented in Figure 5-29 and Table 5-8. It is evident that the effect remains the same as the attenuation is still less for the tracer cements than for the class G cement.

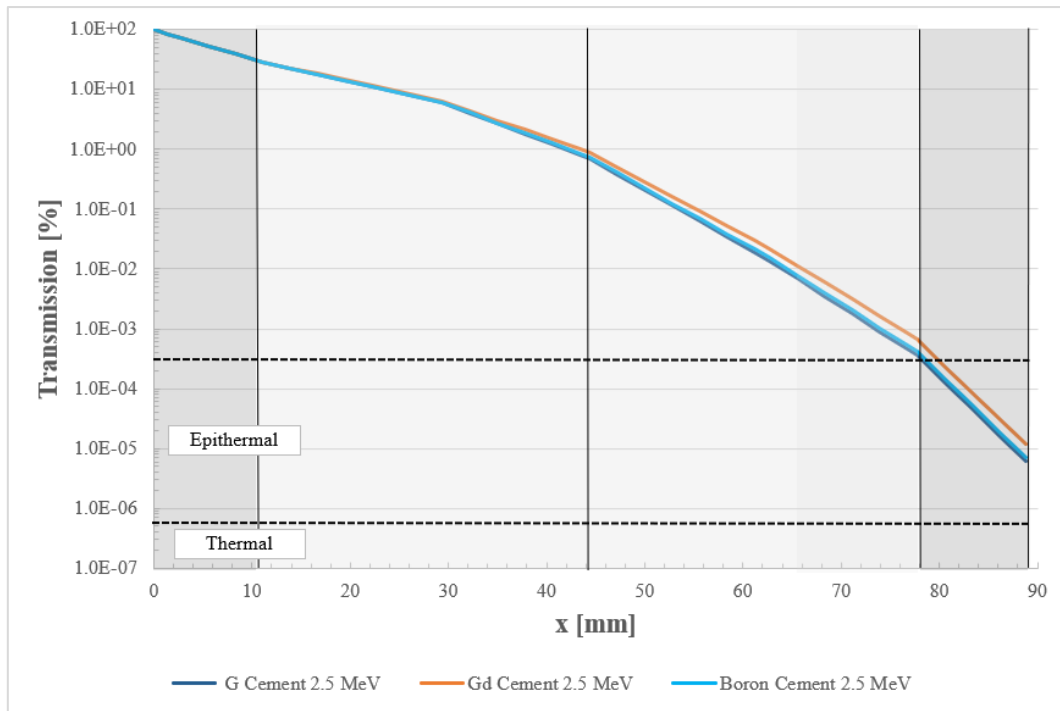


Figure 5-29: Cement with tracer transmission analysis. $E_0 = 2.5 \text{ MeV}$

Table 5-8: Results for tracer analysis at different E_0

	Case	Final eV	% deviation from base case
4.5 MeV	Base Case	0.273	-
	Gd Cement	0.828	203 %
	Boron Cement	0.306	12.1 %
2.5 MeV	Base Case	0.158	-
	Gd Cement	0.296	87.3 %
	Boron Cement	0.181	14.6 %

5.6.5.2 Neutron Absorption in Tracer Material

As previously explained, neutrons have separate probabilities to collide elastically, inelastically and to be absorbed which together makes up the total probability of an interaction to occur, Σ_t . The main reason for the large Σ_t of gadolinium and boron at thermal energy is their rapid increase in absorption cross section. The probability of neutron to be absorbed is defined as (Ragheb, 2006):

$$\text{Absorption probability} = \frac{\Sigma_{abs}}{\Sigma_t} * 100 [\%] \quad \text{Eq. 5-14}$$

The absorption probabilities of the different materials are calculated at different energy and presented below (Figure 5-30). The addition of tracer material severely increases the probability of cements to absorb neutrons. Considering that neutron in previous simulations left the cement in in the 15-50 eV energy range (black dotted line) it seems likely that particularly boron will increase the number of absorbed neutrons increases. Even though the probability is only around 10%, it is still significant considering that it resembles an average of 10% reduction in neutron count rate at

the detector.

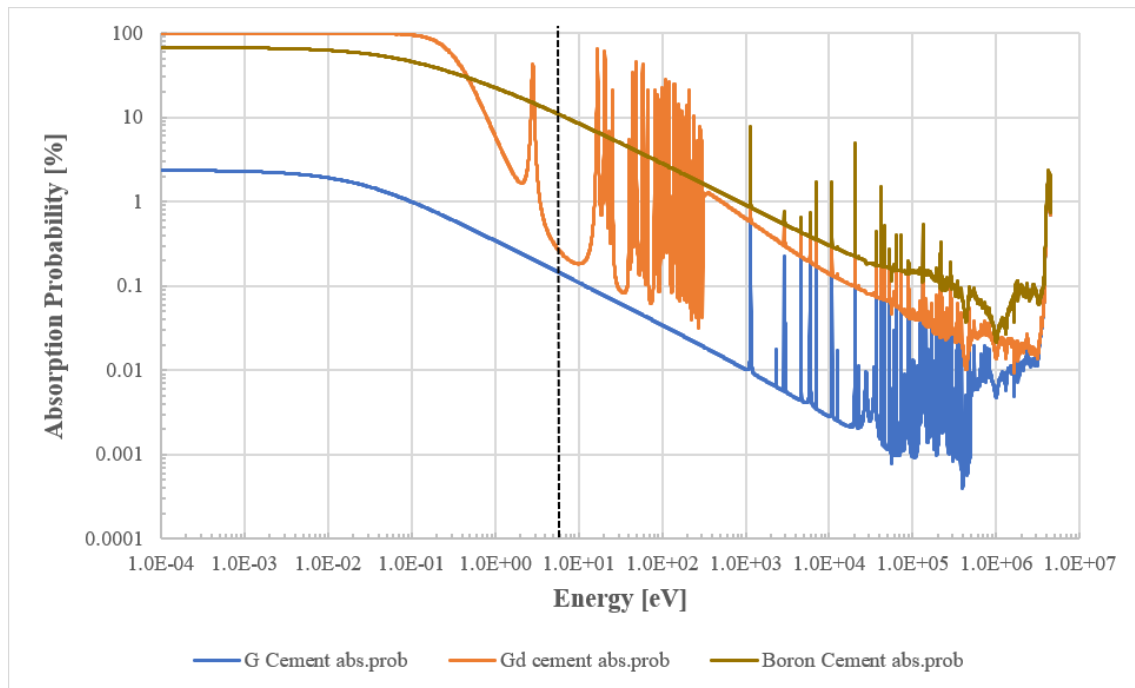


Figure 5-30: Absorption probabilities of cements with and without tracers

5.6.5.3 Spectroscopy for Tracer Logging

When adding tracers, they must be mixed uniformly into the cement before displacement. The amount for tracer needs to be sufficient to be logged through casing and overcome natural background radiation, however it is advantageous if the tracer is not naturally existing in the near wellbore area (Gadeken and Smith Jr, 1996). The study by Kline et al. (1986) (section 5.6.3) presented the possibility of detecting TOC and cement defects using radioactive tracers and gamma ray log. The equivalent method for neutron logging would be by logging gamma rays from inelastic or capture interactions. This section will focus on the inelastic scattering part.

Inelastic microscopic cross sections of all considered elements from the selected recipes were downloaded from the NNDC database (NNDC, 2011). The inelastic macroscopic cross section was calculated from Eq. 3-6 and plotted as shown in Figure 5-31. Iron is not included as it is mainly found in the casing.

4.5 MeV is marked as the black dotted line, and it can be clearly observed that inelastic collisions of some elements mainly occur at energy above this which explains why spectroscopy tools usually include 14.1 MeV neutron generators. All values for inelastic Σ are quite low compared to the total Σ_t . However, it seems that gadolinium has a relatively high probability to interact inelastically compared to the other elements. It is known from literature that tools can

distinguish between elements such as C, O, Si, Ca, Fe, S and Cl (Johnson and Pile, 2006), thus it seems likely that the presence of gadolinium could be detectable as well.

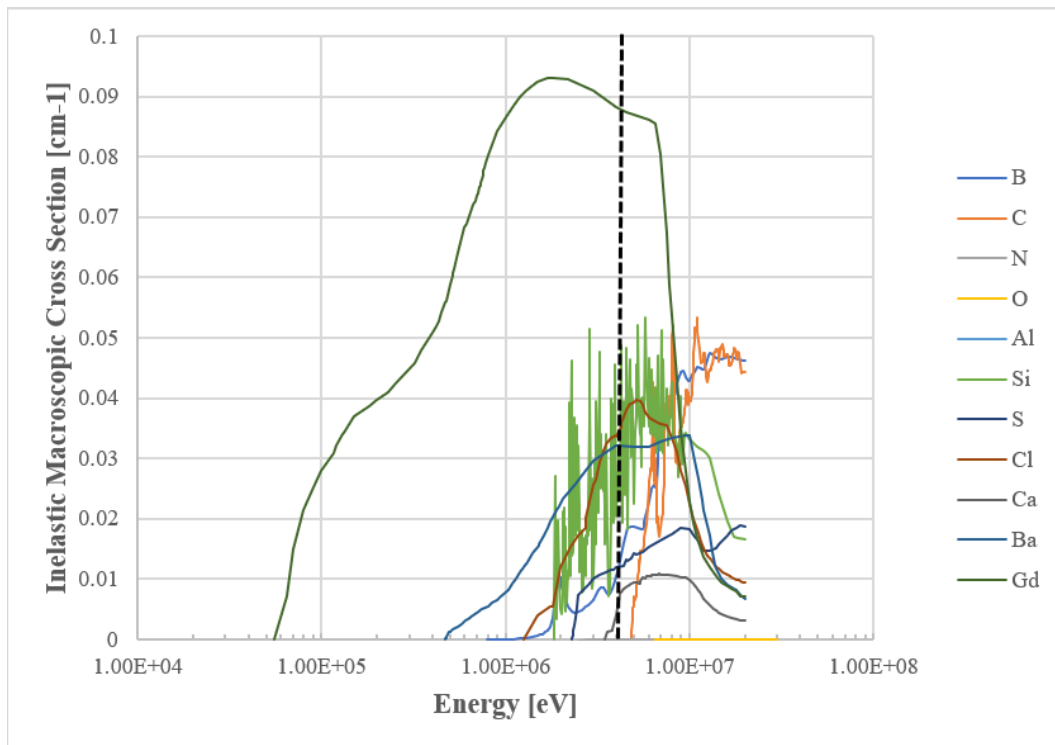


Figure 5-31: Inelastic cross section of selected elements.

5.7 Alternative Approach to Utilize the Technology; Polarization Analysis

From before, we have divided total cross section into absorption and scattering cross sections. Neutron scattering can also be divided into coherent and incoherent scattering. Incoherent scattering is when the incoming neutron interacts with individual nuclei of a specimen independently, while for coherent scattering the interaction between neutron and nuclei is the same in the whole specimen. Most elements have larger coherent scattering cross section. Important exceptions are vanadium and hydrogen (Copley, 2011). It is the sum of the incoherent and coherent cross section that makes up the scattering cross section:

$$\sigma_{inc} + \sigma_{coh} + \sigma_{abs} = \sigma_s + \sigma_{abs} = \sigma_t \quad \text{Eq. 5-15}$$

A property of particles is spin. Neutrons have a spin of $\frac{1}{2}$, which equates to an angular momentum of $\frac{1}{2} \hbar$ where \hbar is the reduced Planck's constant. The incoherent scattering cross section of elements is related to the spin of the element. For example, carbon has zero spin and thus has approximately zero incoherent scattering cross section. Similarly, all nonzero spin elements will exert some incoherent scattering cross section (Hornak, 1997).

The incoherent scattering can in turn be divided into two contributions. One is spin incoherence which is related to the different spins from different atoms in a sample. The other is isotopic incoherence which arises from a mixture of isotopes from the same element in the sample. Interestingly, spin incoherence (accounting for $\frac{2}{3}$ of the incoherent contribution) flips the spin of

the neutron. For isotopic incoherent scattering and coherent scattering, the spin remains the same. Thus by counting neutrons which spin are/are not flipped it can be distinguished between incoherent and coherent scattering thus saying something about the presence of hydrogen atoms (Gaspar et al., 2010).

Schweika (2012) illustrates the principle of polarization analysis. A neutron beam contains neutrons of randomly distributed spin states. When the beam is polarized, all the neutron spins are aligned. A flipper is installed before the sample, so that when the flipper is turned on the neutron must go through spin incoherent scattering (i.e. flip the spin back) to be detected. This principle is illustrated in Figure 5-32. To the left where nickel is used, it is seen that there are essentially no measurements when flipper is on, indicating that no neutrons are flipped back hence nickel has no/negligible incoherent scattering cross section. On the other hand; to the right where vanadium is used, about 2/3 of the contributions are from flipped spins, i.e. the neutrons has undergone incoherent scattering. The remaining 1/3 is from isotropic incoherent scattering which does not flip spin.

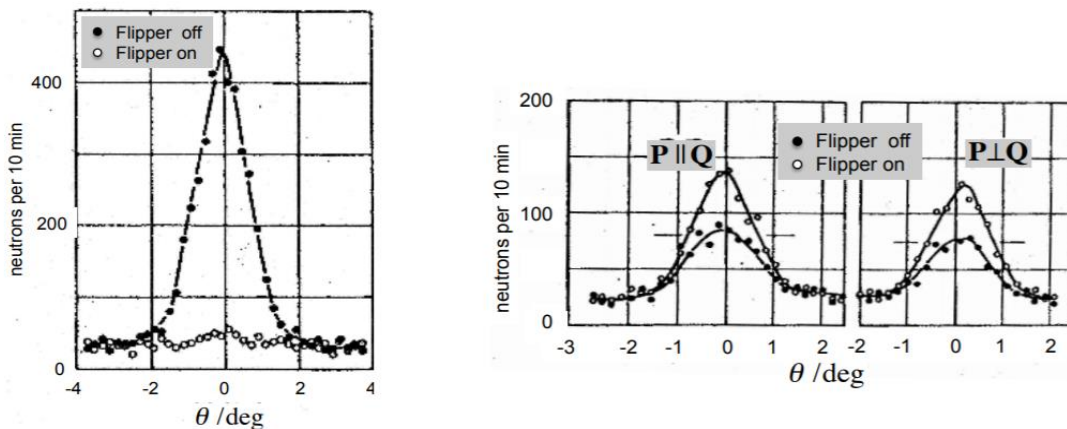


Figure 5-32: Polarization analysis. To the left: Nickel. To the right: Vanadium. Adapted from Schweika (2012)

Even though several works are available to prove the concept of polarization analysis, it has yet to find many applications beyond this (Gaspar et al., 2010). Ideas have been presented where nuclear magnetic resonance (NMR) technology is used to increase sensitivity of spin-polarized neutron scattering analysis (Buckingham, 2003) and recent studies are commenced to research such applications (Kotlarchyk and Thurston, 2017). Despite such technology reaching beyond the scope of this thesis, it is still included to shed light on the alternative aspects of neutrons being used for material analysis, and maybe in the future this technique can be applied to scan the cement behind casing for liquid-filled voids.

6 DISCUSSION

The goal of this thesis was to evaluate the potential to utilize neutron logging for evaluation of casing cement. This has been done by analyzing neutron behavior in different material and assessing other aspects determining the usefulness of this technology for said application. In the following sections the results obtained with associated assumptions are discussed.

6.1 What Are Detectable Results?

For all measured data there will always be some degree of uncertainty. Even though some of the cases modelled fall within detectable energy range they must also be distinguishable from each other. According to available industry tools by Schlumberger (2015) it is reported accuracies of neutron logging tools in the range of $\pm 5-13.3\%$. These are tools measuring thermal and epithermal neutron porosities as well as formation sigma. Accuracy for inelastic/capture gamma ray tools is unknown as it is reported to depend on hydrogen index of the formation. Based on this, it is assumed that a difference of more than 13.3% between compared cases is required to realistically detect changes in modelled results.

6.2 Neutron Transmission Calculations

Among the objectives of this thesis was to investigate the effect of neutron behavior in media such as casing, cement, foamed cement and drilling fluid. The results of such analysis have been presented, and the following sections will discuss these.

6.2.1 Casing

Of the materials under consideration, casing does indeed present relatively significant attenuation especially at intermediate energy levels. At very high energy the presence of resonance peaks of the iron component clouds the visualization of casing Σ_t (Figure 5-1). However, if comparing to the case of Haddad (2017), the issue of X-rays not being able to penetrate the casing is as expected not a concern for neutrons. Appendix B provides calculations of thermal neutron attenuation (i.e. at 0.025 eV) through pure iron which is comparable to casing (about 96 % of the composition). These calculations indicate the “worst case” attenuation that neutrons experience since Σ_t is increasing with decreasing energy. It is therefore not comparable with the analysis of this work, but it is assumed that if the neutron makes it through the casing at such low energy it will certainly also make it at the much higher energy considered in the analysis. This is neglecting eventual scattering, which seems reasonable as pure iron has $\alpha = 0.93$ according to Eq. 5-8.

6.2.2 Foamed Cement

The analysis has shown that foamed cement affects neutrons less than class G cement. The reason is suspected to be comparable to the gas effect presented in section 3.5.1. The gas injected into the cement causes the presence of less atoms per unit volume i.e. lower atomic density. Furthermore, the nitrogen gas has relatively low Σ_t and is assumed to compose 40% of the foamed cement. For case 1-4 the final energy of modelled neutron in foamed cement still falls within the epithermal energy region and can be detectable. This was not the case for through-tubing logging, which is to be discussed in section 6.2.4.

An issue with the CBL log is that foamed cement produced similar response as fluids. This is not the case with the neutron log as they produce opposite responses; results show that liquids will attenuate neutrons more while foamed cement will cause less attenuation relative to class G cement. This agrees well with literature, and it seems reasonable that fluids and foamed cement should be distinguishable on the neutron log.

6.2.3 Channeled Cement

Case 3 and 4 were to simulate the response of a cement channel filled with realistic substances. OBM is shown to attenuate neutrons more than class G cement, and the effect increases with increasing channel width. It is also expected that WBM will have a similar or even larger effect depending on the salinity i.e. the chlorine concentration of the water phase. This effect matches presented theory well, namely that hydrogen-rich liquids would attenuate neutrons more than cement.

The opposite is observed with gas-filled channel. This is also what was expected, as we know that the gas effect causes less neutron attenuation. In total, channeled cement filled with gas causes more attenuation than foamed cement even though natural gas itself has smaller Σ_t . This seems reasonable as the gas channel makes up only 10 and 20% of the cement thickness. The remainder is assumed to be class G cement which attenuates neutrons more than foamed cement. For case 2 the neutrons travel through 100% foamed cement and the resulting total attenuation becomes less than for case 4. It is, however, expected that with increasing channel thickness the attenuation will decrease and even pass the attenuation of foamed cement.

Interestingly, the deviance between 10 and 20% OBM-filled channel is small compared to the deviance between good cement (0%) and a 10% channel, with only a 13.6% relative difference to the base case. Therefore, it seems unlikely that differences in channel thickness of less than 10% are distinguishable. It is also likely that there is a lower limit in channel thickness for it to be detectable.

6.2.4 *Through-Tubing Logging*

For the final case where cases 1-4 were simulated for a configuration with a tubing inside the casing, the results show that the neutrons indeed have the potential to travel to the cement/formation interface and return. However, the attenuation is much larger than for previous cases. The attenuation is heavily dependent on the fluid present in the annulus between tubing and casing. It is therefore also dependent on the radial clearance between the tubing outside diameter and casing inside diameter, and a larger tubing or smaller casing could present different results.

For the cases with OBM present in cement channels, the modelled results are undetectable assuming a 13.3% accuracy of the neutron logging tool. In fact, there seems to be very little difference in attenuation at all. A possible reason is that the attenuation coefficients of OBM and cement are similar at the high energy levels considered.

Gas channels in the cement and foamed cement cause a severe reduction in attenuation. This seems to cause a cumulative effect: Less attenuation through a gas channel will cause the neutrons to enter the next interface with less energy than it would have without the channel. Since Σ_t increases with decreasing energy, they will also be attenuated less through this interface and so on. The resulting total attenuation deviates a lot from the base case, even in small channels, and eventually end up outside the energy range which is considered detectable. Therefore it is not possible, to evaluate gas channels or foamed cement based on the results from the cases considered.

We have in this work only compared the relative response between foamed cement and class G cement, but for actual applications we will be well aware of what material we are cementing with. Therefore, the learning from this part of the analysis is that neutrons can penetrate foamed cement and is distinguishable from fluids but is not attenuated enough to reach detectable energy for the cases considered in this work. A possible solution for this is to increase the spacing further for foamed cement applications so that neutrons must travel further. If acquiring detectable results with increased spacing, one can simulate response of channeling thereafter. This is suggested for further work.

6.2.5 *Limitations of the Analysis*

Modelling of neutrons and their interactions with surroundings is complex at high energy and depends heavily on probability. Therefore, there is an indefinite number of other potential cases which might occur and there is not one exact solution to how much each neutron is going to be attenuated for the given cases. Simplifications and assumptions were made, in particular regarding the initial energy of the neutron, the neutron traveling path, scattering energy loss and energy dependence of Σ_t . However, the cases defined in this work are realistic and the relative response of materials are considered viable.

In the neutron attenuation simulations, it was assumed an initial neutron energy of 4.5 MeV. For some source types, especially generators such as the D-T source, one specific neutron energy is generated. For chemical sources such as Am-Be however there is a wide range of possible energy generated (Figure 3-3) from very low energy up to nearly 11 MeV. This implies that some neutrons will be of higher energy and remain undetected, while those in the lower end of the spectrum will be absorbed quickly. Furthermore, we have assumed that neutrons travel the shortest path from source to cement/formation interface and returns to the detector with varying spacing. The actual path of travel for neutrons is potentially much more complex, causing increased traveling distance. Moreover, in this analysis we have essentially tracked the attenuation of a single neutron traveling through different media. But due to the very high yield of neutron sources ($\sim 10^8$ neutrons/s) it is more appropriate to say that a resulting higher or lower attenuation in this work resembles a likely decreased or increased count rate at the detector compared to the base case of good cement.

To make the modelling possible it had to be assumed constant Σ_t between each simulated step. The strong energy dependency of Σ_t has been illustrated in Figure 5-1, making this assumption relatively weak. However, Σ_t generally increases with decreasing energy, meaning that actual attenuation is likely to be higher than what is reported in this work.

A limitation of the analysis is that we assumed the tool not to be centered, but pressed against the wall. This was considered adequate as the purpose was to study the neutron interactions in cement. Even though it is a viable case, the tool itself will not be measuring symmetrically around the circumference of the wellbore. Neutron tools do indeed present the possibility of centering the neutron tool, by which it will be surrounded by whatever fluid is present in the wellbore. A possibility is drilling fluids such as OBM or WBM which has been shown to cause significant attenuation to neutrons, and effects of these are corrected for on actual logs.

We have seen that gas channels are likely to produce a relative contrast in count rate compared to class G cement. We have also seen that foamed cement, even though attenuating less than class G cement, could still be detectable. One case that was not simulated was presence of gas channel in foamed cement. A concern is that such scenario could produce undetectable results. However, by increasing spacing or reducing initial neutron energy it could be possible to establish a good foamed cement log. If already having established a base case for good foamed cement it could be argued that the presence of gas would simply cause a reduction in count rate.

A limitation of the investigated technology is that it is not a direct measurement of cement integrity, but rather measures neutron attenuation or presence of tracer material which in turn is related to parameters determining if the cement has good integrity. This is, however, also the case for other logs. For example, CBL logs measure acoustic coupling at the cement interfaces. As of today, only a pressure test can verify cement integrity directly.

Even though it has been shown that neutron logging could find applications in detecting channels in cement, this does not necessarily mean that it is a measure of bonding. In cases where there is presence of cement near casing, it does not necessarily mean it is well bonded to the casing. Therefore, it is suggested for further research to determine the elements responsible for the bonding, and thereafter use for example neutron spectroscopy to verify the presence of these.

6.3 Tool, HSE and Cost

Neutron logging technology with associated tools is well-established, and this thesis mainly focuses on applying available technology for a different purpose. Therefore, it seems fair to believe that current tools are able to withstand the operational conditions in a wellbore. Considering the small available tool sizes, there should be no restrictions in applying neutron logging technology in terms of the physical properties of the tools themselves.

The traditional use of radioactive Am-Be sources has been shown to rise concerns in terms of HSE. Several alternatives are being evaluated in recent and ongoing studies, each having their advantages and possible limitations. D-T generators seem beneficial as they have little environmental concerns and have been shown in this work to produce sufficiently high energy neutrons to penetrate two casing strings. It is a concern, however, that high energy neutrons have higher depth of investigation as we want to limit the logging to the cement. For single casing cement evaluation purposes it could possibly be advantageous with sources emitting lower energy neutrons to limit the depth of investigation.

In terms of cost, it is shown that neutron logging technology is likely to increase logging cost compared to the CBL log depending on the application and requirements. Inelastic logging is much slower than both conventional neutron logging and CBL, and has the additional cost of the tracer material itself for this application. Even though the potential consequences of a poor cement log are hard to quantify, they are the same for both current and proposed cement logging technology. Consequently, the potential gain is simply if neutron logs can do a better job, whereas the potential loss is the additional expenses. Furthermore, if neutron log cannot fully replace CBL log there will be a cost increase of around 50% to run both logs in the same operation.

The cost discussed so far has been regarding logging of an entire cement column, where difference in logging speed would produce significant cost differences. For P&A purposes, however, it is reported by NORSOK (2013) that a cross sectional barrier minimum needs to have length of 30 meters of cement behind casing, given it is verified by logging. Consequently, even though there are cost differences these will not be as significant when logging such short sections. Nevertheless, the potential advantages both in cost and HSE with rig-less P&A are so large that it is not a question about whether the technology will be economically viable but rather if it is able to

provide satisfactory evaluation of the cement behind casing for the approximately 300 P&A operations due on the Norwegian Continental Shelf before 2025.

6.4 Cement Evaluation by Neutron Tracer Logging

6.4.1 Neutron Attenuation in Cement with Tracer Material

From this study we have seen that adding a small fraction of tracer material such as boron and gadolinium to the cement unexpectedly caused less attenuation in the studied cases. A possible explanation is that the neutrons does not reach an energy level in the cement where Σ_t starts increasing rapidly. This is particularly the case for gadolinium which requires energy less than 1 eV to be significant. Essentially it seems that the tracer cements attenuate less because the inefficient boron and gadolinium makes the concentration of hydrogen slightly lower.

By isolating the absorption probability, it was shown a stable difference between cements with tracers and conventional cement. Furthermore, that the probability of absorption to occur increased in the lower energy range as expected. Boron could be preferable over gadolinium as it reaches relatively high probability of absorbing neutrons at higher energy. Based on this it can be argued that adding boron and gadolinium to the cement is unlikely to produce more attenuation of neutrons, but a reduction in count rate at the detector can still occur by increased absorption.

A possible limitation for tracer logging in cement is the effect the mixed tracer would have on the cement itself and its setting properties such as bonding and compressive strength. The purpose of adding such tracers to the cement is to evaluate defects, but if it affects the setting properties mixing in tracers becomes unreasonable. Secondly, if addition of high Σ_{abs} tracers to the cement gives effective response on the neutron log, the cement itself could act as a neutron shield around the well. Neutron logging applications involving formation evaluation may become more difficult or lost.

Wells due for plug and abandonment (P&A) often require logging of the cement behind casing to verify its integrity as a permanent barrier. An obvious limitation is that the tracer would have to be present in the cement slurry before setting, hence this method is not applicable in already cemented wells. However, its potential for future drilled and cemented wells remain.

Studies presented in section 5.6 argue both for and against the potential effect tracers have on neutron logging. Chen et al. (2017) characterized fractures by adding small amount of Gd_2O_3 to the fracturing proppant, and Blount et al. (1991) added boron to a solution. A significant difference between these cases and cases presented in this work is that the tracers are mixed into fluids, which also contribute significantly to attenuation. Furthermore, fractures extend beyond the cement/formation interface meaning that neutrons travel further and thus have more distance to be attenuated. The combination of these factors may have caused enough attenuation for the neutrons

to reach the energy range where gadolinium and boron absorption cross section increases rapidly. It does indeed back up the results showing that tracers increase the absorption probability in the cement.

Since the compatibility of tracer materials with the cementing process is unknown, a practical concern arises in terms of cement placement. If cement is contaminated during placement, tracer material could be flushed out of cement and tracer logging would be ineffective. Consequently, using this approach could be more beneficial for secondary cementing.

To summarize, the presented analysis has shown that the attenuation of neutrons is likely to be lower through cement with tracers than for normal cement for the considered energy. Even though the absorption probability is higher in boron-containing cement it is not known how this effect will compare with the lower attenuation. Consequently, there is not foundation to say that presence of gadolinium or boron will produce detectable results in this regard.

6.4.2 Spectroscopy for Cement Evaluation

By calculation of inelastic macroscopic cross section of elements considered in the analysis, it was found that gadolinium has a relatively high probability to interact inelastically with incoming neutrons. The main concern with spectroscopy is that inelastic scattering mainly occurs at high energy. Consequently, a neutron source emitting high energy neutrons is required. This in turn increases the depth of investigation which is undesirable when we wish to limit the logging to the cement behind casing. Neutron tools measuring inelastic cross section such as the RST include a D-T source emitting 14.1 MeV neutrons. It was observed in the analysis however, that the interactions with gadolinium occurs at a wide range of energy starting at approximately 64 KeV. Other elements such as O, C and Ca require energy at or above 4.5 MeV for inelastic interaction to occur and hence would be undetectable in the cases considered in this work where we have assumed an initial emitted energy of 4.5 MeV. Consequently, it could be advantageous to operate at lower energy levels to isolate the gadolinium response.

When running neutron spectroscopy, we want to highlight the presence of elements of significant inelastic cross section. Gadolinium is usually not an element found in abundance near a petroleum well. Given the relatively high inelastic cross section of gadolinium, it seems reasonable that the presence of gadolinium should cause a detectable gamma ray response. It is not known if the measured gamma ray response for neutron logging is possible to relate to the cement radius such as achieved by Kline et al. (1986) (section 5.6.3), nor the required concentration of gadolinium to produce a detectable result. These are proposed subjects for future work.

To summarize, potential advantages of this technique based on the papers discussed include:

- Non-radioactive tracers.

- Does not require punched holes or perforations to inject neutron absorbing material as it would be already mixed in the cement.
- No time limit compared to the gamma ray application studies where only a limited time window was available due to decay of radioactive isotopes.

7 SUGGESTIONS FOR FUTURE WORK

- Monte Carlo N-Particle (MCNP) transport simulations of similar cases as defined in this work.
- Potential utilization of neutron log for foamed cement evaluation. We have shown that neutrons can penetrate foamed cement. The challenge is to attenuate the neutrons enough to produce detectable results.
- Inelastic scattering by cement added gadolinium tracer: required concentration to produce detectable results, and potential relation to cement radius.
- Experimental work: It has been shown that the neutron log theoretically has potential to evaluate cement behind a single casing. Therefore it is proposed to perform further research either by advanced software modelling such as MCNP or by experimental work. A suggested case is to set up a casing with cement block behind. The cement block can be drilled holes of various sizes and filled with fluids to simulate channels, or the cement can be mixed with tracer material to assess its footprint in neutron spectroscopy.
- Determine which elements are key for cement bonding. Thereafter, use spectroscopy tool to determine presence of such elements. Predict bonding based on presence of key elements and verify against actual data from CBL tool.
- Polarization analysis: further studies on its potential and applicability for casing cement evaluation.

8 CONCLUSION

The results of preliminary simulations and literature presented in this work has given rise to the following conclusions:

- Neutrons has potential to travel from source to the cement/formation interface and be backscattered to the detector without being completely attenuated, also for through-tubing configuration.
- Foamed cement causes less neutron attenuation than class G cement.
- Presence of a channel filled with oil-based mud increases attenuation of neutrons at investigated energy levels in a single casing configuration relative to class G cement.
- Presence of a channel filled with natural gas decreases attenuation of neutrons at investigated energy levels relative to class G cement.
- For single casing configuration, cement channels with gas and oil-based mud can be distinguished from one another, and from intact cement.
- For a through-tubing configuration, results show no indication of potential for cement channel evaluation.
- Am-Be chemical neutron source has HSE concerns.
- Neutron logging is more expensive than CBL logging. Increase in cost must be weighed against possible gains of utilizing the technology. Particularly in P&A, there are potential cost savings and reduced uncertainty during cement evaluation.
- Cement containing small amounts of boron causes higher probability of neutron absorption which may be detectable as a reduction in neutron count rate.

REFERENCES

- Aanestad, O.M., 2000. Radioaktive kilder mistet på sokkelen, Stavanager Aftenblad.
- Aitken, J.D., Adolph, R., Evans, M., Wijeyesekera, N., McGowan, R. and Mackay, D. 2002. Radiation Sources in Drilling Tools: Comprehensive Risk Analysis in the Design, Development and Operation of LWD Tools. Presented at the SPE International Conference on Health, Safety and Environment in Oil and Gas Exploration and Production, Kuala Lumpur, Malaysia. 1/1/2002. <https://doi.org/10.2118/73896-MS>.
- Azar, J.J. and Samuel, G.R., 2007. Drilling Engineering, 1st ed. PennWell Books, Oklahoma.
- Badruzzaman, A., Schmidt, A. and Antolak, A., 2019. Neutron Generators as Alternatives to Am-Be Sources in Well Logging: An Assessment of Fundamentals. SPWLA-2019-v60n1a10, 60(01), 136-170.
- Benge, G. 2014. Cement Evaluation - A Risky Business. Presented at the SPE Annual Technical Conference and Exhibition, Amsterdam, The Netherlands. 2014/10/27/. <https://doi.org/10.2118/170712-MS>.
- Blount, C.G., Copoulos, A.E. and Myers, G.D., 1991. A Cement Channel-Detection Technique Using the Pulsed-Neutron Log. SPE-20042-PA, 6(04), 485-492. <https://doi.org/10.2118/20042-PA>.
- Bois, A.-P., Garnier, A., Rodot, F., Sain-Marc, J. and Aimard, N., 2011. How To Prevent Loss of Zonal Isolation Through a Comprehensive Analysis of Microannulus Formation. SPE-35681-PA, 26(01), 13-31. <https://doi.org/10.2118/124719-PA>.
- Boye, N.C., 2009. Kjemis og Miljølære, 4th ed. Gyldendal, Oslo.
- Buckingham, A., 2003. NMR-modulated neutron scattering. Chemical physics letters, 371(5-6), 517-521.
- Burt, J., Zhou, T., Rose, D.A., Grover, R., Ahmad, S., Nemec, J. and Dunston, J. 2018. A Pulsed Neutron Comparison Between an Open and Casedhole Well: An Alaskan Case Study. Presented at the SPE Western Regional Meeting, Garden Grove, California, USA. 2018/4/22/. <https://doi.org/10.2118/190062-MS>.
- Cameron, I. 2013. SPE "Back to Basics" Bond Log Theory and Interpretation, https://higherlogicdownload.s3.amazonaws.com/SPE/5fc0079d-67a5-4dd9-a56f-190534ef5d3d/UploadedImages/April16_BtoB.pdf (accessed 11/03 2019).
- Carey, F.A. 2018. Hydrocarbons, 18/10, <https://www.britannica.com/science/hydrocarbon> (accessed 26/02 2019).
- Cerullo, N., Bufalino, D. and Daquino, G., 2009. Progress in the use of gadolinium for NCT. Applied Radiation and Isotopes, 67(7, Supplement), 157-160. <https://doi.org/10.1016/j.apradiso.2009.03.109>.
- Chen, Q., Zhang, F., Liu, J.-T., Zhang, Q.-Y., Tian, L.-L. and Wu, H. 2017. A New Borehole Gamma Ray Imaging Method To Determine Hydraulic Fracture Using Gd Neutron Tracer Logging. *Proc.*, SPWLA 58th Annual Logging Symposium.
- Chen, Z., Chaudhary, S. and Shine, J. 2014. Intermixing of Cementing Fluids: Understanding Mud Displacement and Cement Placement. Presented at the IADC/SPE Drilling Conference and Exhibition, Fort Worth, Texas, USA. 03/04 2014. <https://doi.org/10.2118/167922-MS>.
- Chilingarian, G.V. and Vorabutr, P., 1983. Drilling and Drilling Fluids, Updated textbook ed., Amsterdam.
- Continental Alloys & Services, 2019. L80 - Chemical Composition. <https://www.contalloy.com/products/grade/l80> (accessed 05/02 2019).
- Copley, J.R.D. 2011. Neutron Scattering. NIST Center for Neutron Research, https://ncnr.nist.gov/summerschool/ss11/pdf/SS2011_Copley_NeutronScattering.pdf (accessed 12/03 2019).
- Darling, T., 2005. Well logging and formation evaluation. Elsevier, USA.

- Das, P.K., 2017. Measurement of Relative Intensity of the Discrete γ Rays From the Thermal Neutron Capture Reaction $^{155,157}\text{Gd}(n,\gamma)$ Using ANNRI Detector (JPARC), Okayama University.
- Date, A.W., 2011. Analytic combustion: with thermodynamics, chemical kinetics and mass transfer, 1st ed. Cambridge University Press, New York.
- Desport, O. and Crowe, J. 2008. Pulsed Neutron Logging Through Multiple Casings. Presented at the SPE Western Regional and Pacific Section AAPG Joint Meeting, Bakersfield, California, USA. 2008/1/1/. <https://doi.org/10.2118/110501-MS>.
- Dewan, J.T., Jacobson, L.A. and Johnstone, C.W., 1973. Thermal Neutron Decay Logging Using Dual Detection. SPWLA-1969-vXn2a2, 14(05), 22.
- Ellis, D.V. and Singer, J.M., 2007. Well Logging for Earth Scientists, 2nd ed. 692. Springer, The Netherlands.
- Elmahroug, Y., Tellili, B. and Souga, C., 2013. Calculation of fast neutron removal cross-sections for different shielding materials. Journal of Physics Research, 3(2), 7-16.
- Encana. 2016. Wellbore Construction, <https://www.encana.com/sustainability/environment/water/protection/construction.html> (accessed 22/01 2019).
- Ferris, N. and Goergen, S. 2017. Gadolinium Contrast Medium (MRI Contrast Agents). Inside Radiology, <https://www.insideradiology.com.au/gadolinium-contrast-medium/> (accessed 22/02 2019).
- Fertl, W.H., Pilkington, P.E. and Scott, J.B., 1974. A Look at Cement Bond Logs. SPE-20314-PA, 26(06), 607-617. <https://doi.org/10.2118/4512-PA>.
- Fidaner, O. 2017. Downhole Multiphase Flow Monitoring Using Fiber Optics. Presented at the SPE Annual Technical Conference and Exhibition, San Antonio, Texas, USA. 2017/10/9/. <https://doi.org/10.2118/187415-MS>.
- FitzGerald, S., Neumann, D., Rush, J., Bentz, D. and Livingston, R., 1998. In situ quasi-elastic neutron scattering study of the hydration of tricalcium silicate. Chemistry of Materials, 10(1), 397-402.
- Fornell, D., 2018. The Debate Over Gadolinium MRI Contrast Toxicity, Imaging Technology News.
- Gabolde, G. and Nguyen, J.-P., 1999. Drilling Data Handbook, 7th ed. Éditions Technip, Paris.
- Gabrovšek, R., Vuk, T. and Kaučič, V., 2006. Evaluation of the hydration of Portland cement containing various carbonates by means of thermal analysis. Acta Chim. Slov., 53, 159-165.
- Gadeken, L.L. and Smith Jr, H.D., 1996. Method for determining cement thickness in a well annulus. Google Patents.
- Gaspar, A.M., Busch, S., Appavou, M.-S., Haeussler, W., Georgii, R., Su, Y. and Doster, W., 2010. Using polarization analysis to separate the coherent and incoherent scattering from protein samples. Biochimica et Biophysica Acta -Proteins 1804(1), 76-82.
- Glover, P.W.J., 2000. Petrophysics, University of Aberdeen, UK.
- Gopinath, D.V., 1983. Use of rare earth oxides in the concrete for reactor shields, International Atomic Energy Agency.
- Gowida, A.H., Ahmad, Z., Elkhatny, S. and Mahmoud, M. 2018. Cement Evaluation Challenges. Presented at the SPE Kingdom of Saudi Arabia Annual Technical Symposium and Exhibition, Dammam, Saudi Arabia. 2018/8/16/. <https://doi.org/10.2118/192360-MS>.
- Greene, D. and Thomas, R., 1969. The attenuation of 14 MeV neutrons in steel and polyethylene. Physics in Medicine Biology, 14(1), 45.
- Grover, R., 2017. Technology Update: Tool Enables Complete Cased-Hole Formation Evaluation, Reservoir Saturation Modeling. SPE-20314-PA, 69(10), 18-20. <https://doi.org/10.2118/1017-0018-JPT>.

- Guillot, D. and Nelson, E., 2006. Well Cementing. Schlumberger Educational Services, 2 ed., Sugarland.
- Guner, D., Ozturk, H. and Erkayaoglu, M., 2016. Investigation of the elastic properties of Class G cement. *Structural Concrete*, 18(1). <https://doi.org/10.1002/suco.201600020>.
- Haddad, M.Y., 2017. Theoretical Study on Utilization of X-ray Techniques for Verification of Casing Cement, University of Stavanger, Norway.
- Harness, P.E. and Frank, W.E., 1996. Neutron Logs Improve Interpretation of Foamed Cement, Even in Concentric Casing. *SPE-35681-PA*, 11(04), 208-213. <https://doi.org/10.2118/35681-PA>.
- Helmenstine, T. 2018. Abundance of Elements in Earth's Crust – Periodic Table and List, <https://sciencenotes.org/abundance-of-elements-in-earths-crust-periodic-table-and-list/> (accessed 22/02 2019).
- Hewlett, P. and Lea, F.M., 2003. *Lea's chemistry of cement and concrete*, 4th ed. . Elsevier, London.
- Hilchie, D.W., Mills, W.R., Dennis, C.L. and Givens, W.W., 1969. Some Aspects Of Pulsed Neutron Logging. *SPWLA-1969-vXn2a2*, 10(02).
- Holbert, K.E. 2014. Atomic Number Density, <http://holbert.faculty.asu.edu/eee460/NumberDensity.pdf> (accessed 22/03 2019).
- Hornak, J.P. 1997. The Basics of NMR, <http://www.cis.rit.edu/htbooks/nmr/> (accessed 04/03 2019).
- Hossain, M.E., 2016. *Fundamentals of Drilling Engineering : MCQs and Workout Examples for Beginners and Engineers*. John Wiley & Sons, Incorporated, Somerset, USA.
- Hveding, F. and Bukhamsin, A. 2018. Distributed Fiber Optic Sensing – A Technology Review for Upstream Oil and Gas Applications. Presented at the SPE Kingdom of Saudi Arabia Annual Technical Symposium and Exhibition, Dammam, Saudi Arabia. 2018/8/16/. <https://doi.org/10.2118/192323-MS>.
- ICRP, 2007. The 2007 Recommendations of the International Commission on Radiological Protection. ICRP Publication 103, *Ann. ICRP* 37 (2-4).
- Jennings, S.S., Al-Ansari, A.A. and Al-Yami, A.S. 2003. Gas Migration After Cementing Greatly Reduced. Presented at the Middle East Oil Show, Bahrain. 2003/1/1/. <https://doi.org/10.2118/81414-MS>.
- Johnson, D.E. and Pile, K.E., 2006. *Well logging in Nontechnical Language*, 2 ed. . PennWell Books, Oklahoma.
- Kennedy, M., 2015. *Practical petrophysics. Developments in Petroleum Science*, 62. Elsevier Science.
- Khalifeh, M., Gardner, D. and Haddad, M.Y. 2017. Technology Trends in Cement Job Evaluation Using Logging Tools. Presented at the Abu Dhabi International Petroleum Exhibition & Conference, Abu Dhabi, UAE. 2017/11/13/. <https://doi.org/10.2118/188274-MS>.
- Kline, W.E., Kocian, E.M. and Smith, W.E. 1986. Evaluation of Cementing Practices by Quantitative Radiotracer Measurements. Presented at the SPE/IADC Drilling Conference, Dallas, Texas. 1986/1/1/. <https://doi.org/10.2118/14778-MS>.
- Kofstad, P.K. and Pedersen, B., 2014. Gadolinium, *Store Norske Leksikon*.
- Kotlarchyk, M. and Thurston, G., 2017. A framework for modeling polarized neutron scattering from NMR spin-modulated systems. *Journal of Physics: Conference Series*, 862(1).
- Lavrov, A. and Torsæter, M., 2016. *Physics and mechanics of primary well cementing*. SpringerBriefs in Petroleum Geoscience & Engineering. Springer.
- Mason, T.O. and Lea, F.M. 2018. Cement. *Encyclopædia Britannica, inc.*, <https://www.britannica.com/technology/cement-building-material/Extraction-and-processing#ref609183> (accessed 31/01 2019).
- McAllister, D.R. 2016. *Neutron Shielding Materials*. PG Research Foundation, <https://www.eichrom.com/wp-content/uploads/2018/02/neutron-attenuation-white-paper-by-d-m-rev-2-1.pdf> (accessed 22/03 2019).

- McLean, R.H., Manry, C.W. and Whitaker, W.W., 1967. Displacement Mechanics in Primary Cementing. SPE-20314-PA, 19(02), 251-260. <https://doi.org/10.2118/1488-PA>.
- MirionTechnologies. 2019. Types of Ionizing Radiation, <https://v2.mirion.com/introduction-to-radiation-safety/types-of-ionizing-radiation/#> (accessed 20/02 2019).
- Morris, C.W., Sabbagh, L., Wydrinski, R., Hupp, J.L., van Kuijk, R. and Froelich, B. 2007. Application of Enhanced Ultrasonic Measurements for Cement and Casing Evaluation. Presented at the SPE/IADC Drilling Conference, Amsterdam, The Netherlands. 2007/1/1/. <https://doi.org/10.2118/105648-MS>.
- Munter, A. 2017. Neutron Scattering Lengths and Cross Sections. NIST Center for Neutron Research, <https://www.nist.gov/ncnr/planning-your-experiment/sld-periodic-table> (accessed 06/02 2019).
- NAS, 2008. Radiation Source Use and Replacement: Abbreviated Version. In: U.N.A.o. Science (Editor). The National Academies Press, Washington, DC, pp. 232.
- Nayfeh, T.H., Wheelis, W.B., Jr. and Leslie, H.D., 1986. The Fluid-Compensated Cement Bond Log. SPE-20042-PA, 1(04), 335-341. <https://doi.org/10.2118/13044-PA>.
- Nikitin, A., Roberts, L.P., Inanc, F. and Kopal, M.M. 2011. Neutron Porosity Measurements Using A Pulsed Neutron Generator And Li-6 Glass Neutron Detectors. Presented at the SPWLA 52nd Annual Logging Symposium, Colorado Springs, Colorado. 2011/5/14/.
- NNDC. 2011. Evaluated Nuclear Data File (ENDF) Retrieval and Plotting. Brookhaven National Laboratory, <https://www.nndc.bnl.gov/sigma/index.jsp?as=10&lib=endfb7.1&sub=10> (accessed 28/02 2019).
- NORSOK, 2013. NORSOK Standard D-010. Well integrity in drilling and well operations, Rev. 4.
- NRC. 2017. Radiation Basics. United States Nuclear Regulatory Commission, <https://www.nrc.gov/about-nrc/radiation/health-effects/radiation-basics.html#alpha> (accessed 22/03 2019).
- NRC. 2019. Category of radioactive sources. US National Research Council, <https://www.nrc.gov/reading-rm/basic-ref/glossary/category-of-radioactive-sources.html> (accessed 22/03 2019).
- Osundare, O.S., Teodoriu, C., Falcone, G. and Ichim, A., 2018. Estimation of plugging and abandonment costs based on different EU regulations with application to geothermal wells. (43rd Workshop on Geothermal Reservoir Engineering, Stanford University).
- Ottolenghi, A., Smyth, V. and Trott, K., 2013. Assessment of cancer risk from neutron exposure—The ANDANTE project. Radiation Measurements, 57, 68-73.
- Pilkington, P.E., 1992. Cement Evaluation - Past, Present, and Future. SPE-20314-PA, 44(02), 132-140. <https://doi.org/10.2118/20314-PA>.
- Piotrowski, T., Tefelski, D., Sokolowska, J. and Jaworska, B., 2015. NGS-Concrete—New Generation Shielding Concrete against ionizing radiation—the potential evaluation and preliminary investigation. ActaPhys Pol A.
- Pynn, R., 2009. Neutron scattering—a non-destructive microscope for seeing inside matter, Neutron applications in earth, energy and environmental sciences. Springer, pp. 15-36.
- Pynn, R. 2017. Neutron Scattering. Los Alamos National Library, https://neutrons.ornl.gov/sites/default/files/intro_to_neutron_scattering.pdf (accessed 08/03 2019).
- Ragheb, M. 2006. Neutron Collision Theory, <http://mragheb.com/NPRE%20402%20ME%20405%20Nuclear%20Power%20Engineeri ng/Neutron%20Collision%20Theory.pdf> (accessed 20/01 2019).
- Rambow, F.H.K., Dria, D.E., Childers, B.A., Appel, M., Freeman, J.J., Shuck, M., Poland, S.H. and Dominique, T., 2010. Real-Time Fiber-Optic Casing Imager. SPE-109941-PA, 15(04), 1089-1097. <https://doi.org/10.2118/109941-PA>.

- REMM. 2019. Radiological Dispersal Devices (RDDs). Radiation Emergency Medical Management, US Department of Health & Human Services, <https://www.remm.nlm.gov/rdd.htm#isotopes> (accessed 22/03 2019).
- Rider, M. and Kennedy, M., 2011. The Geological Interpretation of Well Logs, 3rd ed. Rider-French Consulting Ltd., Scotland.
- Rinard, P., 1991. Neutron interactions with matter. Passive Nondestructive Assay of Nuclear Materials(375-377).
- Schlumberger. 2015. Wireline Services Catalog, https://www.slb.com/~media/Files/evaluation/catalogs/2015_wireline_services_catalog.pdf (accessed 14/02 2019).
- Schlumberger. 2018. Pulsar Multifunction Spectroscopy Service, https://www.slb.com/~media/Files/evaluation/brochures/wireline_open_hole/petrophysic/s/pulsar-spectroscopy-br.pdf (accessed 17/01 2019).
- Schlumberger. 2019a. Hydrogen Index. Schlumberger Oilfield Glossary, https://www.glossary.oilfield.slb.com/en/Terms/h/hydrogen_index.aspx (accessed 16/01 2019).
- Schlumberger. 2019b. Packer Fluid. Schlumberger Oilfield Glossary, https://www.glossary.oilfield.slb.com/en/Terms/p/packer_fluid.aspx (accessed 23/04 2019).
- Schlumberger. 2019c. Pulsed neutron determination of reservoir saturation, porosity, and borehole fluid flow and three-phase holdup. Schlumberger, https://www.slb.com/services/production/production_logging/reservoir_saturation_tool.aspx (accessed 16/01 2019).
- Schlumberger. 2019d. Spacers. Schlumberger Oilfield Glossary, <https://www.glossary.oilfield.slb.com/en/Terms/s/spacer.aspx> (accessed 29/01 2019).
- Schlumberger, D., 1984. Cementing technology. Nova Communications Limited, London.
- Schweika, W., 2012. Polarized Neutron Scattering and Polarization Analysis. Scattering Methods for Condensed Matter Research: Towards Novel Applications at Future Sources 2019.
- Sears, F.W., Zemansky, M.W. and Young, H.D., 2012. University physics with modern physics, 13 ed. Addison-Wesley.
- Seshadri, B., 1989. Transmission measurements of DT neutrons through gadolinium loaded concrete and polypropylene. Journal of Nuclear Science, 26(9), 881-886. <https://doi.org/10.1080/18811248.1989.9734400>.
- Sharp, T. 2017. What is an Atom?, <https://www.livescience.com/37206-atom-definition.html> (accessed 20/02 2019).
- Simpson, G., Jacobson, L. and Salazar, F. 1998. Evaluating and Monitoring Reservoirs Behind Casing With a Modern Pulsed Neutron Tool. Presented at the International Petroleum Conference and Exhibition of Mexico, Villahermosa, Mexico. 1998/1/1/. <https://doi.org/10.2118/39872-MS>.
- Simpson, J.P., 1969. Stability and Corrosivity of Packer Fluids. PETSOC-69-01-04, 8(01), 24-29. 10.2118/69-01-04.
- Sommer, F.S. and Jenkins, D.P. 1993. Channel Detection Using Pulsed Neutron Logging in a Borax Solution. Presented at the SPE Asia Pacific Oil and Gas Conference, Singapore. 1993/1/1/. <https://doi.org/10.2118/25383-MS>.
- Sowerby, M.G. and Forrest, R.A. 2017. Neutron cross-sections. Kaye&Lady, http://www.kayelaby.npl.co.uk/atomic_and_nuclear_physics/4_7/4_7_2.html (accessed 24/04 2019).
- SPE-International. 2013. Tail Cement. PetroWiki, https://petrowiki.org/Glossary:Tail_cement (accessed 29/04 2019).
- SPE-International. 2015a. Drilling Fluid Types. Petrowiki, https://petrowiki.org/Drilling_fluid_types (accessed 28/01 2019).

- SPE-International. 2015b. Neutron Porosity Logging Tools. PetroWiki, https://petrowiki.org/Nuclear_logging_while_drilling#Neutron-porosity_log_tools (accessed 20/04 2019).
- SPE-International. 2015c. Pulsed Neutron Lifetime Logs. PetroWiki, https://petrowiki.org/Pulsed_neutron_lifetime_logs (accessed 28/01 2019).
- Stark, G. 2018. X-ray. Encyclopædia Britannica, inc. , <https://www.britannica.com/science/X-ray> (accessed 21/01 2019).
- Stewart, D. 2012. Gadolinium Element Facts/Chemistry, <https://www.chemicool.com/elements/gadolinium.html> (accessed 22/02 2019).
- Sun, Y., Xue, Z. and Hashimoto, T., 2018. Fiber optic distributed sensing technology for real-time monitoring water jet tests: Implications for wellbore integrity diagnostics. *Journal of Natural Gas Science and Engineering*, 58, 241-250. <https://doi.org/10.1016/j.jngse.2018.08.005>.
- Sørheim, M. 2018. Cutting Plugging Cost, 03/01 2018, <https://www.hartenergy.com/exclusives/cutting-plugging-costs-176895> (accessed 22/03 2019).
- Thomas, S., Smith, C.H., Williams, B.W. and Hamilton, L., 2016. Ultrasonic-Log Response in Lightweight-Cement Conditions. SPE-35681-PA, 30(04), 326-333. <https://doi.org/10.2118/171612-PA>.
- Thorstensen, E. 2019. Roadmap for New P&A Technologies. Norsk Olje&Gass, <https://www.norskoljeoggass.no/contentassets/f60cf93f2c9c4c129b0a73303ff8081c/00---welcome.pdf> (accessed 16/04 2019).
- Total. 2014. EDC 95-11, http://www.icckor.com/admin/data/product/1512250001_2.pdf (accessed 18/02 2019).
- Trefil, J., Bertsch, G.F. and McGrayne, S.B. 2018. Atom. Encyclopædia Britannica, inc., <https://www.britannica.com/science/atom> (accessed 21/01 2019).
- UiS, 2016. Øving i Bore- og Brønnvæsker (PET210). Universitetet i Stavanger.
- United States Department of Agriculture, 2005. A Rare-Earth Approach to Tracing Soil, *AgResearch Magazine*.
- Walker, I. and Carr, D. 2003. Fibre Optic Leak Detection. Presented at the Offshore Technology Conference, Houston, Texas. 2003/1/1/. <https://doi.org/10.4043/15360-MS>.
- Wang, W., Wan, X., Chen, H., Zhang, Y. and Wang, J. 2000. Application of Boron(Gadolinium) Neutron Lifetime Logging in Oil Field Development. Presented at the SPE Asia Pacific Oil and Gas Conference and Exhibition, Brisbane, Australia. 2000/1/1/. <https://doi.org/10.2118/64472-MS>.
- Wikipedia. 2019. Abundance of Elements in Earth's Crust, https://en.wikipedia.org/wiki/Abundance_of_elements_in_Earth%27s_crust (accessed 22/02 2019).
- Wilson, A., 2017. Cement Placement With Tubing Left in Hole During Plug-and-Abandonment Operations. SPE-20314-PA, 69(05), 85-86. 10.2118/0517-0085-JPT.
- Wu, Q., Nair, S., Shuck, M., van Oort, E., Guzik, A. and Kishida, K., 2017. Advanced distributed fiber optic sensors for monitoring real-time cementing operations and long term zonal isolation. *Journal of Petroleum Science and Engineering*, 158, 479-493. <https://doi.org/10.1016/j.petrol.2017.08.072>.
- Xu, L., Huiszoon, C. and Schultz, W., 2010. A Comprehensive Investigation of Source Effects On Neutron Porosity Response For Logging-While-Drilling Measurements. SPWLA-2019-v60n1a10, 51(03), 14.
- Yip, S., 2014. Nuclear radiation interactions. World Scientific Publishing Company.
- Zhou, T., Rose, D., Millot, P., Grover, R., Beekman, S., Amin, M.F.M., Zamzuri, M.D.B., Ralphie, B. and Zakwan, Z. 2018. A Comprehensive Neutron Porosity From a Pulsed Neutron Logging Tool. Presented at the SPWLA 59th Annual Logging Symposium, London, UK. 2018/6/2/.

Zhou, T., Rose, D., Quinlan, T., Thornton, J., Saldungaray, P., Gerges, N., Bin Mohamed Noordin, F. and Lukman, A. 2016. Fast neutron cross-section measurement physics and applications. *Proc.*, SPWLA 57th Annual Logging Symposium.

APPENDIX A – DATA INTERPOLATION

```
clear all
close all

ev_vector = logspace(-4,6.6532,10000)'; % Evenly distributed between 10^-4 and 4.5*10^6

load('barns_B'); % Insert sigma file name, downloaded from online database
load('ev_B'); % Insert corresponding energy file name

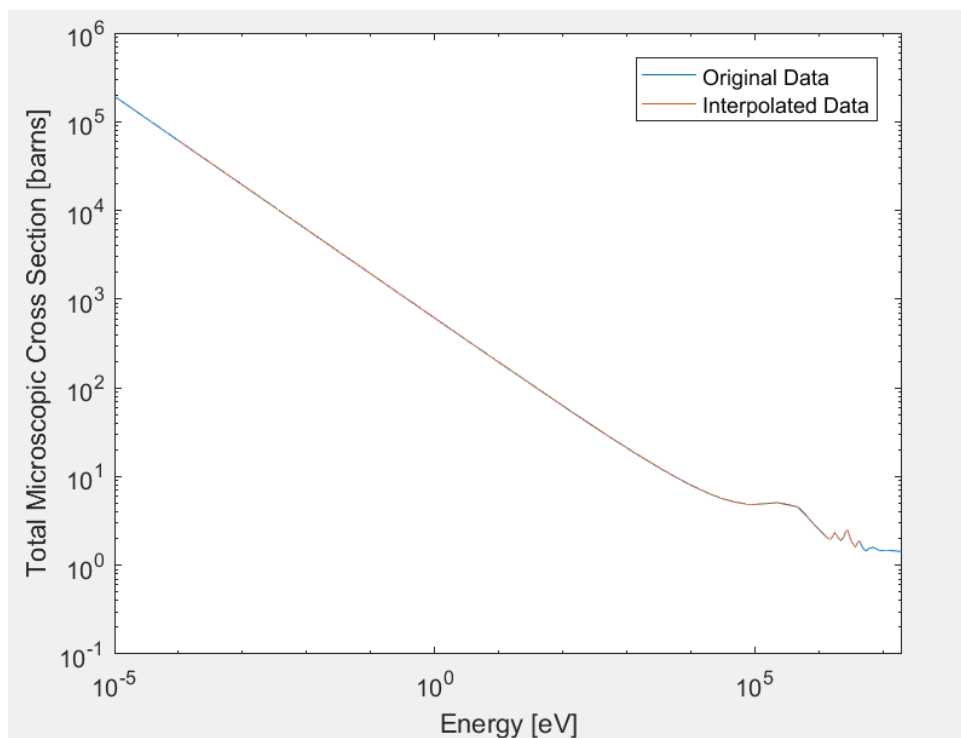
x = ev_B;
y = barns_B;

xq = ev_vector;

[x, index] = unique(x); % Make sure no duplicates which causes interpolation error
yq = interp1(x, y(index), xq); % Interpolate

loglog(x,y);
hold on
loglog(xq,yq); % Plot original vs interpolated values to check validity
xlabel('Energy [eV]');
ylabel('Total Microscopic Cross Section [barns]');
legend('Original Data','Interpolated Data');
axis([10^-5 20*10^6 10^-1 10^6])

barns_int_0 = yq; % Array to be saved and imported to Excel
```



APPENDIX B – THERMAL NEUTRON CALCULATIONS

<i>ELEMENT</i>	σ_t [barn]	u [g/mol]	ρ [g/cm ³]	Ni [at/cm ³]	Σ_t [cm ⁻¹]
<i>C</i>	5.56	12.01	2.26	1.13E+23	0.630
<i>H</i>	82.35	1.01	0.07	4.18E+22	3.444
<i>Cl</i>	50.33	35.45	3.21	5.46E+22	2.747
<i>Fe</i>	14.18	55.85	7.87	8.49E+22	1.204
<i>Al</i>	1.73	26.98	2.70	6.03E+22	0.105
<i>Si</i>	2.34	28.09	2.33	5.00E+22	0.117
<i>N2</i>	13.41	28.04	0.00125	2.69E+19	0.00036
<i>He</i>	1.35	4.44	0.18	2.43E+22	0.033
<i>Si</i>	2.34	28.09	2.33	5.00E+22	0.117
<i>S</i>	1.56	32.07	1.96	3.68E+22	0.057
<i>O</i>	4.23	15.60	1.43	5.52E+22	0.234
<i>Ca</i>	3.26	40.08	1.55	2.33E+22	0.076
<i>Mg</i>	3.77	24.31	1.74	4.31E+22	0.163
<i>K</i>	4.06	39.10	0.86	1.32E+22	0.054
<i>Gd</i>	259000.00	156.90	7.89	3.03E+22	7843.408
<i>B</i>	4000.00	10.81	2.37	1.32E+23	528.072

Transmission [%]

<i>ELEMENT</i>	x [mm]							
	0	1	3	5	10	15	20	100
<i>C</i>	100.00	93.90	82.79	72.99	53.28	38.89	28.39	0.18
<i>H</i>	100.00	70.87	35.59	17.87	3.19	0.57	0.10	0.00
<i>Cl</i>	100.00	75.98	43.86	25.32	6.41	1.62	0.41	0.00
<i>Fe</i>	100.00	88.66	69.68	54.77	30.00	16.43	9.00	0.00
<i>Al</i>	100.00	98.96	96.91	94.91	90.08	85.49	81.14	35.17
<i>Si</i>	100.00	98.84	96.56	94.33	88.97	83.93	79.16	31.09
<i>N2</i>	100.00	100.00	99.99	99.98	99.96	99.95	99.93	99.64
<i>He</i>	100.00	99.67	99.02	98.38	96.78	95.22	93.67	72.12
<i>Si</i>	100.00	98.84	96.56	94.33	88.98	83.93	79.17	31.10
<i>S</i>	100.00	99.43	98.30	97.18	94.43	91.77	89.18	56.40
<i>O</i>	100.00	97.69	93.23	88.98	79.17	70.45	62.69	9.68
<i>Ca</i>	100.00	99.24	97.75	96.27	92.69	89.24	85.91	46.80
<i>Mg</i>	100.00	98.39	95.24	92.20	85.00	78.37	72.25	19.69
<i>K</i>	100.00	99.47	98.41	97.36	94.79	92.28	89.85	58.55
<i>Gd</i>	100.00	0.00	0.00	0.00	0.00	0.00	0.00	0.00
<i>B</i>	100.00	0.00	0.00	0.00	0.00	0.00	0.00	0.00

Potential Utilization of Neutron Logging Technology for Casing Cement Evaluation - A Theoretical Study

Espen Dommersnes¹, Mahmoud Khalifeh¹,

¹Dept. of Energy and Petroleum Engineering, University of Stavanger, Norway

Abstract

Reliable cement evaluation is crucial for well integrity and optimal production. Current cement evaluation technologies have limitations and a preliminary analysis is performed to assess neutron logging for this purpose. Basic modelling has been performed to study neutron attenuation for several realistic cases including good cement, channeled cement, foamed cement and through-tubing configuration. For a comprehensive review, other aspects such as HSE, cost and alternative approaches have also been assessed.

Achieved results show that neutrons have the potential to travel to cement-formation interface and return to the detector without being completely attenuated for all cases considered. For single casing configurations, results indicate that cement channels produce distinguishable results from intact cement. For through-tubing logging it cannot be concluded that detected results are distinguishable. Even though neutron logging itself is likely to be more costly than cement bond logs, potential benefits in terms of other cost savings and decrease in HSE risks must also be considered.

Introduction

When a casing is placed inside a drilled wellbore, it is cemented in place. The purpose of the cement is not only to hold the casing in place and protect it from corrosion, but among others also providing zonal isolation to avoid unwanted flow of fluids to surface (Guillot and Nelson, 2006). To ensure the cement fulfils its purposes, it must be logged. Cement logging technology has been a hot research topic for years, and different technologies attempting to solve limitation of previous ones are continuously being developed. These technologies and their current limitations and advantages have been comprehensively reviewed by Khalifeh et al. (2017). Examples of these technologies are:

- Acoustics